MODELLING OF REEFS AND SHALLOW MARINE CARBONATES

Jon Hill

THESIS SUBMITTED FOR THE DEGREE OF

DOCTOR OF PHILOSOPHY

UNIVERSITY OF EDINBURGH

2006

Declaration

I attest that:

All material presented in this document was compiled and written by myself unless otherwise acknowledged.

JON HILL, 2006

Acknowledgements

I always wondered what I would write for this page. Should I go for something witty and clever or stick to the tried and tested? Given my lack of time towards the end of my time as a PhD student, I think I shall stick to the latter. So here goes…I would first like to thank my supervisors, Andrew Curtis, Rachel Wood and Roger Scrutton for all their help and assistance over the years. Special thanks to Dan Tetzlaff, the original author of GPM for our day long debugging sessions and the plethora of questions I bombarded him with over the last four years. I would also like the thank Schlumberger and NERC for funding this PhD and (in the case of Schlumberger) letting me get my hands on GPM in the first place. I would also like to thank the folk at EPCC, for whom I spent the final year on my PhD working for – they put up with a very stressed employee. My colleagues and friends from the Grant Institute also deserve a mention, particularly Clare B, Alex, Tim, Dave, Sarah and Clare W. A pint was always welcome after a hard day debugging. Finally, I would like to thank my future wife, Katie. Despite doing her own PhD at the same time, she always had time for my work, never complained about it and gave me encouragement when needed and for all that I will be eternally grateful.

Jon Hill, 2006.

Abstract

Carbonate sediments are often highly heterogeneous due to the numerous factors that control deposition. Understanding the processes and controls that are responsible for such complexity has, however, proved problematic. In addition, several of these processes are non-linear, so that depositional stratigraphies may consequently form complicated, perhaps even chaotic, geometries. Forward modelling can help us to understand the interactions between the various processes involved. Here a new three-dimensional forward model of carbonate production and deposition is presented, Carbonate GPM, which is specifically designed to test the interactions between the three main carbonate production controls: light intensity, wave power and carbonate supersaturation, the latter of which is unique to this model. The model also includes transport processes specific to the reef sediment only. The effect of supersaturation and reef transport is demonstrated by comparing the output of three, otherwise, identical runs. From these simulations the need to accurately model the flow of water around a reef system and to correctly take into the account the binding nature of reefal sediments can be seen. Analysis of the stratigraphy generated by changing the antecedent topography by 1m in one locality over a 50km square platform suggest that it may be impossible to predict in detail the stratigraphy of carbonate deposits due to its sensitivity to initial conditions or controlling parameters. This reinforces the conclusions reached using previous process models. However, unlike previous models, this model does not explicitly include nonlinear biological interactions as a control. Instead it shows that similar sensitive behaviour may originate from physicochemical processes alone. External factors, such as sea-level changes, will also influence the complex stratigraphy generated by the model. The effect of several different relative sea-level curves was assessed, each corresponding to a combination of three different hierarchies of sea-level oscillations. Large-scale external processes dominate internal processes, dampening their effect on stratigraphy. However, small-scale, high frequency external processes coupled with autocyclic processes do not show any discernable stratigraphic differences from autocyclcic processes alone. The model also produces an exponential-like cycle thickness distributions that are similar to those found in ancient deposits.

Table of Contents

Chapter 1

Forward Modelling of Reefs and Shallow Marine Carbonates

1.1 Introduction

Limestones and dolomites, collectively know as carbonates, are a large component of the geological record. Carbonates are sediments that are predominately formed from calcium or magnesium carbonate: $CaMg(CO_3)_2$. Modern carbonates are generally biological in origin and the organisms producing the carbonate form the world's only living structure that can be seen from space, the Great Barrier Reef, which despite its vast size is the product of a symbiotic relationship between corals and small zooxanthellae plankton (Figure 1.1). Carbonates form in a range of environments, from deep pelagic oozes to speleothem deposits in caves, but a large proportion of modern carbonate sediment is deposited in shallow, tropical seas, such as the Bahamas.

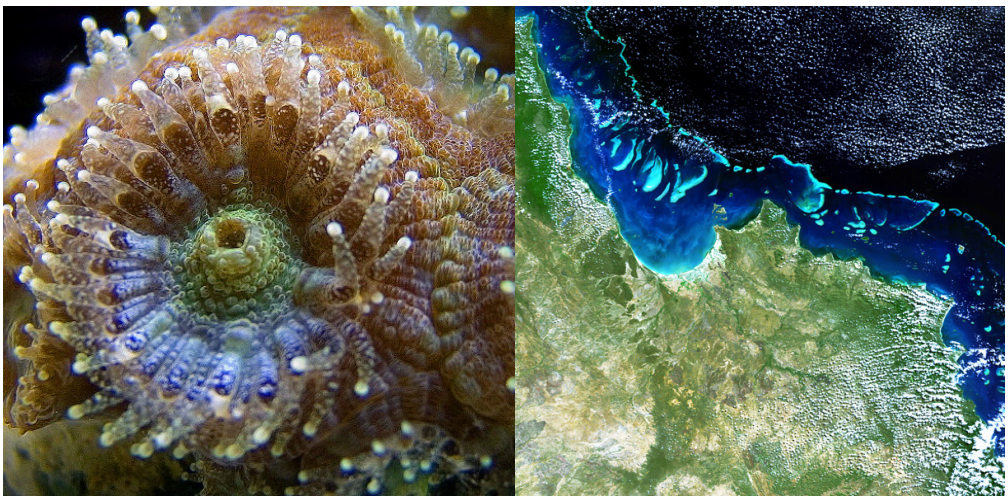

Figure 1.1. From tiny carbonate producing organisms to the only living structure that can be seen from space. Left: a single coral polyp, Acanthastrea lordhowensis (courtesy of Mike Giangrasso) which can be found on the Great Barrier Reef (right). The image of the Great Barrier Reef is an Envisat MERIS image of Australia's Queensland coast (courtesy of ESA).

Carbonates play a vital role in the carbon cycle of the planet by storing carbon dissolved in the oceans. It is estimated that 3×10^{12} g C $year^{-1}$ is stored by coral reefs alone (Crossland *et al.*, 1991). This has important consequences on global climate due to carbon dioxide interchange between the atmosphere and oceans. However, reefs are also affected by climate change and the effects of this are only now beginning to be understood (Kleypas *et al.*, 2001; Hughes *et al.*, 2003; Feely *et al.*, 2004). Ancient carbonates may also provide a high-resolution stratigraphic framework if they respond predominantly to external forces such as sea-level change rather than internal forces. This would allow for the measurement of sediment accumulation rates, biological evolution and correlation in unprecedented detail (Drummond and Wilkinson, 1993b).

Despite the importance and prominence of carbonate sediments, there are still several problems that exist in the understanding of carbonate production and deposition. Several processes affect the production and deposition rates of carbonate sediment. These processes and factors exhibit a non-linear relationship with production and deposition rates and interact in a complex fashion (e.g. Burgess, 2001; Rankey, 2002; Rankey, 2003; Wilkinson and Drummond, 2004; Wright and Burgess, 2005). The carbonate that is finally deposited is the sum effect of all these processes and the effect of an individual process is extremely difficult to extract, but this is an essential part of understanding how to decipher ancient carbonate deposits.

This thesis aims to increase understanding of the processes that control carbonate sedimentation, which is the aggregate of both the production and deposition of carbonate sediments, and does so by implementing a new model of carbonate platform production. This has particular relevance to the use of carbonates as high resolution frameworks in stratigraphy as it gives insight into the factors that influence the highly heterogeneous nature of ancient carbonate deposits and, as such, identify what information can be extracted from them. The method used in this thesis is forward modelling which is a numerical, dynamic modelling technique that can be used to simulate both production and sedimentary processes over geological temporal and spatial scales.

1.2 Depositional Processes of Carbonates

The raw material for carbonate sediment is drawn directly from the dissolved load carried in water, which is fundamentally different from how siliciclastic sediments are generated. Most modern carbonate production is biological in origin, but some production such as the whitings in the Bahamas are thought to be inorganic (Morse *et al.*, 2003). Due to the largely biological origin, and the intimate relationship with seawater chemistry, carbonate production is heavily dependent on the regional and local environmental conditions both spatially and temporally. Light intensity, carbonate supersaturation and temperature are the environmental parameters that are thought to exert most control on carbonate production rates (Kleypas *et al.*, 1999b). Carbonate is precipitated as either calcite or aragonite, which are polymorphs of the same chemical compound, calcium carbonate ($CaCO_3$) and differ only in the crystalline structure. The type of carbonate precipitated is currently dominated by aragonite and has fluctuated over time due to the dependence on water chemistry and the organisms producing the carbonate (Tucker and Wright, 1990).

Once produced, either inorganically or organically, carbonate sediment is subject to the same controls as other sediments, namely erosion, transport and deposition. However, the in-situ nature of carbonate sediment means that sediment does not have to be brought into a sedimentary basin, unlike terrigeneous sediment. The interaction of biology, environmental parameters and sedimentary transport processes give rise to complex and heterogeneous stratigraphies which are difficult to interpret in terms of their formative processes.

1.3 Diagenetic Processes of Carbonates

Diagenesis is the process that occurs soon after sediment has been deposited. It plays a key role in the final carbonate exposed in the field as carbonates make extremely reactive rocks. The flow of water through a carbonate rock is highly complex as the water reacts with the carbonate as it travels through it, precipitating carbonate in places, dissolving carbonate in others (Tucker and Wright, 1990). This changes the permeability and porosity of a rock, affecting the flow of the pore water.

The result of these interactions is a highly heterogeneous rock which can vary in composition on a metre-scale (Tucker and Wright, 1990). Although diagenesis is clearly a key process in the formation of the final outcrop, its effect depends heavily on the sediment that is deposited in the first instance. This thesis concentrates on the depositional and production processes only, but it is important to consider the effect that diagenesis may have on the final lithology recorded.

1.4 Intrinsic Vs. Extrinsic Controls on Stratigraphy

The basin-scale geometry of carbonate deposits is largely controlled by antecedent topography (Tucker and Wright, 1990). On a smaller scale, the geometries depend on several controlling factors, which is the focus of this thesis. Not only are carbonate geometries governed by the external forcing mechanisms universal to all sedimentary systems, such as sea-level oscillations, subsidence rates, and local climatic conditions, but carbonate production itself is further controlled by the interplay of biological, ecological, and physicochemical processes that operate over multiple time scales.

These processes can be divided into two groups; extrinsic and intrinsic. Extrinsic processes affect the production and deposition of carbonates, but are not affected by this deposition. Instead, eustatic sea-level changes can be caused by orbital cycles: the Milankovitch cycles (Hinnov, 2000). Changes in sea-level clearly affect the stratigraphy of carbonates, causing progradation during a sea-level fall for example, but eustatic sea-level does not respond to deposition of sediments. Other examples of extrinsic controls are climate changes (although there is some relationship between carbonate and climate, carbonates are not a dominant control but act as a sink for carbon), large-scale tectonics, and mass-extinctions; which can cause massive shifts in the biota producing carbonate sediment.

The second group are intrinsic processes which affect the carbonate deposited, but in turn respond to this deposition. Intrinsic processes interact with each other via the production of carbonate sediment. For example, the deposition of sediment can alter the flow, whether tidal or oceanic, in an area. The change in flow may reduce the supersaturation of the area as there may no longer be a free exchange of water with the open ocean to replenish the carbonate being precipitated. This change affects the

rate of carbonate production, which can lead to changes in the topography, affecting the flow again. In this way, the intrinsic processes form a complex web of non-linear interactions, which may be an ingredient for chaotic behaviour (Nicolis and Nicolis, 1991).

The interaction of these processes (both extrinsic and intrinsic) is responsible for the abundant cyclicity seen in carbonate deposits, particularly ancient peritidal deposits. These deposits are of particular interest as they could form a high-resolution stratigraphic framework, if they record high-frequency (so-called 5^{th} order) sea-level changes (Drummond and Wilkinson, 1993b). This may be the case as there is evidence of an orbital control as cycle duration corresponds to Milankovitch cycles in some ancient deposits, meaning glacio-eustatic sea-level changes may well be the main causative process and the cycles are therefore termed allocycles (e.g. Koerschner and Read, 1989; Hinnov and Goldhammer, 1991; Read *et al.*, 1991; Goldhammer *et al.*, 1993; McLean and Mountjoy, 1994; Grotsch, 1996; Balog *et al.*, 1997; Barnett *et al.*, 2002). However, this explanation of the origins of these cycles does not satisfy all authors (e.g. Drummond and Wilkinson, 1993a). It has been shown that these cycles can form from purely intrinsic processes and are therefore termed autocycles (e.g. Ginsburg, 1971; Pratt and James, 1986; Burgess, 2001; Burgess *et al.*, 2001). Moreover, statistical analysis on the cycle thickness distribution shows good agreement with a random event mechanism of formation, possibly ruling out non-random forcings as the main influence (Drummond and Wilkinson, 1996; Wilkinson *et al.*, 1996; Wilkinson *et al.*, 1997; Wilkinson *et al.*, 1998; Wilkinson *et al.*, 1999).

Given that these processes, whether intrinsic or extrinsic, are recorded in the final carbonate rock (and have not been obliterated by diagenetic effects), how does one know which, if any, is the dominant process? Unfortunately, from the rock record alone, this could be a futile exercise as carbonates show evidence of abundant hiatus events and only around 10-20% of the sediment deposited is actually recorded, eradicating much evidence of the main formative processes (Sadler, 1981). However, these processes may be simulated with a computer, providing a virtual laboratory where the effect of each process on the final stratigraphy can be investigated.

1.5 Forward Modelling

A powerful tool for analysing the cyclical carbonates described above, and carbonate stratigraphy in general, is forward modelling. Forward models are computer based numerical models that dynamically calculate parameters while running forward in time. The methodology of forward modelling is covered in more detail in chapter 3, but essentially forward modelling allows the construction of a virtual geological laboratory which aims to predict sediment deposition over millions of years (Harbaugh and Bonham-Carter, 1970). Both sides of the cyclic carbonate argument have used models to construct arguments to support both their cases (e.g. Read *et al.*, 1986; Koerschner and Read, 1989; Demicco, 1998; Burgess, 2001). However, it is only recently that computers have been powerful enough to run these models with sufficient detail to satisfy some fundamental requirements such as three-dimensional sedimentation (Burgess *et al.*, 2001; Burgess and Wright, 2003; Wright and Burgess, 2005).

There are many carbonate production and depositional processes that have previously been implemented in forward models. These now cover many of the main processes known to govern carbonate production and deposition. However, some implementations do not simulate the processes with enough accuracy or the assumptions on which the algorithms are based are too simplistic. There are two important processes that are included in the model, which is called Carbonate GPM, presented in this thesis. The first is correct treatment of reef sediment. Due to the binding and size of reef sediment it cannot be simply modelled as "a sediment" (Hughes, 1999; Rasser and Riegl, 2002). For Carbonate GPM, "sediment" means a spherical grain which has the same density as quartz. Instead the lack of advective transport and the ability to create steep slopes has to be incorporated in to the models algorithms. Carbonate supersaturation is the second process that has been incorporated into Carbonate GPM. Carbonate supersaturation of water is believed to act on both a global (Walker *et al.*, 2002) and local scale (Demicco and Hardie, 2002). Previous attempts at modelling the localised effects of supersaturation have assumed that fully saturated waters occur at a platform's edge and undersaturated waters are found nearshore (Bosence and Waltham, 1990; Warrlich *et al.*, 2002). While this is a reasonable assumption, this is not always the case as the flow of water around a

platform is not as straightforward as simply onshore (Tartinville and Rancher, 2000; Wolanski and Spangnol, 2000). The supersaturation of water is heavily dependent on the amount of time the water has spent on the platform (Demicco and Hardie, 2002) and hence to the flow regime.

1.6 Approach Taken

To decipher the effects of the multitude of processes that influence carbonate a forward model of carbonate sedimentation has been written that extends an existing siliciclastic model, GPM (Geological Process Modeller), to include carbonate production (Tetzlaff and Priddy, 2001; Tetzlaff, 2005). Many processes have previously been explored using forward models; for example sea level change, sediment transport and tectonic movement have been used to explain carbonate cyclicity (see chapter 2 for more details). One process that has not been explored in any detail is supersaturation. It is clear that supersaturation is a major controlling factor in carbonate deposition, both for coral reefs and carbonates in general (Kleypas *et al.*, 1999b; Demicco and Hardie, 2002). However the effects of supersaturation on depositional geometries are not well understood. Does it add to the complexity of carbonate deposition as described and documented by many authors (e.g. Wilkinson *et al.*, 1996; Rankey, 2004)? Does it smooth out any variances? In short, the questions that this thesis will try to answer using the forward model are:

- To what extent could supersaturation affect the deposition of carbonate stratigraphy?
- Could supersaturation increase or decrease the complexity of carbonate stratigraphy?
- Which processes control the complexity?
- Do external forcings dominate internal forcings?
- Can some of the features previously attributed to other (e.g., biological) controls/feedbacks be explained by a simple physicochemical control?
- Does this control introduce other features that are not included in previous models?

The hypotheses that will be tested in this thesis are:

- Supersaturation is not a major factor in producing carbonate complexity.
- Transport of reefal sediment does not need to be differentiated from other sediments in shallow marine carbonate systems in order to create realistic stratigraphic geometries.
- Physicochemical processes alone cannot create apparently chaotic carbonate stratigraphic sections.
- External forcings dominate internal processes and control the amount of carbonate deposition.

1.7 Outline of Thesis

The next chapter deals with geological processes. What are the processes that control sediment, and in particular carbonate, deposition? This chapter examines the processes that are thought to affect deposition and looks at the data that can be gathered to elucidate these processes.

In order to test the hypotheses stated above, the processes controlling carbonate production and deposition must be modelled with a computer in order to tease apart the effect of each process. The previous efforts in modelling carbonate stratigraphy are detailed in chapter 3.

The fourth chapter describes the forward model that was produced as part of this thesis, validates and verifies the model against data and other models. The processes and algorithms used in the model are also detailed in this chapter. The effect of transport on reef sediment is also assessed.

The chapter five deals with the importance of supersaturation as a controlling process and the effect of reef sediment on carbonate deposition. It establishes that residence time (the proxy for supersaturation), which is unique to this model, produces “patchy” production rates, which in turn cause the formation of autocycles in the stratigraphy.

Using the model described in chapter 4, the possibility of chaotic behaviour in carbonate stratigraphy is explored in chapter 6 by changing the initial topography by a small amount at one location on the platform.

Chapter 7 examines the auto- vs. allo-cyclic debate. The effect of an external forcing is tested on the final stratigraphy and the complexity produced. This is tested using a hierarchy of sea level changes and the effect of each is assessed independently.

The final discussion chapter brings the previous four chapters together and analyses the consequences of the findings produced in this thesis. This chapter also assesses whether the hypotheses tested have been successful or not, lists the main conclusions of this work and suggest areas of further work.

Chapter 2

Carbonate Processes

This chapter describes the parameters and processes that control and affect carbonate precipitation and deposition. These processes form a complex system of non-linear interactions and feedbacks, making it difficult to extract the effect of a single process in isolation. Nevertheless, this has been the focus of many studies, as summarised here. Most research effort focuses on modern, tropical coral reefs and their associated platforms as they are the most visible portion of global carbonate production, but there have been attempts to isolate the effect of various processes on many other types of carbonate depositional settings.

2.1 Introduction

Carbonates are deposited in a wide range of environmental settings, ranging from lacustrine to deep, pelagic oceans (Figure 2.1). One thing that unites all these environments are the factors that control the production and deposition of carbonate sediments; of which biology and carbonate supersaturation are the most important. One of the most prominent of these environments is the shallow, tropical, marine environment of which coral reef communities are the most well-known producers of carbonate sediment, although calcareous green algae such as *Halimeda* also play an important role and have been the subject of several studies (Drew, 1983; Kleypas, 1997). The shallow-marine environment is responsible for around 10% of the global carbonate production (Tucker and Wright, 1990). This creates an immediate problem for understanding ancient deposits: what knowledge extracted from modern systems is applicable to ancient systems? For example, the current day chemistry of seawater is not thought to be the same as existing during the Phanerozoic (Tucker and Wright, 1990; Walker *et al.*, 2002). This type of fluctuation in controlling parameters must be incorporated into any attempt to understand the effect on ancient carbonate deposits.

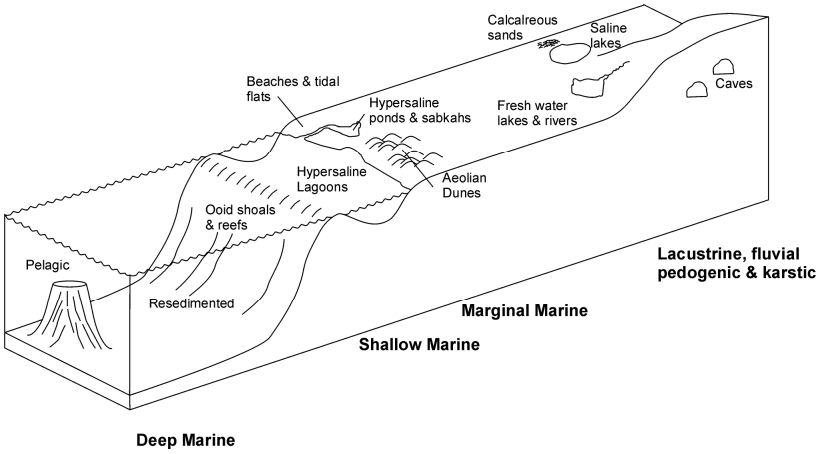

Figure 2.1. A cartoon showing the environments where carbonates are produced and deposited. After Tucker and Wright (1990).

The limestone or dolomite found in the field is the end result of a number of non-linear and interacting processes. These processes act on the carbonates at a number of stages. The first stage is carbonate precipitation or production from seawater. This is the fundamental difference between carbonates and siliciclastic rocks, as carbonates can be deposited in-situ whereas siliciclastic sediments must be eroded from pre-existing rocks and transported into a sedimentary basin. Modern carbonate production is mostly organic in nature, and is the product of organisms creating skeletons, frameworks, shells or other structures. Production can also occur inorganically, such as the so-called "whitings" in the Bahamas (Morse *et al.*, 2003), or can be biologically aided, as is the case with ooids (Simone, 1980).

Once produced, the carbonate must be deposited in the basin as sediment, rather than be subjected to chemical erosion. It is at this point the carbonate sediment starts to behave more like siliciclastic sediment, being subject to erosion, transport and re-deposition by wave actions, tides, currents and gravity flows. There are still, however, key differences. Carbonate particles are generally less dense than an equivalent-sized quartz grain, the main component of siliciclastic sediment. Calcite has a slightly higher specific gravity than quartz, but many carbonate grains are not solid grains, instead having cavities and hollows due to the biological origin of the sediment, reducing the overall density of the grain to below that of quartz. Secondly, carbonate grains produced by organisms have a shape that is adapted to the life habits of the organisms and is may not be a near-spherical shape as in a clastic sediment. Both of

these factors have implications on the transport of such grains. Some corals and other organisms generate vast skeletons, sometimes metres in size and additionally, large boulders may be formed due to the binding action of organisms. Both these processes result in large grain sizes, which if considered in a siliciclastic setting, would be indicative of an extreme high energy event, rather than the action of steady production processes that is the case in carbonate systems. The large size of the grains will also have an effect on the transport of such sediments. In addition to these sedimentary factors, carbonates are also susceptible to rapid cementation soon after deposition. This depends on the local environmental conditions but can produce so called "hardgrounds" (Tucker and Wright, 1990).

The large-scale geometries produced by carbonate deposition are controlled by the extrinsic global and regional processes that affect all sedimentary systems. These controls, such as sea-level, and subsidence rates dictate how much sediment can be deposited and where it can be deposited and as such controls the large-scale geometries that are observed in the rock record.

Overprinted on the sedimentary record left by all these processes is the effect of diagenesis, which spans a large range of effects. Although diagenesis is vital to the final carbonate observed in the field, this thesis concentrates on the production and depositional processes only.

This chapter is divided into three main sections. Section 2.2 deals with the factors and processes that control the precipitation and production of carbonates. Section 2.3 concentrates on those factors that affect the deposition of carbonate sediment, including subsequent erosion, transport and re-deposition. This section also includes the physics of sediment transport and deposition. Section 2.4 deals with the controls on carbonate geometries at a range of scales which includes the sequence stratigraphy of carbonate systems. The chapter concludes with a discussion on what our current understanding of the processes controlling carbonate is and where the gaps in our knowledge exist.

2.2 Processes Controlling Precipitation

It is well known that modern shallow carbonate production generally occurs in the warm, shallow, tropical marine environment, which are some distance from terrigeneous input, i.e. are not affected by clastic sedimentation, freshwater and nutrients (Wood, 1999). While cool water carbonate deposits can be found in the arctic waters at great depths (Roberts *et al.*, 2006), most organic carbonate is produced in less than 15m of water (Tucker and Wright, 1990).

Environmental conditions can affect carbonate production in two ways. Firstly, they can control the global distribution of carbonate producing organisms. Secondly, they can affect the rate at which carbonate is produced, whether the sediment is abiotic or biotic in origin. The environmental parameters act on a number of scales, from global scales, such as aragonite and calcite supersaturation to more localised scales, such as wave energy, which can fluctuate rapidly both temporally and spatially.

The primary control on modern carbonate production (assuming sufficient accommodation is available) is mostly likely to be aragonite supersaturation, as shown by carbonate production rates measured against latitude which show a very good correlation with supersaturation variation with latitude (Figure 2.2). The other key factors on carbonate production, temperature and light, show a positive correlation, however, only supersaturation shows an equivalent decrease to the decrease in carbonate production in equatorial regions. The reason for this decrease is due to increased rainfall in this region, diluting the carbonate supersaturation (Opdyke and Wilkinson, 1993).

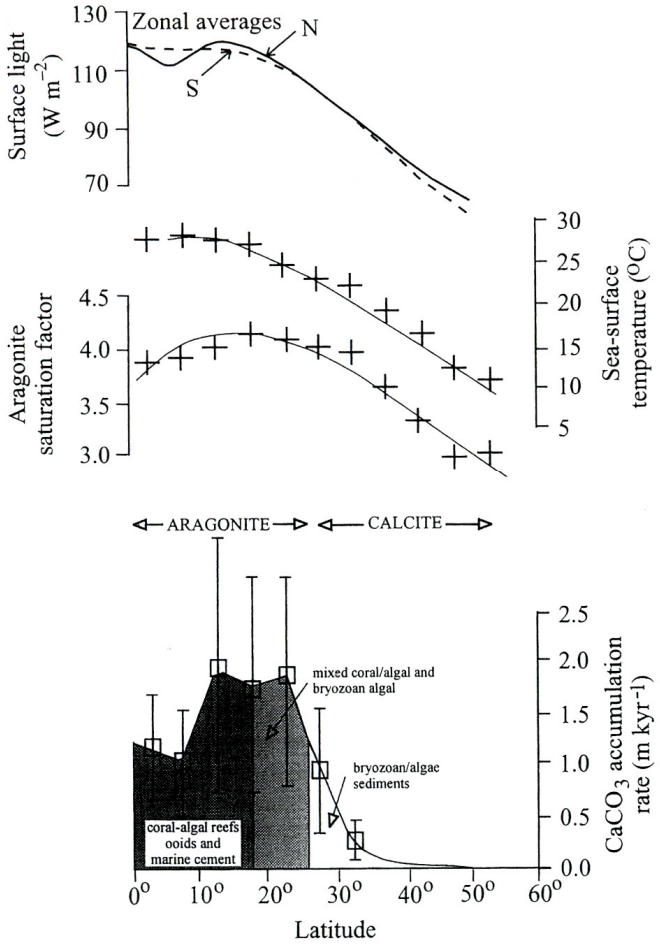

Figure 2.2. Distribution of various carbonate producing biota (bottom panel) with latitude. Note how this correlates very well with aragonite supersaturation (middle panel), including at equatorial latitudes. Both temperature and light show very good correlation at high and tropical latitudes. From Wood (1999)

As the majority of carbonate production is biological in origin, this section first reviews the effects of biologically induced production, before discussing the effect of supersaturation, temperature, light, nutrients, waves, and finally tides.

2.2.1 Biology

Many types of carbonate sediment are the product of biological activity (Wood, 1998). In considering the processes that govern carbonate production, the effect of biological organisms is an overprint on the parameters and processes discussed later in the chapter, as most modern carbonate sediment is derived directly or indirectly via biological processes. Biology adds additional complexity to the other processes and parameters that affect carbonate production via the competition and co-operation of

species and individuals and plays an important role in the type of carbonate sediment produced.

Coral reefs are a major producer of modern day carbonate and produce large, framework structures that have a high cohesive strength, whereas other carbonate producers, such as coccoliths, produce vast amounts of carbonate ooze in deep water. As such, biology plays a key role in the type of facies observed in both modern and ancient carbonate deposits. One clear effect that is undoubtedly the result of biological controls is the change in sediment type through geologic time, an example of how the law of uniformitarianism cannot be blindly applied to carbonate sediment. Species of carbonate producing organisms do not exist throughout geological time. Neither, in fact, do entire groups. Coccoliths, the main producer of carbonate sediment today only evolved in the Mesozoic (Figure 2.3). Likewise, brachipods, which were a major producer of carbonate sediments in the Palaeozoic are not so now (Tucker and Wright, 1990). These two groups produce vastly different carbonate facies; coccoliths produce a fine mud, while brachipods produce shells that range from a few mms to tens of centimetres (Clarkson, 1998).

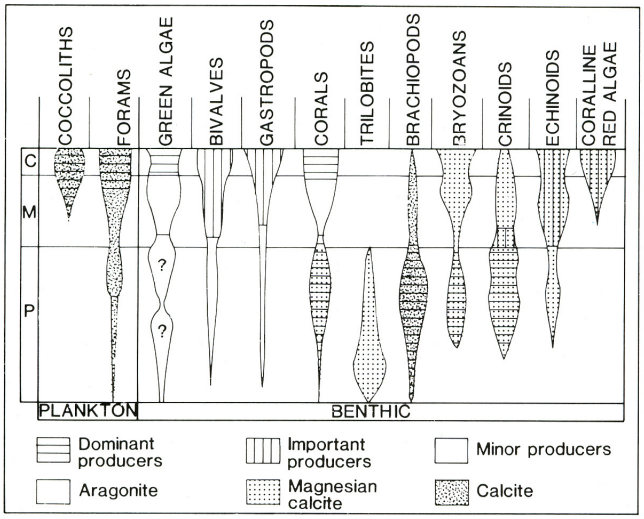

Figure 2.3. Changes in carbonate producing organisms through time. From Tucker and Wright (1990).

2.2.2 Supersaturation

A solution that is carrying more solute than the maximum stable amount is said to be supersaturated. Supersaturation of carbonate is usually quoted with respect to

aragonite and is represented by a dimensionless number (Ω-arag). Values of less than 1 indicate undersaturation and supersaturation is given by numbers greater than 1. The entire surface ocean is supersaturated, but the amount varies according to latitude, with the tropics averaging around 3.3 and the poles around 1.5, which is largely a temperature control (Kleypas *et al.*, 1999b).

In seawater there are three species of dissolved inorganic carbon (DIC): CO_2, bicarbonate (HCO_3^-) and carbonate ions (CO_3^{2-}). The distribution of these species is set by two equilibrium constants:

$$K_1 = \frac{[HCO_3^-][H^+]}{[CO_2]}$$
$$K_2 = \frac{[CO_3^{2-}][H^+]}{[HCO_3^-]} \qquad (2.1)$$

Where [*X*] is the total free concentration of component *X* in seawater and K_1 and K_2 are the equilibrium constants. Changes in both temperature and pH cause a change in K_1 and K_2, which in turn affects the concentrations of the species involved. Finally, the carbon also interacts with carbon in the gaseous and solid states, meaning atmospheric carbon dioxide can also affect the concentrations (Gattuso *et al.*, 1999). The change in aragonite supersaturation with temperature and the carbon dioxide in the atmosphere is well understood and documented (Figure 2.4) This does have important implications on understanding the effect of global climate change on coral reefs and carbonates in general as global levels of CO_2 are expected to rise.

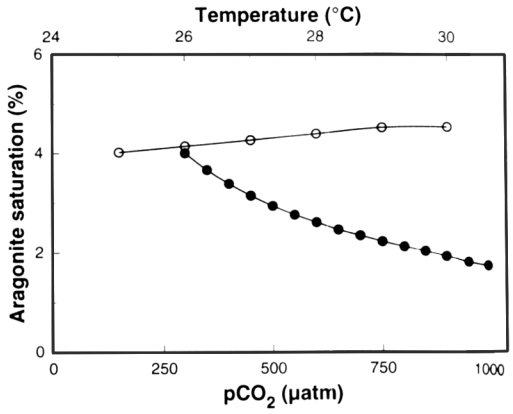

Figure 2.4. Changes in aragonite supersaturation as a function of temperature and atmospheric CO_2. From Gattuso et al. (1999).

Due to the fact that all carbonate must be extracted from water, the supersaturation of the water with respect to calcium carbonate is a key control on the amount of carbonate produced. The overall effect of supersaturation, however, is closely tied to photosynthesis and temperature (Suzuki *et al.*, 1995; Gattuso *et al.*, 1999). Studies by Broecker and Takahashi (1966), Morse et al. (1984) and Demicco and Hardie (2002) on the Bahama Banks carbonate platform show that carbonate precipitation is a function of water depth and residence time (Figure 2.5). The change in production rates with respect to water depth can already be explained by the change in light intensity (see section 2.2.4). In particular the study by Demicco and Hardie (2002) shows a strong exponential relationship between carbonate production rates and residence time. Residence time is defined as the length of time that water has remained on the platform. As the production rate is related to the saturation state of the water, the more highly supersaturated the waters, the more calcium carbonate can precipitate. On the Bahaman platform, water evolves as it moves onto the platform and at approximately 250 days is very nearly at equilibrium and is incapable of producing very much additional aragonite (Demicco and Hardie, 2002). This change in supersaturation state affects the production rates of organisms, such as calcareous red algae (Borowitzka, 1981), and corals (Gattuso *et al.*, 1998a) and production rates of non-biotic carbonate sediments, such as ooids (Davies *et al.,* 1978).

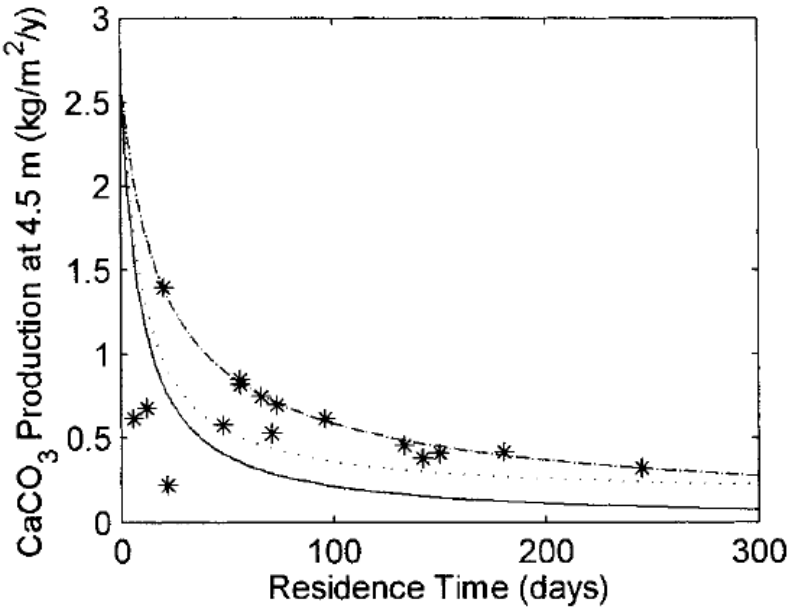

Figure 2.5: Calcium carbonate production rates at 4.5m depth as a function of residence time from the Bahaman Bank. Modified from Demicco and Hardie (2002).

For corals reef growth, water must have a minimum supersaturation (Buddemeier and Smith, 1999). The minimum for reef growth is around 3.1 Ω-arag (Kleypas *et al.*, 1999b). However, the uncertainty of the effect of supersaturation on reefs is rather large. Langdon et al (1998) measured a 30% drop in carbonate production of the BIOSPHERE 2 coral reef community (a self-contained study area) as the aragonite supersaturation of the water dropped from 5.0 to 3.2 Ω-arag, a 46% drop. The response of calcification rates in corals to supersaturation is thought to be non-linear, remaining near constant within certain limits, but decreasing rapidly with a smaller change in supersaturation state (Gattuso *et al.*, 1998a). Global analysis by Kleypas *et al.* (1999) also shows higher calcification rates in areas of higher supersaturation when other key factors, such as temperature and light, were similar.

Non-biotic carbonate sediment production rates are also affected by supersaturation. Ooids are spherical or ellipsoid concretions of calcium carbonate, usually less than 2mm in diameter (Donahue, 1969; Tucker and Wright, 1990). There have been examples in the Neoprotozoic of ooids that are 16mm in diameter (Sumner and Grotzinger, 1993), but all modern ooids are 2mm or less. Supersaturation plays two important roles in ooid formation, controlling the growth rate of an individual ooid as well as the form of the ooid. Monoghan and Lytle (1956) investigated the effect of carbonate concentration on the formation of ooids. They found that the concentration needed to be above 0.002 moles/litre and below 0.0167 moles/litre for ooids to form successfully. Below 0.002 moles/litre only aragonite needles or poor ooids formed. Above 0.0167 moles/litre the ooids formed an amorphous mass.

2.2.3 Temperature

Temperature is one of the three main controls on carbonate production as, for example, it determines reef distribution at a global scale. In terms of carbonate production as a whole temperature affects the supersaturation of the water, which in turn affects the precipitation rate (Gattuso *et al.*, 1999; Kleypas *et al.*, 1999b). Clearly, low temperatures are not an indicator of no carbonate production as cool-water carbonate factories are found in seas which have a temperatures as low as 4°C and these kinds of reef are widely distributed and therefore other controls are of more importance. (Roberts *et al.*, 2006).

Tropical reefs have a fairly narrow temperature range. The minimum sea surface temperature is around 11.5°C, but this can only be withstood for a number of days. Longer term minimums that a reef can withstand are around 18°C (Kleypas *et al.*, 1999a). Reductions in temperature can reduce the amount of reef growth and lead to drowning of the reef (Isern *et al.*, 1996; Flood, 2001), but there is little data available on the exact relationship between growth rates and temperature.

2.2.4 Light

Light penetration is of particular importance to modern coral reefs and to all photosynthetic organisms that produce carbonate skeletons or frameworks. Carbonate is produced via photosynthesis in both corals and phytoplankton, which together account for the majority of modern day carbonate production (Tucker and Wright, 1990). Almost all the data concerning the effect of light on carbonate production has been collected for modern coral reefs, but much of it applies to any photosynthetic organism that produces carbonate, such as calcareous red and green algae (e.g. Pentecost, 1978; Borowitzka, 1981; Drew, 1983).

The majority of corals grow in depths of less than 25m and the maximum growth rate occurs in depths of less than 10m (Stoddart, 1969). Other photosynthetic, carbonate producing organisms have a different range of light tolerance, such as the calcareous green algae, *Halimeda*, which can grow as deep as 200m (Hillis-Colinvaux, 1986). As can be seen in Figure 2.6, both temperature and oxygen are largely invariant of water depth (at least until 50m depth), making light the main controlling factor on the depth at which corals can grow (Stoddart, 1969). The long-term light levels reaching the seabed are a function of two variables: the light reaching the ocean surface and the attenuation of light in the water. The first of these is largely controlled by the angle of the sun and atmospheric conditions and is therefore a latitudinal control. The second factor depends on water clarity, which can vary due to suspended sediment and time of year (Kleypas *et al.*, 1999b). For example in the Bahamas the light intensity at a depth of 15m is 2.7% that of the surface intensity in the summer, but in the winter, the percentage drops to just 1.5% (Stoddart, 1969).

The absolute limits on reef growth in terms of light are not expressed as light intensity, but as a percentage of surface light intensity. Individual coral species can survive at around 5-10% of surface intensity, but reefs generally grow where the light intensity on the sea floor is around 15-20% of the surface intensity. Reduced growth at higher latitudes is often attributed to temperature, but just as light attenuation with depth can explain the depth profile of a reef, it can also explain how reefs can be restricted to shallow water at these higher latitudes (Kleypas *et al.*, 1999b).

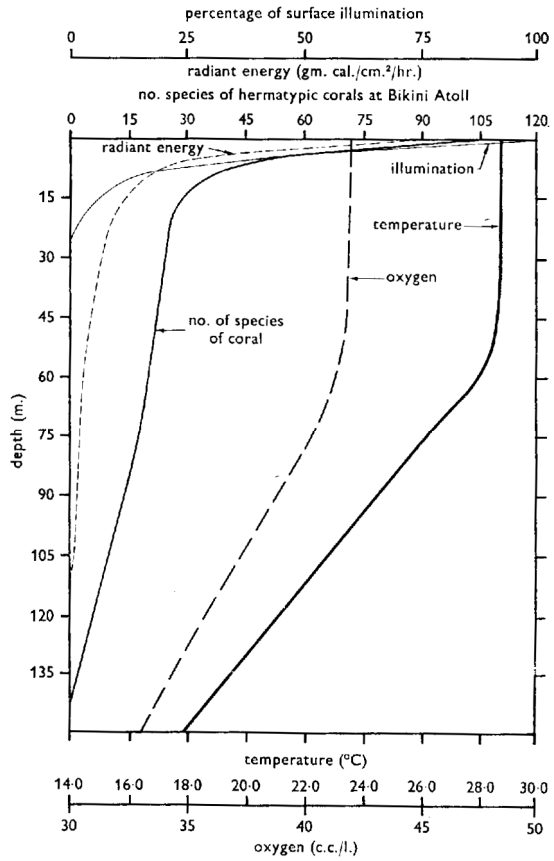

Figure 2.6. Variation of light, oxygen and temperature with increasing depth. From Stoddart (1969).

As well as the depth to which corals can grow, light also controls the rate at which a reef, dominated by photosynthetic organisms, produces carbonates. Growth rates of individual coral species show a strong correlation with water depth (Bosscher and Schlager, 1992) as does the morphological form of the coral species (Chappell, 1980). In addition, if the growth rates of corals in a Caribbean reef are measured at various depths, they are very close to the theoretical curve produced by considering the

extinction of light with depth linked with changes in photosynthetic rate with light intensity (Chalker, 1981; Bosscher and Schlager, 1992). *Halimeda* also require a minimum amount of light intensity (which is lower than that of corals) in order to grow and the rates of calcification vary with changing light intensity and species (Littler *et al.*, 1988).

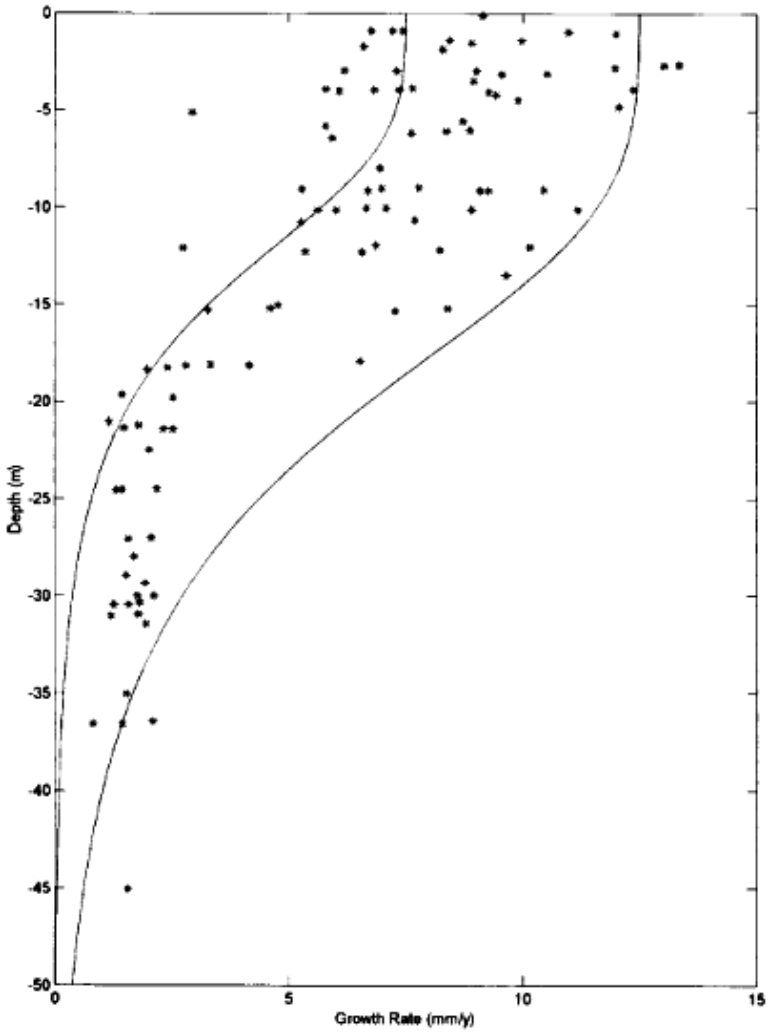

Figure 2.7: Growth rates of Caribbean corals. Solid lines show the theoretical growth rates calculated using the attenuation of light and photosynthesis with different attenuation coefficients. Dots show measured coral growth rates. After Bosscher and Schlager (1992).

2.2.5 Nutrients

Nutrients are necessary for any organism to exist. The nutrient levels important for reef growth are nitrate (NO_3) and phosphate (PO_4). Reef corals require very low levels of both these compounds in order to thrive. Reefs have been recorded in areas where

nutrient levels are as high as 5.61μmols litre^{-1} of nitrate and 0.54μmols liter^{-1} of phosphate (Kleypas *et al.*, 1999b). Corals do need minimum nutrient amounts in order to survive (Atkinson *et al.*, 2001; Hearn *et al.*, 2001). The reason that higher nutrients levels are so detrimental to a reef's health is not thought to be due to poisonous effects, but to the competition of species that thrive with higher nutrient levels, such as benthic algae, reducing water clarity (Tucker and Wright, 1990). However, other effects such as the decrease in the translocation of photosynthetic products from the zooxanthellae to the coral with increasing nutrient levels, a higher abundance of bioeroders in nutrient rich waters and the fact that most nutrient rich waters occur as upwellings and as such are at a lower temperature than would be normal for the area could all be confounding factors (Szmant, 2002).

Nutrient levels are not so detrimental to other carbonate producing organisms. *Halimeda* appears to be adapted to take advantage of brief increases in both nitrate and phosphate levels, increasing the calcification rates. However, the exact response depends on the species, with *H. lacrimos* and *H. copiosa* adapted to nitrate increases and *H. tuna* and *H. simulans* adapted to phosphate increases (Littler *et al.*, 1988).

2.2.6 Waves

Although waves are not a first order control on how fast, and where reefs, can grow, they are a regionally important control (Kleypas *et al.*, 1999b; Storlazzi *et al.*, 2003). Waves show a large effect on coral reefs, determining morphology and growth rates, but they are also an important factor in the effect of storms (section 2.3.5) and in sediment transport in general (section 2.3.1).

The morphology of individual corals shows a general decrease in branching complexity as the hydrodynamic stress increases (Chappell, 1980). This can affect precipitation rates as different species of corals also have different growth rates. The type of corals that can grow in any particular area of a reef is a function of light intensity and subaerial exposure due to tidal fluctuations. Measurements of waves across a reef show that the wave height decreases as the waves travel from the forereef to the backreef areas, which in turn decreases the wave energy by around 65-71% (Lugo-Fernández *et al.*, 1994; Lugo-Fernández *et al.*, 1998a). Changes in wave

energy and light levels give rise to changes in zonation patterns and cross-section profile of a reef (Graus and Macintyre, 1989).

As well as controlling the morphology of the whole reef and individual coral species, waves also play an important role in the maintenance of the reef community. The currents that are caused by waves sweep away sediment and waste products (Lugo-Fernández *et al.*, 1994), and contribute to mechanical cleaning of the coral polyps (Stoddart, 1969). Waves also contribute to the currents circulating in and around a reef due to wave set-up, which has important implications on the residence time of the waters contained in a lagoon (Kraines *et al.*, 1999). All these factors may explain the observation that reefs are often more productive on the windward side of an atoll where wave energy is greatest (e.g. Munk and Sargent, 1948; Roberts, 1974; Grigg, 1998; Kench, 1998; Cruz-Piñón *et al.*, 2003; Yamano *et al.*, 2003). However, there is little quantitative data that explicitly states how changing wave energy affects production rates, but the reason for the increase in growth in high energy areas is thought to be due to an increase in nutrient uptake from waters that are nutrient poor (Atkinson *et al.*, 2001; Hearn *et al.*, 2001).

2.2.7 Tides

When considering the effect of tides on carbonates there are two main things to consider. The first that tides modify the flow in and around reefs (Roberts *et al.*, 1975; Wolanski and Spangnol, 2000). This has an effect on the transport of sediment and water circulation around the lagoon in conjunction with winds (Kraines *et al.*, 1999; Kraines *et al.*, 2001; Mathieu *et al.*, 2002). Secondly there is the effect of waves impacting the reef or shoreline. As described in the previous section, waves are important factors in determining local coral growth and general reef morphology.

The effect of tide on waves is generally associated with the energy dissipated and the wave properties. Larger waves occur at high tides (Brander *et al.*, 2004). However, lower tides cause the energy dissipated by waves breaking to increase due to the reduction of water depth and increased friction (Lugo-Fernández *et al.*, 1998a). Finally, because of the daily change in water level, tides can leave part of a reef exposed. However, the coral species that live in the areas that are exposed show a

morphological adaptation to this change (Chappell, 1980). The species can therefore tolerate emersion of up to 3 hours without any damage. However, this time is dependent on the time of day as exposure to sunlight will shorten this (Stoddart, 1969). As with wave energy, this controls the location of individual coral species, affecting the overall production rate in an area. In addition, production can only occur during submersion, therefore any time spent exposed will reduce the overall production rate.

2.3 Processes Controlling Deposition

This section covers the processes that affect carbonate deposition. These are very similar to the processes that control the sedimentation of siliciclastic sediments and include erosion, transport and re-deposition of sediment. The section first covers general physical principals of sediment erosion and transport, before considering the specific effects of wave, tides and biology on carbonate sediment.

2.3.1 The Physics of Erosion, transport and re-deposition of sediment

The movement of sediment grains is controlled by grain properties such as density, size, shape and composition, the flow that is transporting them, and the bulk characteristics of the sediment, for example, porosity, sorting and cementation. The entrainment and transport of grains can change the properties of a grain that is being transported, affecting its shape and size, or even destroying it completely. In this way the composition of any sedimentary rock that has undergone any form of transport can give vital clues to the sedimentary provenance, transport history and depositional conditions (Pye, 1994).

All sediment transport takes place in a fluid, which is either water or air. A fluid flow is a portion of that fluid which is in motion. Most fluids that are of sedimentological interest are restricted by a closed boundary of some kind, for example river channels bottoms or the sea bed. Friction between this boundary and the fluid gives rise to a boundary layer in which a gradient of velocity occurs from zero at the solid boundary to the flow velocity. This gradient is equivalent to the stress that arises between the solid boundary and the fluid, which is important for the entrainment of sediment (Allen, 1994). If the stress is above the threshold stress, Shields' Criterion, for a

particle (which depends on the particle size, density and neighbouring particle sizes) then the flow can lift the particle and entrain it (Shields A, 1936). Equally, an entrained particle can be deposited when the flow slackens, causing the stress to drop below the threshold value (Figure 2.8). The type of movement also depends on the grain size as to whether it is carried as suspended load or bedload (Figure 2.8).

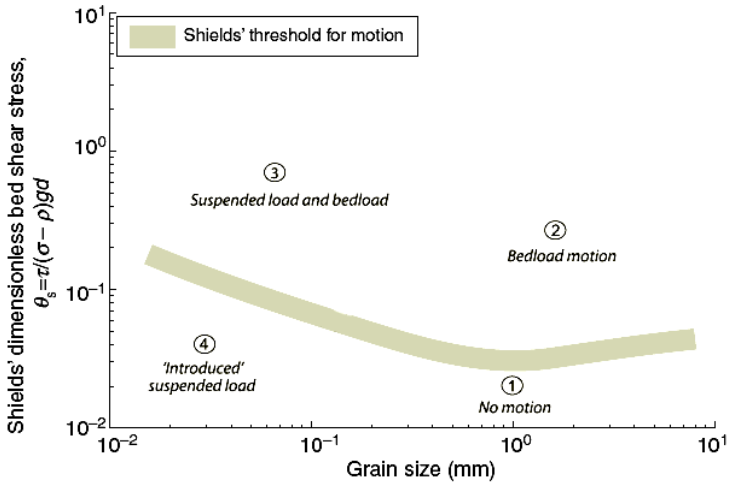

Figure 2.8: Shields Threshold for siliciclastic sediment movement and transport. Modified from Leeder et al., (2005).

Entrained grains travel in a number of ways which depends on their size shape and the excess shear in the flow as well as the properties of the transporting fluid. There are four modes of transport in water: sliding, rolling, saltation and suspension. Particles that are sliding, rolling or saltating are considered to be the bed load. Suspended grains make up the suspended load. Similarly in air there are three recognised modes of transport: creep, saltation and suspension (Allen, 1994). Again, the entrained sediment can be divided into the bedload (creeping and saltating grains) and the suspended load (suspended grains).

The sediment movement considered so far has been within a seperate moving fluid. Gravity, however, also plays a major part in sediment transport. Mass wasting encompasses all types of sediment movement due to gravity and covers intermittent events such as avalanches, debris flows and rock falls and also constant processes such as soil creep.

2.3.2 Waves

Of particular interest to this thesis are the transport processes that occur in the nearshore and beach environment, which is mostly the product of waves. Most processes act either perpendicular to the shoreline (orthogonal or cross-shore processes) or parallel to the shoreline (longshore processes).

Waves are the most visible aspect of shoreline sediment transport. Waves occur due to the transfer of energy from the wind to the water in the *fetch* area. Waves are oriented such that the crests are normal to the wind direction and they travel in the down-wind direction. The properties of a wave, such as its period, wavelength and amplitude, are directly related to the wind speed in, and the size of, the fetch area (Pinet, 1992). Waves impacting along a shoreline will have a range of periods and wavelength. The water moves in an elliptical path as a wave passes through. This can generate a current due to the fact that the oscillatory, elliptical motion induced by a wave is not a perfectly closed ellipse. When waves enter water that is approximately the same depth as its height, they break, dissipating energy. This also sets up the longshore current, caused by waves approaching the shoreline at an angle other than normal (Hardisty, 1994).

The action of waves has several effects on the sediment transport processes. In addition to the forces described in section 2.3.1, waves also an acceleration of the fluid past the plane on which the sediment rests, increasing the stress at that point. This allows for more sediment to be entrained. Longshore currents transport sediment along the shoreline, causing the formation of such geomorphological features as spits and bars. Waves also sort sediment, leading to coarser sediment nearshore and finer sediment offshore.

2.3.3 Tides

As described in section 2.2.6, tides affect the wave properties, therefore affecting the transport properties of waves. The daily change in water height also generates tidal currents. These currents are strong enough to move sediment. The effect of tides on carbonate deposition is most effectively demonstrated by looking at the ooid shoals on the Bahaman Platform. Ginsburg (2005) showed that not only do tides affect the

sedimentary bedforms (which is not surprising), but that the arrangement of these bedforms can then affect the tidal currents that formed the bedform in the first instance. The constant shifting of the sediment is essential for ooid formation as they require constant agitation (Newell *et al.*, 1960; Davies *et al.*, 1978). It is not only ooid shoals that cause a feedback between the tides and the topography. Studies at Muruoa Atoll show that cross-reef tidal current is highly dependent on the reef geometry (Tartinville and Rancher, 2000), but tides also affect the rim of reef-protected area (Andrefouet *et al.*, 2001a).

Figure 2.9. Aerial view of a flood parabolic bar or spillover lobe from the Cat Cay sand belt on the western margin of Great Bahama Bank. The effect of sediment movement is clear in the ooid shoal. All sediment movement here was created by tidal flow. From Ginsburg (2005)

2.3.4 Bioerosion

The eroders of carbonate include those that graze on the plant tissue above or close to the substrates, and so ingest some calcareous materials in addition and those that bore into live coral. The amount of sediment removed depends highly on the species involved, but it involves groups as diverse as fish, molluscs, echinoderms and annelid worms (Wood, 1999).

Bioerosion of coral reefs was first recorded by Darwin (1842) when he noted that "*…[opening] several of these fish, which are very numerous and of considerable size, …I found their intestines distended by small pieces of coral, and finely ground calcareous matter.*"

The fish most commonly observed feeding from corals is the family Scaridae, commonly known as Parrotfish (Figure 2.10). Studies have shown that an individual of the species *Chlorurus guibbus* can consume around 1000kg of sediment per year (Bellwood, 1995b). When compared to other bioeroders, such as echinoids and sponges, which may erode between 0.1 to 15kg of sediment per year per individual, the effect of parrotfish on the reef system is not negligible (Bellwood, 1995b).

Figure 2.10. A male Bicolor Parrotfish (Cetoscarus bicolor) at North Horn, Osprey Reef, Australia. Courtesy of Richard Ling

In addition to the net removal of corals, parrotfish are also responsible for sediment transport and a change in grainsize. Bellwood (1995) observed two species of parrotfish, *C. gibbus* and *C. sordidus*, both of which reduce the grain size of any carbonate material they consume, whether fresh coral or reworked sediment. *C. gibbus* also transports sediment from the growing reef to deeper water (which could be the reef slope or a reef gully), but *C. sordidus* deposits the sediment in the same area as it consumes it. The fish also prefer to eat certain areas of reef, in particular reef stumps on the reef crest. The overall effect is the removal of higher topography on the reef.

However, the effect of parrotfish is a recent phenomenon as Scaridae evolved in the Cenozoic, increasing the total amount of bioerosion occurring on a reef (Bellwood, 2003). Studies on other types of bioeroders show that they are still capable of

removing significant amounts of sediment, 2.6kg m^{-2} yr^{-1}, with water depth, light and nutrient supply having an effect on the amount eroded (Chazottes *et al.*, 1995).

2.3.5 Storms/Hurricanes

Storms are infrequent, but high energy events that may have a large effect on carbonate deposition. More obvious effects include the increase in wave power and wave induced currents for a short time. This can move vast amounts of sediment around (Lugo-Fernández *et al.*, 1994), destroy areas of coral growth and change the zonation and species around a reef due to re-colonisation of bare substratum (Woodley *et al.*, 1981; Scoffin, 1993). However, the long term effect on zonation and the diversity of species may not be that great as the period between successive storm events is typically lower than the recovery rate (Graus *et al.*, 1984).

2.4 Processes Controlling Geometries

Geometries formed by carbonate sedimentation can be recognised at a range of scales (Figure 2.11). On the bed and facies scale, the geometries formed are controlled by local environmental processes, such as the strength of the tidal currents, much in the same way as siliciclastic sediments and of course biological controls which are of particular importance to carbonate geometries. These geometries are covered only briefly in section 2.4.1 as some occur at a smaller scale than the resolution of the forward model described in the thesis. However, their overall effects on the larger-scale geometries are incorporated into a sedimentary model. The parasequence-scale geometries are on the order of a metre in size and are described in section 2.4.2. The term parasequence is derived from the nomenclature of sequence stratigraphy (see section 2.4.3 and chapter 7). The scale of these geometries is the same order of magnitude as the cycles that are particularly common on ancient peritidal platforms. The debate around these cycles centres on whether they are largely controlled by internal or external controls (e.g. Wilkinson *et al.*, 1999). It is at this scale, the effects of the principal depositional processes can be seen and modelled (Figure 2.12). The largest scale geometries occur at basin level (section 2.4.3). This is largely controlled by antecedent topography, but can be modified by the production and depositional processes as well as changes in relative sea-level.

2.4.1 Bed-Scale Geometries

The bed-scale geometries of carbonate deposition are controlled by local processes such as wave action, much like siliciclastic sediments. In the shallow marine environment the type of sedimentary depositional system is largely a control of energy (Tucker and Wright, 1990). There is a spectrum of possible depositional systems that can develop and are analogous to their siliciclastic counterparts, such as beach-barrier systems and strandplain complexes (Tucker and Wright, 1990). Various sedimentary structures can be formed, such as cross-bedding, hummocky cross stratification (HSC) and ripples. If a barrier reef forms, this can significantly affect the depositional system that occurs. On a windward facing barrier system with strong tides channels with spillover lobes can form behind the reef. Where tides are less of an influence, tidal flats (see later) will occur in the lagoon. These tidal flats exhibit bed-scale geometries such as laminated muds, HSC and channels. The channels in these areas may migrate laterally, forming a shallowing-upwards sequence. A small cluster of such channels is within the range of resolutions of the model used in this thesis, as an individual channel can be up to 3m in depth and 100m wide in modern tidal deposits in the Bahamas (Tucker and Wright, 1990).

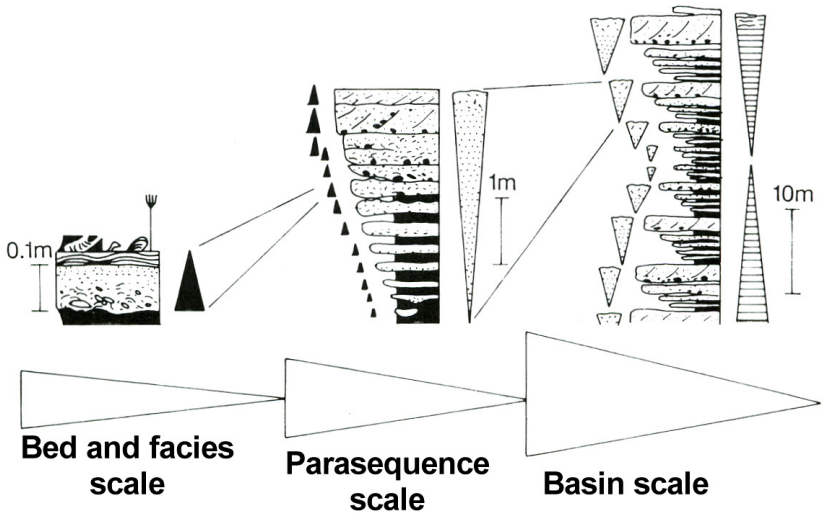

Figure 2.11. The range of scales that depositional processes affect from single beds (left) to whole sedimentary basins (right). After Tucker and Wright (1990).

2.4.2 Parasequence-Scale Geometries

Parasequence geometries are largely controlled by accommodation, which is the available volume for sediment deposition in marine environments. Accommodation is a function of relative sea-level changes, which is the sum effect of eustatic sea-level changes, tectonic changes and compaction of existing sediments.

This balance between accommodation and sediment supply can be described using three basic terms: aggradation, progradation and retrogradation. Progradation occurs when the sediment supply is greater than the accommodation. Each successive parasequence is deposited in deeper water, moving the system as a whole seaward. If the sediment supply and rate of increase in accommodation are approximately equal, then each parasequence is deposited directly on top of the preceding sequence resulting in aggradation. Retrogradation is caused when the sediment supply is less than the accommodation. The parasequences then move landward (Schlager, 1999). Localities such as the Capitan Reef, New Mexico, and the Canning Basin, Australia show classic progradation of the reef front through time (Tinker, 1998; Stephens and Sumner, 2003).

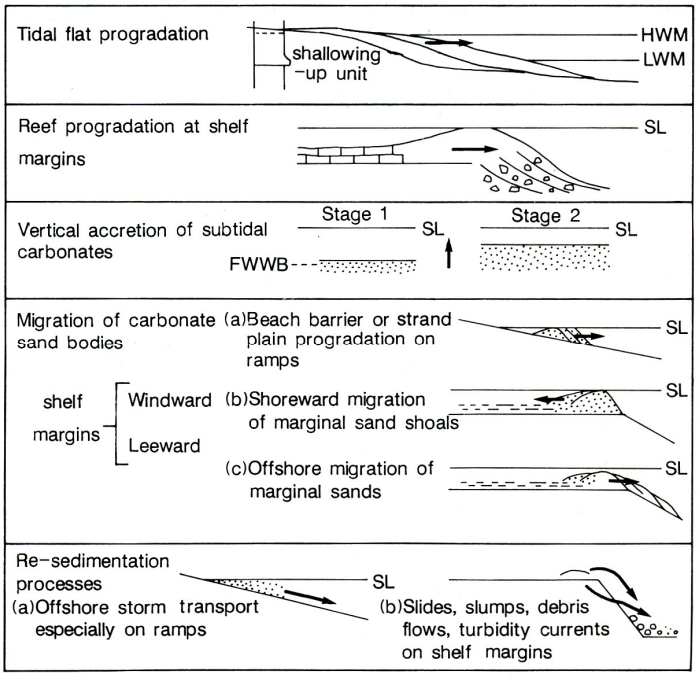

Figure 2.12. Processes of deposition that occur at the parasequence scale. From Tucker and Wright (1990).

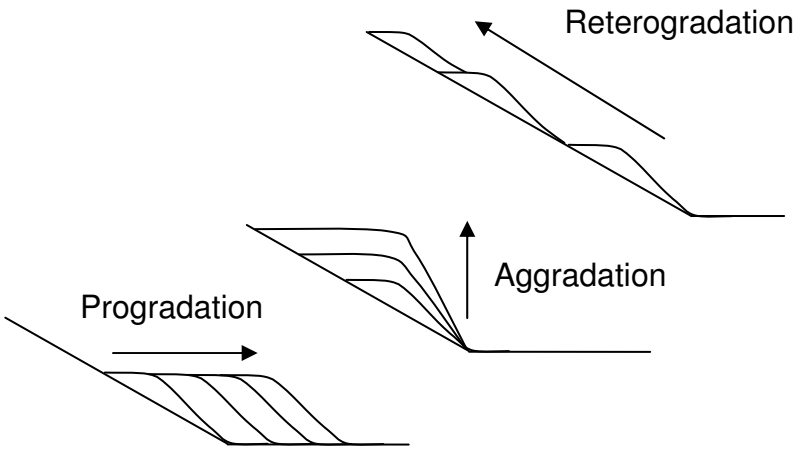

Figure 2.13. Geometries produced by progradation, aggradation and retrogradation. There is a continuum of all responses.

Through the processes of progradation of tidal flats, lateral migration of tidal islands and channel and vertical accretion of subtidal sediment, carbonate sequences typically show a shallow-upwards sequence: a regressive sequence. Repetitions of these metre-scale units are common in carbonate formations (e.g. Ginsburg, 1971; Goldhammer and Elmore, 1984; Goldhammer, 1988; Goldhammer *et al.*, 1990; Goldhammer *et al.*, 1993; Balog *et al.*, 1997; Dargenio *et al.*, 1997; Altiner *et al.*, 1999; Balog *et al.*, 1999; Diedrich and Wilkinson, 1999; Barnett *et al.*, 2002). In detail, however, the microfacies within one cycle vary both laterally and vertically. There are two main hypotheses as to how these cyclical carbonate deposits occur – each aligning with the dominance of one of internal or external processes. The first is periodic exposure and flooding of the areas by eustatic sea level changes and the associated changes in accommodation space which drive the formation of cycles. The opposing hypothesis is that proposed by Pratt and James (1986), which was based on that of Ginsburg (1971) of prograding tidal flat islands which starve areas of sediment and hence allow them to become flooded (Figure 2.14). The latter mechanism is supported by the lack of lateral continuity in such successions (Adams and Grotzinger, 1996) but is criticised due to the lack of explanation for non-uniform parasequence thickness, lack of subaerial exposure surfaces and purely subtidal sections.

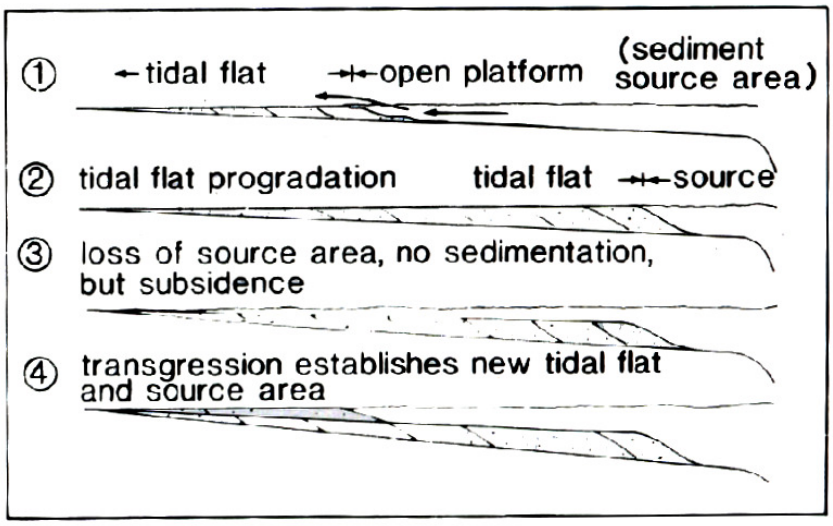

Figure 2.14. Model of peritidal cycle formation proposed by Pratt and James (1986).

Studies of the attributes of the carbonate cycles have shown some interesting results. The thicknesses of cycles from various localities were found to be indistinguishable from cycles produced from random using a statistical distribution: a Poisson process (Wilkinson *et al.*, 1997; Wilkinson *et al.*, 1998; Wilkinson *et al.*, 1999). Poisson processes are random events that are taken from an exponential distribution of possible outcomes. In the case of carbonate cycles this implies that each cycle thickness is random and not related to the preceding cycle. In addition there are exponentially more thin cycles than thick cycles. This would appear to support an autocyclic interpretation as external forcings, such as sea level changes, are not random and therefore would not manifest as random cycles. This is supported further by looking at the sequence of cycles and the repeatability of cycle thicknesses also show no difference from random sequences (Drummond and Wilkinson, 1996; Wilkinson *et al.*, 1998). The horizontal extent of lithologies also appears to obey a Poisson model (Wilkinson *et al.*, 1999) and facies in a modern system have a fractal distribution (Rankey, 2002). The formation of these cycles is covered in more detail in chapter 7.

2.4.3 Basin-Scale Geometries

Large-scale carbonate geometries are classified into a scheme useful for sequence stratigraphic work using morphology and the genesis of the platform (Tucker and Wright, 1990; Pomar, 2001; Bosence, 2005). They are broadly categorised into four

different platform geometries: rimmed shelf, ramp, epeiric platforms, and isolated platforms (Figure 2.15). Each type has a distinctive pattern of carbonate facies and is initially controlled by antecedent topography. However, this can be modified and changed during sedimentation depending on accommodation, as discussed above.

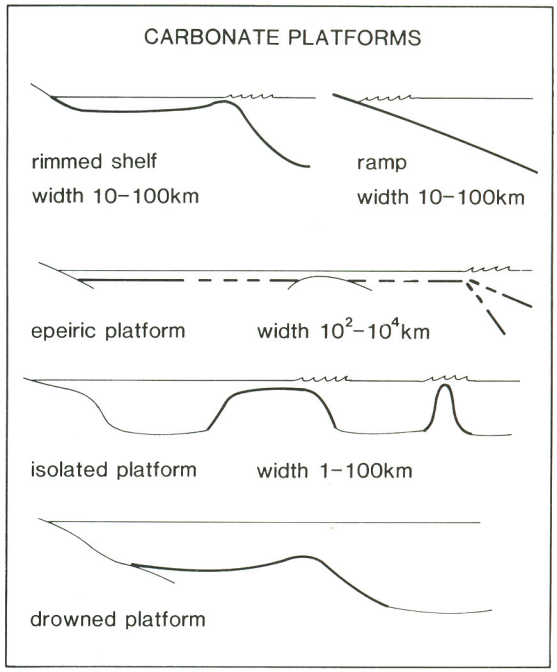

Figure 2.15. Five broad categories of carbonate platforms that can be recognised from sequence stratigraphy. After Tucker and Wright (1990).

Sequence stratigraphy is the nomenclature used to describe the grouping of the parasequences described above into sequences. These sequences are then divided into 'system tracts' each of which represents a particular section of a cyclical change in the balance between accommodation and sediment supply (Figure 2.16). The highstand system tract (HST) occurs during the initial sea-level rise which creates new accommodation up to the time the relative sea-level reaches the crest of the first cycle. This is separated from the falling stage system tract (FSST) by the Sequence Boundary. The FSST represent the fall from the highest relative sea-level to the lowest. The period after the lowest point in the curve is the lowstand system tract (LST) which continues until the sea-level rise reaches a maximum; the so-called Transgressive Surface. This ends at the maximum flooding surface, when the locus of sedimentation is at its most landward. Any sea-level rise at this point will result in new accommodation space being created and hence the start of a new HST.

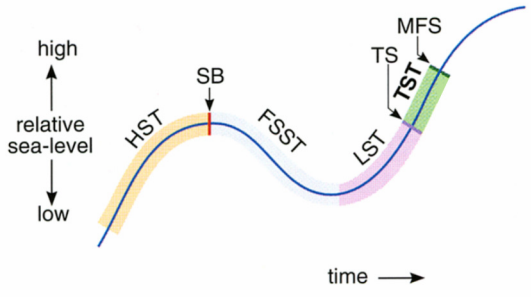

Figure 2.16. Sea level changes and the sequence stratigraphic terms used to describe parts of a single sea-level oscillation.

All the terminology above can be used in both siliciclastic dominated and carbonate dominated areas, as well as mixed siliciclastic-carbonate systems. However, the responses of a carbonate system to changes in sea-level are markedly different to the responses of a siliciclastic system.

The differences between siliciclastic and carbonate sedimentation are largely due to the production of carbonate in-situ. Although this does not change how carbonates can be described by sequence stratigraphy, it does mean that different geometries form. It is still therefore possible to pick out and describe the HST, LST and TST.

Carbonates prograde, aggrade and retrograde in response to sea level changes depending on the production rate (rather than sediment supply) and the change in accommodation (Schlager, 1992). A carbonate platform that produces more sediment than can be accommodated progrades or aggrades depending on the platform geometry, producing a HST. Similarly, a platform not producing enough sediment to fill the available space will retrograde, producing a TST. If sea-level has dropped to below the platform, allowing only a limited space for carbonate production and deposition, a LST is produced. All these geometries are broadly similar to siliciclastic systems. Carbonate can also produce other geometries. Reefs generally have a higher production rate than other carbonates. This can mean that the reef can keep-up with the rate of sea-level rise, while the non-reef sediments cannot. This gives rise to the "bucket-fill" morphology (Schlager, 1999). The final carbonate geometry that can be observed is that of the drowned platform. This occurs when the rate of sea-level rise

increases, eventually pushing the carbonate producing areas into a non-production zone, such as pushing a reef into the non-photic zone, halting all carbonate production.

In addition to the differences in geometries, carbonates also differ in other ways. They shed sediment at HST, not LST as with siliciclastic systems. This is for two reasons. Firstly, during a highstand, the available areas for carbonate production are increased. The increased sediment production means that more sediment is shed downslope. In contrast, during lowstand, there is little to no carbonate production. Furthermore, the exposed carbonates are subject to chemical erosion – karstification – instead of just physical erosion, dissolving the carbonate, resulting in fewer grains to transport. Finally, carbonates are subject to cementation in-situ and can form much steeper sediment build-ups than siliciclastic sediments (Schlager, 1992).

2.5 Discussion

It is clear that many of the processes that control carbonate production have been well studied. The effects of light, temperature and supersaturation on coral reefs are now broadly understood in terms of understanding and describing the effect quantitatively. Factors that are less well understood, such as tides, are understood to have an effect and the cause of this effect is known and can be described qualitatively, if not quantitatively. The effect of some factors, such as waves, can be described, but there is little understanding of the underlying cause and even less quantitative information.

However, the combined effects of parameters are less clear. Traditionally, authors dismissed supersaturation, claiming it is a proxy for temperature, but this recently changed as the effect of increasing carbon dioxide concentrations in the atmosphere became a topic of study (Gattuso *et al.*, 1999). This fuelled research into the effect this has on seawater chemistry, which in turn led to a greater understanding of seawater chemistry on reefs (Gattuso and Buddemeier, 2000; Leclercq *et al.*, 2000; Reynaud *et al.*, 2003; Feely *et al.*, 2004). How supersaturation and waves, for example, interact to produce carbonate geometries is something that has not been studied.

The processes that control deposition are much better understood, mainly because they also affect siliciclastic sediments. The physics underpinning sediment transport and erosion has been extensively studied. Although gaps do remain in our understanding and there is still active research into sediment transport and deposition, this area of sedimentation is well understood.

Like the depositional processes, the geometries that can be observed in carbonate sequences are again, generally well understood. There are still, however, some fundamental questions to answer in this area of carbonate research with respect to the interaction between these processes and those controlling precipitation and deposition. For example, the causes of metre-scale, upwards shallowing carbonate cycles that are common in ancient deposits remains something of an enigma. It is unclear whether it is largely controlled by large-scale processes, such as accommodation, or whether the interactions of production and depositional processes are the main cause.

There are, however, difficulties in untangling the effect of individual processes. It is impossible to do so using ancient deposits as they are an amalgamation of all the separate processes into a single record (Wright and Burgess, 2005). In addition, ancient deposits have also been subjected to diagenesis, further complicating the situation. In order to decipher the effects of individual factors and processes, one must use alternative methods, such as forward modelling. The next chapter describes how previous carbonate models have attempted to implement the processes and factors described here.

Chapter 3

Modelling of Carbonate Processes

A number of computer models have been developed in the past to both simulate and visualise carbonate stratigraphy. These employ a wide range of both methods and algorithms to represent and simulate the physical, chemical and biological processes that govern both carbonate production and deposition. This chapter describes how those processes pertinent to shallow marine carbonate deposition, as detailed in the previous chapter, have been implemented in computer forward models and discusses the limitations and advantages of modelling carbonate deposition in this manner.

3.1 Introduction

Forward modelling of carbonate stratigraphy has been carried out in earnest since the late eighties (Bice, 1988) in order to test hypotheses as to the processes that govern carbonate production and deposition and how these processes might interact (Watney *et al.*, 1999; Dalmasso *et al.*, 2001). There have been many models constructed since then, some adding additional processes onto existing frameworks (e.g. Bosence *et al.*, 1994; Hüssner *et al.*, 2001) while others employ innovative algorithms in order to understand phenomena key to understanding carbonate depositional processes. Such phenomena include "lag" (Tipper, 1997), the observed delay between the sea-level rising above a platform to the commencement of sedimentation, and the widespread cyclicity seen on ancient platforms (e.g. Read *et al.*, 1986; Koerschner and Read, 1989; Demicco, 1998; Burgess, 2001; Burgess *et al.*, 2001; Burgess and Wright, 2003; Burgess and Emery, 2004).

This chapter is a brief introduction to forward modelling and how the carbonate production and depositional processes detailed in the previous chapter can be implemented in a computer-based forward model. The chapter starts by describing forward modelling and some of the common numerical methods employed in

carbonate depositional forward models (henceforth referred to as 'carbonate models'), such as the representation of continuous data as series of discrete points. Section 3.3, which forms the bulk of this chapter, focuses on how the most significant carbonate production and depositional processes (section 2.2) have been implemented in previous models. The effect these processes have on carbonate deposition was detailed in the previous chapter. Section 3.4 considers the problems inherent to any forward modelling. Section 3.5 is a brief description of how to verify, validate and calibrate a forward model to ensure that the model is representative of the processes embodied within it, rather than numerical artefacts. The final section (3.6) discusses the implications presented in the chapter, including some weaknesses in current carbonate models that fail to properly represent the processes they seek to simulate.

3.2 Forward Modelling

Forward models form a subset of all the modelling techniques that a geologist may use (Figure 3.1).

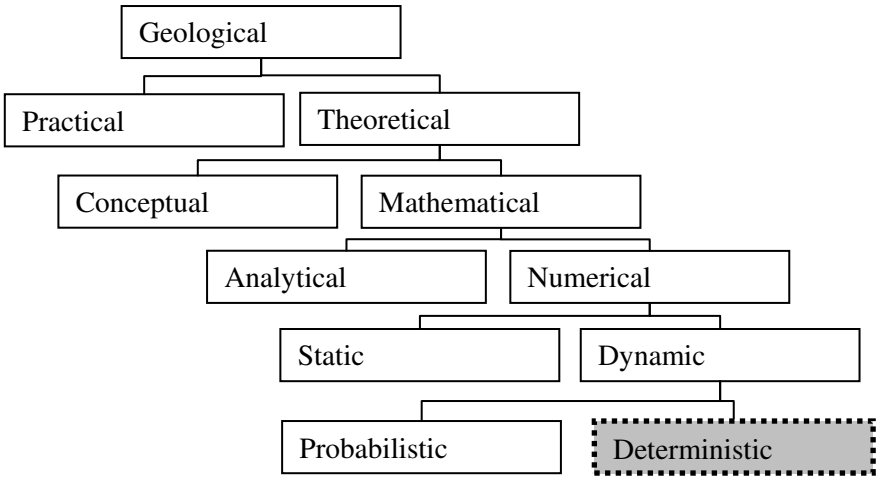

Figure 3.1. The range of modelling techniques used by geologists classified by their methodology. The models described in this thesis are deterministic forward models (after Tetzlaff (2004)).

Forward models offer the geologist a "virtual laboratory" in which to carry out experiments. Only numerical models can deal with both the scale of geological time and formations, both of which are impossible to simulate in a laboratory. One could create a 1/10,000 scale model of the Mississippi delta for instance, but one cannot scale grain size effects or the fluid viscosity and density (Tetzlaff and Harbaugh,

1989). Geological forward models are a mid-scale simulation. They are not on the scale of full earth models of climate or oceanic behaviour (e.g. Saunders *et al.*, 1999) and they do not model the movement of individual grains of sediment (e.g. Calantoni *et al.*, 2006). However, the processes included in a model need to incorporate the smaller scale effects as they influence basin scale processes. Various sedimentary structures, such as bars, channels, turbidites and deltas are ultimately determined by the processes acting on individual grains and the continental-scale forces that determine their location and evolution. As such basin scale modelling of geological processes is challenging to model deterministically (Tetzlaff, 2004).

3.2.1 Uses of Forward Models

Forward models have many uses, even within geology, from predicting fluid flow paths in a 3D hydrocarbon reservoir incorporating porosity, permeability, compaction and other confounding factors (e.g. Adams *et al.*, 2004), to simple 2D models (Bice, 1988).

The main use of forward models is to supplement the information gleaned from observations in the field or by instruments. Forwards models can be constrained at points where parameters are known and can then be used to predict stratigraphy between these points. They do this by incorporating mathematical knowledge about geological processes to produce realistic stratigraphy within the confines of the mathematics used and, as such, can determine if properties such as aquifer architecture, formation thickness, etc. are sedimentologically plausible. Furthermore they can also prevent the invention of scenarios which at first glance may appear plausible, but are not. An example could be where a delta deposits more sand than the river feeding it could possibly deposit in the given time; something even the most expert geological eye might miss (Tetzlaff, 2004).

A second use of forward models is to attempt to determine geologically important parameters that would not normally be possible to obtain, such as the sea level within a sedimentary basin at a given time. With a suitable model and data, it is possible to get a better estimate than the best educated guess. This type of approach has been used to derive sea-level curves for the Last Glacial period (Chappell, 2002). In other

words models can be used to quantify uncertainty in parameters. This is not limited to past parameters either. Currently, climate modelling is using a similar approach to determine all possible scenarios of the future climate based on past records (e.g. Allen *et al.*, 2000). By using the uncertainty of the past records, the amount of uncertainty in the future can also be determined. This is a more rigorous method than simply guessing what may happen in the future based on past records because there is some accountability in the model (if the physics embodied are documented and understood).

The third and final use, and the approach used in this thesis, is to use the model as a virtual laboratory – the "what if...?" test. Because models can contain all the important processes governing any system, they can be used to test the effect any process has in isolation from the others, something which is unachievable by other methods. Geologists see the strata as the sum effect of all physical, chemical and biological processes that have occurred pre-, syn- and post-deposition. Forward models allow us the extraction of the effect of a single process. This information can then be used when interpreting strata. Here, the emphasis is not on accuracy of prediction based on a few hard data points, but on what happens when a parameter is changed. For example, forward models have been used to demonstrate how a change in the transport rates of sediment affect cycle thickness in epi-continental carbonate successions (Burgess, 2001).

3.2.2 Model Formulation

Like other digital modelling techniques, forward models must discretise data, which is the process of representing a continuous function as a series of discrete points. They are dynamic numerical models that run forward in time, i.e. they start in the past or present and run into the future. Typically starting with a set of parameters, they increase time by a small amount (an iteration), before calculating the changes in any parameters that are being modelled. This continues until the desired time has passed. All the models described here are finite difference models, which means they calculate the parameters over a regular Cartesian grid, either in two- or three-dimensions, which is divided into a series of cells (Figure 3.2). A two-dimensional model will have one vertical dimension and one horizontal direction. Three-dimensional models have two horizontal dimensions in addition to a vertical

dimension. The horizontal size of the cell is usually input by the user while the vertical size depends on the thickness of sediment deposited in the output time step. The representation of data in these cells is the second discretisation that all forward models must employ.

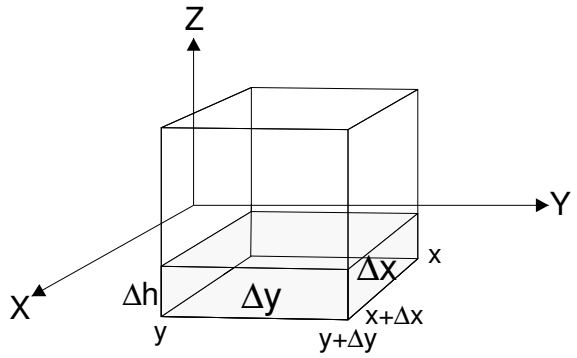

Figure 3.2: A typical cell as used in finite difference models.

Most carbonate models follow the same set of rules when simulating depositional processes. The user is requested to create a set of input data, normally a starting topography along with any pertinent geological and numerical parameters that are necessary for the simulation. Numerical parameters are values that control the numerical algorithms implemented in the model. Grid size, time step and any tolerance values are all typical numerical input parameters. It is essential that numerical parameters are within the range of stability for any particular model (see section 3.5). A geologist, however, is mainly interested in the effect of the geological parameters incorporated into the model. These parameters represent real physical, chemical or biological processes. For example, a material diffusion coefficient controls the rate at which material is shed downslope, and embodies a number of real sedimentary transport processes such as slumps, slides and creep (Kenyon and Turcotte, 1985). Both numerical and geological parameters are then used to step the model forward in time and at each timestep calculate the change in any measured parameter of interest. All basin-scale sedimentary models must calculate the change in accommodation space at each timestep. This is a function of any change in eustatic sea level along with any changes in topography due to both tectonic movement and sediment deposition (Figure 3.3).

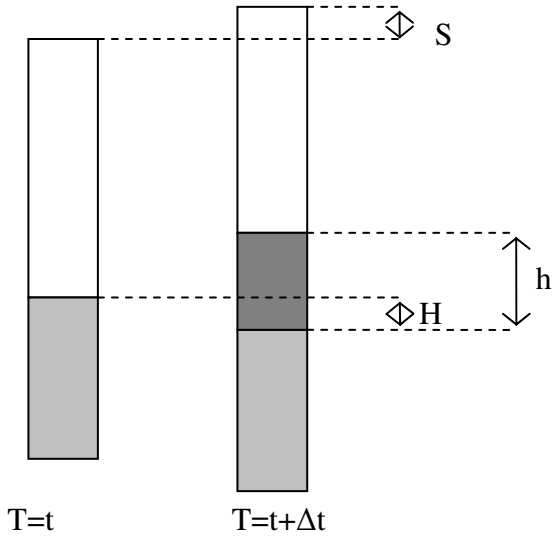

Figure 3.3: Accommodation space is generated by the subsidence of the basement (light grey, H), and changes in sea level (white, S).This results in deposition of some (h) sediment (dark grey). Here T is the time, starting at t with a Δt increment.

In calculating the change in topography, the model must not violate some basic principles, such as conservation of mass, which states that the volume of sediment (*V*) produced plus the volume of sediment input minus the volume output from the model must equal the volume deposited (Tetzlaff and Harbaugh, 1989):

$$V_{deposited} = V_{produced} + V_{input} - V_{output} \qquad (3.1)$$

It assumed in equation 3.1 that the volume of sediment is of constant density and porosity. Each process modelled has similar basic requirements, all of which can be used to verify the output of the model (see section 3.5).

Output is generated after a set number of timesteps for most models. This output can then be viewed using generic or bespoke visualisation tools. Generally output is in the form of a block model with layers represented by timelines. This represents a fundamental difference between a virtual outcrop produced by a model, and a real one found in the field: the modelled layers are produced a set time after the previous one, whereas in a field locality there is no such guarantee – indeed some layers may be diachronous.

Carbonate deposition is a two stage process. First, the carbonate is precipitated by both organic and inorganic processes. This sediment is then deposited by processes

that are similar to siliciclastic systems. Ideally, when modelling carbonate systems all processes should be included. However, to do so would take an immense amount of computational power. In order to make forward models useable, assumptions and simplifications must be made. No single carbonate model includes all of the processes highlighted in the rest of this chapter, although some do include many (e.g. Warrlich *et al.*, 2002; Burgess and Emery, 2004).

3.3 Modelling Techniques for Carbonate Sedimentation

This section reviews the processes that are pertinent for shallow marine carbonate production and deposition. The implementation of production processes is described first, such as depth-dependent production and production controlled by carbonate supersaturation. The physical processes that control the deposition of carbonates are then reviewed, including the effect of erosion, transport and re-deposition of sediment.

3.3.1 Depth-Dependent Production

Water depth is a primary control on carbonate production, as it is a key control on the amount of light reaching a carbonate-producing, photosynthetic organism, which is known to be a major control on the amount of carbonate produced in modern, shallow-water, tropical systems (Stoddart, 1969; Chalker, 1981; Bosscher and Schlager, 1992; Kleypas *et al.*, 1999b). As such, water depth is a proxy for light attenuation and photosynthetic carbonate production, and all carbonate models use a profile where production decreases with increasing depth. There are two ways of modelling the relationship between water depth and carbonate production rates, using either an empirically or a physically derived profile (Warrlich *et al.*, 2002). A physical profile is one based on increasing light attenuation with increasing water depth (Chalker, 1981; Bosscher and Schlager, 1992). Profiles based on measured production rates have a similar profile but may include other factors such as the influence of tides (Burgess *et al.*, 2001).

3.3.1.1 Physical Based Modelling of Depth-Dependent Production

The amount of light reaching the sea floor can be calculated using the Beer-Lambert Law,

$$I_z = I_0 e^{-kz} \tag{3.2}$$

where I_z is the light intensity ($\mu Em^{-2}s^{-1}$) at depth, z (m), I_0 is the light intensity at the surface and k is the extinction coefficient (Chalker, 1981). This is then combined with a photosynthetic rate equation to give the carbonate production due to light at the sea bed (Figure 3.4),

$$p = \tanh\left(\frac{I_0 e^{-kz}}{I_k}\right)$$
$$P = pP_M \tag{3.3}$$

where P is the growth rate, P_M is the maximum growth rate and I_k is the saturating light intensity (Chalker, 1981).

3.3.1.2 Empirical-Based Modelling of Depth-Dependent Production

All carbonate models, except for SIMSAFADIM (Bitzer and Salas, 2002), use a non-linear curve (Figure 3.4) to control carbonate production as a function of depth, which are based on empirical measurements of carbonate production rates measured at different depths, rather than on the physical derivation outlined above (Bosence and Waltham, 1990; Bosence *et al.*, 1994; Burgess, 2001; Burgess *et al.*, 2001; Warrlich *et al.*, 2002). By using empirically derived measurements, these models implicitly include the effect of other factors that control carbonate production, such as tides, wave action, etc, as these will be included in any measurements used to derive a depth-dependent production curve. This may be a disadvantage of such methods as it becomes difficult to differentiate or distinguish the effects of the amalgamated processes from each other. However, the advantage of using such curves is that the model can incorporate a range of processes that may be difficult to include in a geological forward model, such as tides. In addition, the model can also simulate different carbonate types, such as mud mounds, that have a different depth profile to that of corals (Bridges *et al.*, 1995) by altering the depth-dependent production profile accordingly.

An example of an empirically derived curve is the profile employed in Carbonate 3D (Warrlich *et al.*, 2002). This model constructs a depth-dependent profile using four depth points; the minimum depth of carbonate production, two depths between which

carbonate production is at maximum, and a minimum carbonate production depth. Between these four points is either a linear, constant or exponential relationship, which leads to a curve very similar to that of process based models (Figure 3.4).

A.

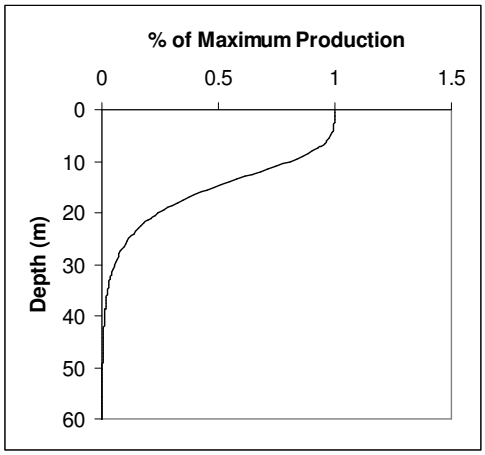

B.

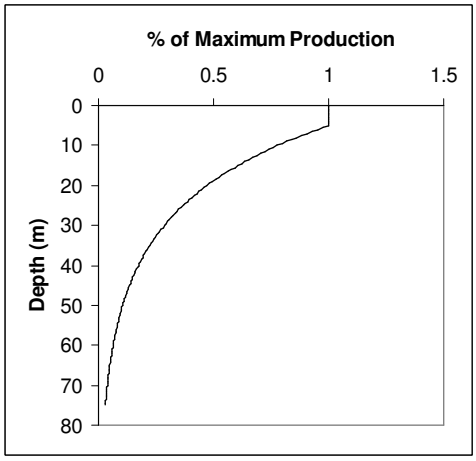

C.

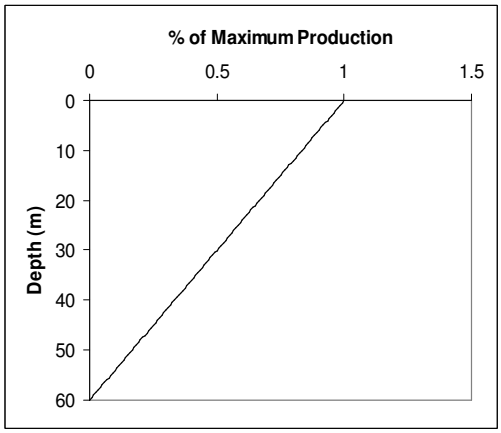

Figure 3.4: Production profiles for three carbonate models: A. Bosscher and Schlager (1992), B. Warrlich et al, (2002) and C. Bitzer and Salas (2002).

There is one current carbonate model, SIMSAFADIM, that does not use some form of exponential for the production of carbonate with increasing depth, instead using a linear profile (Bitzer and Salas, 2002). This model uses a predator-prey simulation to control the population of three carbonate producing species (Bitzer and Salas, 2001; Bitzer and Salas, 2002). Each species population is controlled by the population of the other two species and water depth. So, for example the birth rate, γ, of a species is a function of water depth:

$$\gamma_i(z) = \frac{\gamma_{i\max}(z_{\max} - z)}{z_{\max}} \qquad (3.4)$$

where z_{max} is the maximum depth of carbonate production and $\gamma_{i\max}$ is the maximum birth coefficient of the species in optimum conditions (Bitzer and Salas, 2002). Carbonate production is then controlled by the relative populations of the three species,

$$P = \sum_{i=1,3} c_i \left(\frac{\chi_i}{\gamma_i / \beta_i} \right) \tag{3.5}$$

These equations give a linear depth-dependent profile (Figure 3.4).

The authors give no reason for using this form, but the basic form of decreasing carbonate production with increasing depth is consistent with other carbonate models and real-world observations.

3.3.1.3 Summary

The majority of carbonate models use some sort of exponential decrease of carbonate production with water depth, with SIMSAFADIM being the only known exception. There are, however, variations on the two more standard curves presented above. Burgess and Emery (2004) modify the standard process-based curve (Bosscher and Schlager, 1992) slightly to account for the effects of tide on production (see section 2.2.7). Other variations are due to the way in which an empirical profile has been represented in the model, for example Demicco (1998) uses a series of points and interpolates linearly between them. The resulting profile is very similar to those shown in Figure 3.4. An advantage of using an empirically derived profile is that changes in the parameters can change the shape of the curve allowing the simulation of other carbonate production environments, such as mud mounds.

3.3.2 Supersaturation

As discussed in the previous section, all carbonate models have a function relating carbonate production to water depth, where the maximum carbonate deposition rates are found in the shallowest water. However, the restriction of fluid flow over a carbonate platform also affects carbonate production and deposition via supersaturation as discussed in chapter 2. Authors have attempted to model the relationship between carbonate production and supersaturation in one of two ways: a

lag between recommencement of sedimentation and a transgression, or by making carbonate production a function of distance from fully supersaturated water.

3.3.2.1 Lag Depth and Lag Time

As all models use an increase of carbonate production with decreasing depth, it becomes difficult to explain both how platforms drown and to reproduce shallowing-upwards cycles that are frequent in the geological record (Tipper, 1997). A common mechanism employed in early carbonate models was to use a lag between sea-level change and sedimentation (Ginsburg, 1971; Enos, 1991). The lag can be implemented as a lag depth (Read *et al.*, 1986), where carbonate sedimentation commences after a certain water depth has been reached after exposure, or as a lag time (Goldhammer *et al.*, 1987), where sedimentation commences after a prescribed time after a sea-level transgression. These two modelling parameters are meant to simulate the phenomenon of lag, for which the best current explanation is a reduction in water circulation (Bosence and Waltham, 1990; Enos, 1991).

Other explanations of the lag are biological in origin and are covered in detail in section 3.3.5. However, it is worth mentioning briefly that using a simple cellular automata model for a biological population also gives the necessary lag, without any lag depths or times (Tipper, 1997).

3.3.2.2 Distance from Platform Edge

The second method of simulating the effects of supersaturation is to make carbonate production a function of distance from the platform edge. There have been two approaches to this. The first is to explicitly make the production a function of the distance from some arbitrary point defined as the shelf edge (Bosence and Waltham, 1990). In this case the carbonate production rate is defined as (Bosence and Waltham, 1990):

$$P(x,z) = P(z) \cdot f(x) \qquad (3.6)$$

The form of $f(x)$ is then defined by (Bosence and Waltham, 1990):

$$\begin{aligned} f(x) &= 0 && x < 0 \\ &= (x/X)^n && 0 < x < X \\ &= 1 && x > X \end{aligned} \qquad (3.7)$$

Where x is the distance from the shoreline and X is the distance at which the platform margin exists (taken to be the final point at which the depth is 2m or less). The model described by Bosence and Waltham (1990) use a value of 3 for n (Figure 3.5)

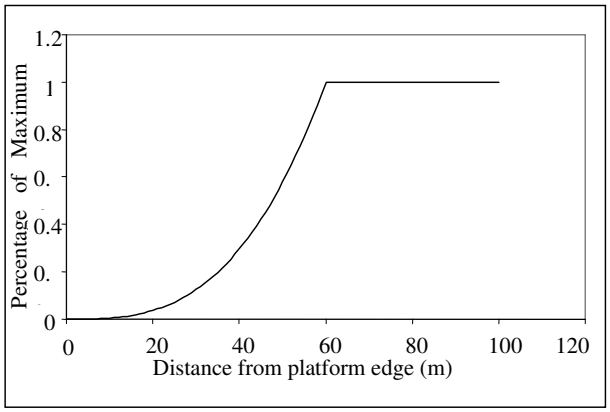

Figure 3.5: Production rates as a function of distance from shoreline. The production increases from the shoreline until the platform edge (60m) where it is then at maximum. Derived from Bosence and Waltham (1990).

The second method is to use the topography of the simulation to produce an estimation of the distance from open marine sources (Warrlich *et al.*, 2002), again, in addition to the other processes that govern carbonate production. This method attempts to include fluctuations in production due to variations in salinity, temperature and nutrient supply, which all affect biological carbonate production (Warrlich *et al.*, 2002). Carbonate 3D uses the concept of "stress", which reduces the maximum carbonate production rate by a "stress function". The calculation of the stress function to simulate the effect of supersaturation uses the smoothed topography (Figure 3.6), which is calculated using:

$$z_s(x, y) = z(x, y) * F(x, y) \qquad (3.8)$$

Here $*$ indicates convolution between the water-depth, z*(x,y)*, and a smoothing function *F(x,y)* to give the smoothed water depth, $z_s(x,y)$, where:

$$F(x, y) = \frac{3}{\pi \ell^2} \exp\left(1 - \frac{r}{\ell}\right), \text{ where } r \le \ell \qquad (3.9)$$

$r^2 = x^2 + y^2$ and ℓ is the horizontal length scale for the restriction. Increasing ℓ will smooth the topography to a greater extent.

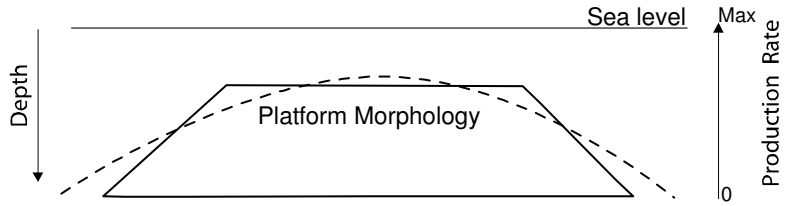

Figure 3.6: The platform morphology and smoothed depth curve (dashed).

The final production profile is then calculated using:

$$U = 1 - \exp\left(-\frac{z_s(x,y)}{\sigma_R}\right) \qquad (3.10)$$

where σ_R is a scaling constant. This gives a profile as shown in Figure 3.7 across a symmetrical platform, with suppressed production in the interior of a platform and maximum production on the margin edges (Warrlich *et al.*, 2002).

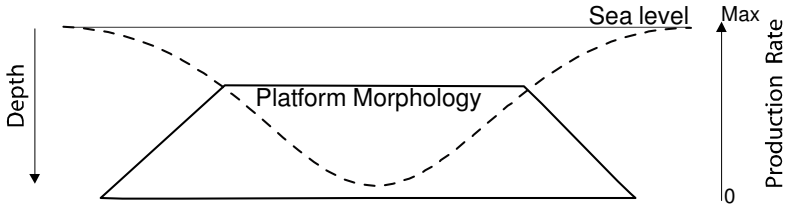

Figure 3.7: The stress function, U (dashed line), used to estimate the effect of water condition instability (and therefore restriction in water circulation) on carbonate production.

3.3.2.3 Summary

Carbonate production is heavily dependent on the supersaturation of water with respect to calcium carbonate (Demicco and Hardie, 2002). The two main methods used to simulate this process are a lag, or using a distance from fully supersaturated waters. However, neither method takes into account the true pattern of the water flow over a carbonate platform.

Data exists for the supersaturation of carbonate over a platform (Demicco and Hardie, 2002). These authors have shown that simple relationships between carbonate production and some physical parameterisation of supersaturation, e.g. distance from the margin edge, are not sufficient to replicate these data. Supersaturation is clearly a key component in understanding carbonate deposition, but as yet, cannot be

adequately modelled. Residence time, which could be used as a proxy to supersaturation (Demicco and Hardie, 2002) could provide a more accurate method of simulating the effects of supersaturation on carbonate stratigraphy. To implement a control in this manner is the next logical progression from the *a priori* numerical representation of this phenomenon, such as distance from the platform edge, as it takes into account flow patterns due to changes in topography. Oceanic flow has been shown to be non-trivial on the Great Barrier Reef (Kleypas and Burrage, 1994; Wolanski and Spangnol, 2000) and around atolls (Tartinville *et al.*, 1997; Tartinville and Rancher, 2000) meaning that neither implementation described above may be adequate to representing the full complications of supersaturation on carbonate production.

3.3.3 Wave Energy

Wave energy affects both the production rate of corals and affects the rate of erosion and transport of sediment. Wave energy therefore becomes a proxy for a number of things, such as siliciclastic sediment dispersal in high-energy areas, water chemistry changes around breaking waves (Archer, 1999; Kleypas *et al.*, 1999b) and as a maximum depth for sediment transport via advective processes. There are three carbonate models to date that explicitly use wave energy to affect the growth of reefs. Two of the models use an identical approach, but use different parameters. The third uses fuzzy logic to describe the relationship between wave energy and reef growth. Other models may incorporate wave energy implicitly.

3.3.3.1 Explicit Modelling of the Effect of Wave Energy

Two current carbonate models implement the effect of wave energy in a similar manner. First, CSM Carbsim (Duan *et al.*, 2000) reduces carbonate reef production in areas of low wave energy. The relationship between carbonate production and wave energy is linear in this case. Second, Dionisos (Granjeon and Joseph, 1999) uses the same methodology, i.e. reduce carbonate reef production in areas of low energy, but the form of the relationship is not described in current literature (Granjeon, 2003).

The third model that includes wave energy related carbonate production is Fuzzim (Norland, 1999), which is also the basis of the carbonate model used in Sedsim

(Griffiths, 2003 pers. comm.). Fuzzy logic allows the construction of models using qualitative descriptions, rather than using mathematical rules (Norland, 1999). Fuzzim uses wave energy to control both where coral reefs are deposited and whether the corals are branching or massive (Norland, 1999). In addition, wave energy is also used to differentiate the depositional locations of coarse (high energy) and fine (low energy) sediments.

3.3.3.2 Implicit Modelling of the Effect of Wave Energy

The effect of wave energy has also been included implicitly in some models. For example CARBPLAT (Bosscher and Southam, 1992) simulates the transport by waves. It does this by specifying a wave base. Any sediment that is deposited above this level is stored separately and is not deposited in-situ, instead it is deposited down the reef slope at the end of the time step using a function to control the geometry of the sediment moved (see section 3.3.6) (Bosscher and Southam, 1992).

Similarly, CYCLOPATH 2D (Demicco, 1998) does not remove sediment below a user defined wavebase. Above this level a certain proportion of sediment (set by the user) is moved landward (Demicco, 1998).

The transport of sediment due to wave action was also included in a semi-emprical, heuristic manner in the recent model of Burgess and Emery (2005). Here, the transport rate initially increases with increasing depth, to a maximum of 10m, then decreases with depth in order to simulate the exponential decrease of wave orbit with depth.

3.3.3.3 Summary

Waves are an important factor in carbonate production and subsequent erosion and deposition (Munk and Sargent, 1948; Lugo-Fernández *et al.*, 1994; Cruz-Piñón *et al.*, 2003). Most models that include transport (see section 3.3.6) acknowledge that some, if not all, of the transport simulated is due to wave action. From the few studies that have been carried out incorporating wave power or energy dissipated, it is clear that waves have an important effect on the geological carbonate record (Munk and Sargent, 1948; Lugo-Fernández *et al.*, 1994; Grigg, 1998; Kench, 1998; Lugo-

Fernández *et al.*, 1998a; Lugo-Fernández *et al.*, 1998b; Yamano *et al.*, 2003). They affect tides (see next section), have control over both coral extension rates and zonation patterns, and are a major factor in sediment erosion and transport. However, despite these facts, little work has been undertaken to correlate wave power or energy, and especially the effect of large waves during hurricanes, with coral extension rates (Lugo-Fernández *et al.*, 1994).

3.3.4 Tides

Given that tides happen on a daily scale, whereas geological models must simulate millions of years, tides are currently impossible to simulate explicitly (Burgess *et al.*, 2001). The effect of tides on carbonates is not well understood, although they have an effect on the water circulation on a platform and obviously cause diurnal changes in water depth. Because of this lack of understanding, tides are not included explicitly in any current carbonate model. However, there have been attempts to include their effect on carbonate processes. Burgess et al. (2001) reduce the production of carbonates in the top 1m of water, implying a 1m tidal range. This is due to reduced circulation and frequent (on a geological timescale) subaerial exposure (Burgess *et al.*, 2001; Yamano *et al.*, 2003). A similar approach has been used in a few other models (Read *et al.*, 1991; Bosence *et al.*, 1994).

3.3.5 Biological Communities

The biological interactions that affect carbonate production and deposition are obviously a complex and dynamic system in their own right and are intensively studied. There are three ways in which a model can incorporate biology: implicitly, assuming a spatially homogeneous distribution of biology, implicitly but assuming a heterogeneous distribution of biology, and by explicitly modelling biological communities and their interactions. Implicit biological activity is a basic assumption in any carbonate model as all carbonate models include depth-dependent production and hence include biological processes via photosynthetic processes. Including more than one carbonate type assumes more than one type of biological activity, i.e. reef organisms and non-reef organisms, are included in the model. This is more complex than a single sediment type, but can be implemented using the processes already discussed earlier in this section. Both the implicit methods amalgamate processes and

use the other techniques outlined in this chapter to represent the activity of biological organisms. This section reviews the two attempts that have been made at explicitly modelling biological activity.

There are two main algorithms for simulating the effects of biological activity: cellular automata (Tipper, 1997; Burgess and Emery, 2004) and predator-prey (Bitzer and Salas, 2002).

3.3.5.1 Cellular Automata

Cellular automata algorithms use the values of the four neighbouring two-dimensional, horizontal cells to determine the value in the centre cell (Figure 3.8), a so-called five-point stencil. Other sizes of stencils may also be used, but a five-point stencil is most common. The value is based on a set of defined rules, which can greatly alter the dynamics of the system and represents the colonisation of biological organisms. Tipper (1997) first used a cellular automaton algorithm to model the effect of colonisation in order to explain the lag phenomenon (see section 3.3.2.1). The cells had a simple "1" or "0" pattern to describe if they were "filled" or "empty". A cell was filled according to the number of filled nearest neighbours and a given probability representing a birth rate. Cells were emptied probabilistically, where the probability depended on the environmental parameters at the cell location. These environmental parameters included water depth, which acted as a common proxy for other variables (Tipper, 1997). Tipper (1997) concludes that colonisation results in a natural lag phenomenon, without explicit inclusion of such a process.

In contrast, Burgess and Emery (2004) used a fractional value in the cell to construct a production mosaic. This value (M_{xy}) was then used to control production rates at every location:

$$P_{xy} = M_{xy} \cdot P_{\max} \cdot P_z \cdot T \qquad (3.11)$$

Where P_{xy} is the production rate at location (x,y), P_{max} is the maximum production rate, P_z is the depth-dependent function of production and T is the transport rate. The production mosaic, M, is determined by seven rules (Table 3.1) which alter the value of M in the current cell.

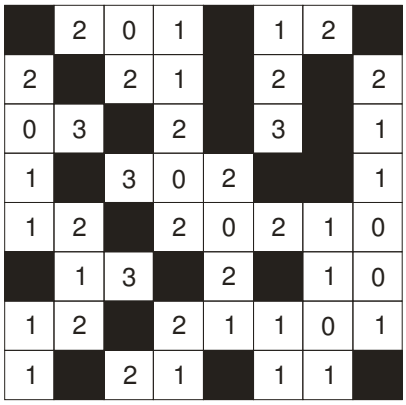

Figure 3.8: A simple example of a cellular automaton grid. The black squares are "filled". The "empty" squares contain a digit which is the number of neighbours that are filled. The empty squares may be filled in the next timestep depending on the number of neighbours they have that are already filled. Conversely, the filled squares may be emptied according to the number of neighbouring empty squares.

Table 3.1: The rules employed in the cellular automata to determine the mosaic production factor per model grid cell. From Burgess and Emery (2004)

Value of production mosaic element M	Number of occupied neighbours, n	Action Comment
M = 0	n < 2	None
M = 0	n = 2	M = 0.2. Optimal conditions, production commences
M = 0	n > 2	None
0 <M < 1	n < 2	M = M - 0.5. Underpopulated, production decreases
0 < M < 1	n = 2 or n = 3	M = M + 0.2. Population optimal, production increases
0 < M < 1	n > 3	M =M - 0.5. Overpopulated, population decreases
M = 1	n/a	M = 0. Population mature, production ceases

Burgess and Emery (2004) found that using such a production mosaic resulted in reasonable autocyclic production without any relative sea-level oscillations. Moreover, they found that a small change in initial conditions resulted in a large

change in final output, showing that true chaotic behaviour in carbonate systems may be explained by a simple biological process.

3.3.5.2 Predator-Prey

Predator-prey algorithms attempt to simulate the interactions between different competing or co-operating species (see for example, Berryman, 1992; Harrison, 1995; Bitzer and Salas, 2001; Xiao and Chen, 2002). Only one carbonate model, SIMSAFADIM, uses a predator-prey algorithm to simulate the activities of biological colonies (Bitzer and Salas, 2001). The model uses three carbonate-producing species, which can co-operate or be in competition with each other. The three species have similar equations to calculate their populations. For example, the change in population of species 1 (χ_1) is calculated using,

$$\frac{d\chi_1}{dt} = \gamma_1\chi_1 - \beta_1\chi_1^{\,2} - \phi_{12}\chi_1\chi_2 - \phi_{13}\chi_1\chi_3 - \omega_1\chi_1\psi - \xi_1\chi_1 \qquad (3.12)$$

where γ_1 is the birth rate of the species, $\beta_1\chi_1$ limits the maximum population size, ϕ_{12} and ϕ_{13} dictate the co-operation or competition between species 1 and 2 then 1 and 3 respectively, ω_1 determines the species response to carbonate mud and ξ_1 determines the species response to suspended carbonate in the water. The population is scaled to one, by setting $\gamma_{\max} = \beta_i$ (where i=1, 2 or 3). Carbonate production rate is calculated as the sum of the carbonate of all three species,

$$P = \sum_{i=1,3} c_i \left(\frac{\chi_i}{\gamma_i / \beta_i} \right) \qquad (3.13)$$

and the birth rate, γ, of a species is a function of water depth,

$$\gamma_i(z) = \frac{\gamma_{i\max}(z_{\max} - z)}{z_{\max}} \qquad (3.14)$$

where z_{max} is the maximum depth of carbonate production and $\gamma_{i\max}$ is the maximum birth coefficient of the species in optimum conditions (Bitzer and Salas, 2002). More details of this formulation are given in section 3.3.1.2.

3.3.5.3 Summary

Biology is included implicitly in every carbonate model that includes a depth-dependent function to simulate photosynthetic organisms. However, this misses a lot of the complex interactions that occur between competing and co-operating species. Efforts to include biological activity explicitly have resulted in two algorithms being used; cellular automata (Tipper, 1997; Burgess and Emery, 2004) and predator-prey (Bitzer and Salas, 2002). In addition to simulating the effects of biology on carbonate systems, cellular automata algorithms have also been used to assess the self-organisational properties of carbonate sedimentation (Drummond and Dugan, 1999) and to simulate transport of sediment (Claudia *et al.*, 2001). Predator-prey algorithms use a first-order differential equation to approximate the interplay between several biological species, which may represent whole communities, not just individual species. Both of these algorithms can be used to determine both carbonate production rates and the locations where deposition occurs.

Although biology is a key part of understanding carbonate deposition and production, much of the complexity is interwoven with the other processes described here. One aspect of biology that has not yet been implicitly included is bioerosion, which is of particular interest in Cenozoic reef systems (Bellwood, 1995b, a, 2003).

Although the inclusion of biological processes can clearly produce complex, perhaps even chaotic, behaviour in models it is not obvious firstly, how one should initialise such models, secondly how complex such models should be for a purpose (i.e. how many species should be simulated), nor thirdly whether the emergence of such complex behaviour *requires* the inclusion of biological processes. Later, the answer to the third question is shown to be negative.

3.3.6 Transport

The erosion, transport and re-deposition of sediment are important processes of all sedimentary system. The methods used here are therefore used in many other, non-carbonate, sedimentary forward models. For carbonates, transport is of particular importance when attempting to simulate shallowing-upwards carbonate cycles by autocyclic mechanisms (see chapter 7 and section 2.4) as this is the fundamental

mechanism of their formation as proposed by Ginsburg (1971). The transport of sediment attempts to simulate all the physical processes that move sediment, from saltation of individual grains to large scale landslides and slumps.

Carbonate models employ three mechanisms to redistribute deposited sediment: geometrical transport, which uses some function to determine the large-scale geometry that the eroded sediment forms when it is deposited; diffusive transport, which smoothes topography; and advective transport, which transports sediment as a Lagrangian particle in a flow field. Older models tend to use geometric or diffusive algorithms for transport whereas more recent models have utilised both diffusive and advective transport.

3.3.6.1 Geometrical Transport

Geometrical transport re-deposits sediment according to defined geometric functions. This method is usually found in older models as it is computationally inexpensive to calculate (in contrast to advective transport). Carbonate models that employ this method re-distribute the "surplus" sediment either downslope or landward (Bice, 1988; Bosence and Waltham, 1990; Bosscher and Southam, 1992; Demicco, 1998). For example, CYCLOPATH 2D (Demicco, 1998) takes a user defined proportion of sediment from each point along the platform. This accumulation of eroded sediment is then deposited in a wedge at the current shoreline. In this manner carbonate autocycles can be reproduced (Demicco, 1998). In a slightly different variation on the same mechanism CARBPLAT (Bosscher and Southam, 1992) produces sediment up to sea level. However any sediment produced above the wave base is stored separately for deposition downslope (Figure 3.9). A simple exponential function is then used on this sediment as it is re-deposited, to produce the shape of the slope below the wave base,

$$h(x) = h_0 e^{-fx} \qquad (3.15)$$

Here $h(x)$ is the height of the slope, x is the distance from the platform margin and f is the slope coefficient. This function is meant to simulate transport of materials onto the reef slope from the platform (Bosscher and Southam, 1992).

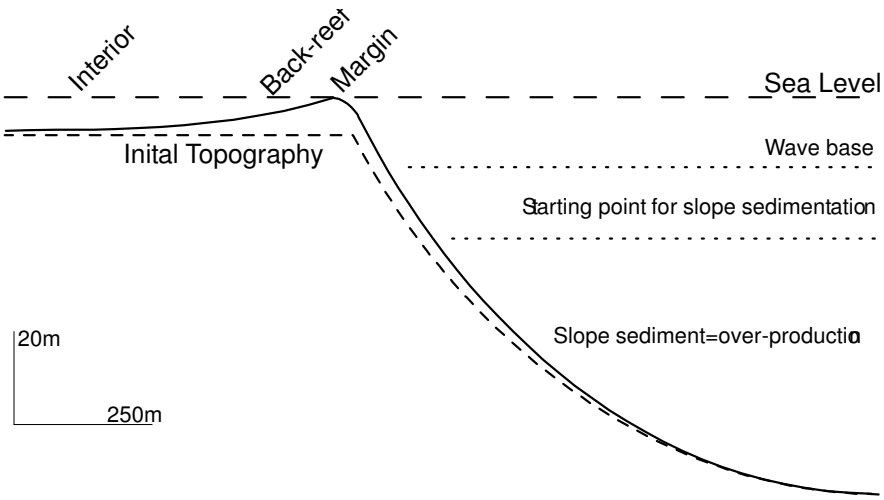

Figure 3.9: Defined depths and platform geometry used in CARBPLAT (Bosscher and Southam, 1992).

A model that uses a form of geometric transport that is unique from other models is Fuzzim (Norland, 1999), which was described in section 3.3.3.1. Fuzzim uses a total of sixteen simple rules to define transport of sediment. For example "If at surface then erode some". The terms "surface" and "some" are defined by appropriate probability functions. These rules control the amount of erosion and deposition, the slope, and grain size (Norland, 1999)

3.3.6.2 Diffusion

Diffusion is a process that smoothes any topographic highs by moving mass into topographic lows. A number of authors have used diffusion to model sediment transport and geomorphologic evolution (e.g. Kenyon and Turcotte, 1985; Flemings and Jordan, 1989; Martin, 2000). Sediment diffusion in the modelling context is the assumption that sediment moves downslope at a rate that is proportional to the tangent of the steepest gradient and to the physical characteristics of the sediment, jointly represented by a diffusion coefficient (Tetzlaff and Harbaugh, 1989). Typically, for a two dimensional model, the diffusion is controlled by:

$$\frac{\partial h}{\partial t} = D_x \frac{\partial^2 h}{\partial x^2} + D_y \frac{\partial^2 h}{\partial y^2} \qquad (3.16)$$

Where D_x and D_y are the diffusion coefficients in the x and y directions respectively, h is the topography and t is time. However, the two separate diffusion coefficients are usually the same, yielding (see for example Granjeon and Joseph, 1999):

$$\frac{\partial h}{\partial t} = D\left(\frac{\partial^2 h}{\partial x^2} + \frac{\partial^2 h}{\partial y^2}\right) \qquad (3.17)$$

In carbonate models diffusion has been applied in exactly the same manner as in other sedimentary models. Carbonate models that use this method are able to shed material down into the basin, simulating mass transport (Hüssner *et al.*, 2001).

Clearly the particular value of the diffusion coefficient used is of great importance and can have a large influence on resultant topography (Kenyon and Turcotte, 1985; Kaufman *et al.*, 1991). Typical values vary from $0.1m^2/yr$ (Bosence *et al.*, 1994) through $100m^2/yr$ (Burgess and Emery, 2004) and even as high as $5000m^2/yr$ (Kaufman *et al.*, 1991). Appropriate values for the diffusion coefficient can also vary with depth (Kaufman *et al.*, 1991; Granjeon and Joseph, 1999).

3.3.6.3 Advective Transport

Advective transport is transport of sediment by fluid flow, which could be caused by tidal currents, wave-induced currents or even ocean currents. Due to constraints in computing power it is impossible to perform a fully three dimensional flow calculation over the timescales required for a geological model (Tetzlaff and Priddy, 2001). Therefore, all sedimentary forward models make some simplifying assumptions when representing fluid flow. Within carbonate models there are many methods of simulating advective transport of sediment, however they all share common themes and techniques.

Burgess et al. (2001) use a relatively simple advective model. Transport rates are dependent on water depth, such that the transport rate increases linearly with depth up to a defined wavebase, before decreasing linearly with depth to a maximum depth (Figure 3.10). The direction of transport is always shoreward but can be affected by a random walk process which represents small changes in transport directions due to changes in wind direction (Burgess *et al.*, 2001). In later versions of the same model the random walk algorithm was replaced with another pseudo-random algorithm and the refraction of waves was also included (Burgess and Wright, 2003).

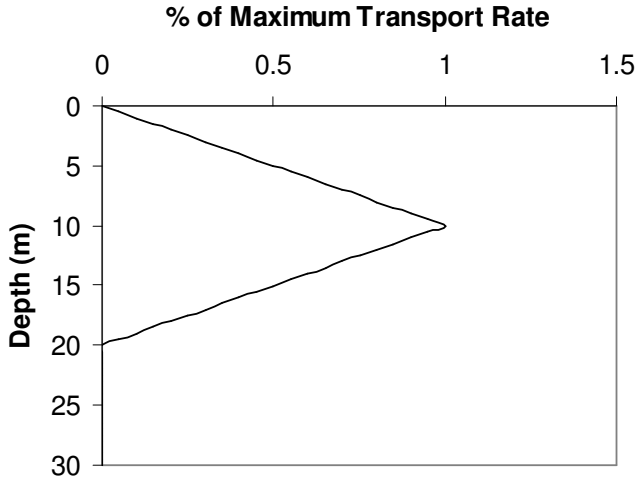

Figure 3.10: Erosion rate as a function of depth. After Burgess et al. (2001)

SIMSAFADIM also includes an advective transport component (Bitzer and Salas, 2002). The flow is a function of water depth and hydraulic potential:

$$\left(\frac{\partial}{\partial x}\right)\left(z\frac{\partial h}{\partial x}\right)+\left(\frac{\partial}{\partial y}\right)\left(z\frac{\partial h}{\partial y}\right)=0 \qquad (3.18)$$

Where z is the water depth and h is the hydraulic potential (elevation of surface multiplied by gravitation acceleration) (Bitzer and Salas, 2002). When solving an equation like this, the boundary conditions must also be specified. These are generally altered to match the area being simulated but can be a fixed flow rate or a fixed hydraulic potential (Figure 3.11A). The resultant flow field (Figure 3.11B) can then be used to erode, transport and deposit sediment.

Sediment is eroded when the flow velocity is greater than a threshold value (Figure 3.12), known as Shields Criterion. The actual value of the threshold depends on both the fluid velocity and sediment grain size. Deposition occurs when the flow falls below Shields Criterion. SIMSAFADIM employs a very similar mechanism to this, but there is no distinction of grainsize (Bitzer and Salas, 2002), unlike other models which do include the effect of grain size with Shields Criterion (e.g. Warrlich *et al.*, 2002).

3.3.6.4 Summary

Erosion, transport and re-deposition of sediment are common to all sedimentary models. Most carbonate models include some form of sediment transport and those that do so employ one or more of the three methods described above. In common with siliciclastic sedimentary systems, the erosion, transport and deposition of sediment plays a vital role in shaping the final stratigraphy

Transport of sediment is a well understood and studied process. The only limitation is the computing power needed to fully simulate a flow, and therefore, the movement of sediment (Tetzlaff and Priddy, 2001).

In modelling the erosion, transport and re-deposition of sediment no model as yet includes specific implementations for modelling different carbonate facies. As described in the previous chapter, carbonate sediment does behave differently from its siliciclastic counterpart. Grains often have a lower density than an equivalent sized quartz grain because of cavities and hollows formed due to the biological origin of such grains. This effect can be incorporated into transport rates or by adjusting the size of a grain to simulate a different density. However, it is coral reef sediments that require special consideration. Coral reefs do not produce large amounts of sediment that can be transported advectively as the corals themselves can be too large to transport and the binding of sediment by algae and microbes can increase the grain size of the sediment (Rasser and Riegl, 2002). However, they are subject to transport downslope, forming the reef talus slope, which contains grain sizes varying from pebbles to boulders (Hughes, 1999). As such, the transport of sediment in reefal areas must incorporate diffusive transport (simulating landslides and rockfalls downslope) but advective transport must be restricted to simulate the large “grains” of sediment and the binding of any loose sediment.

A)

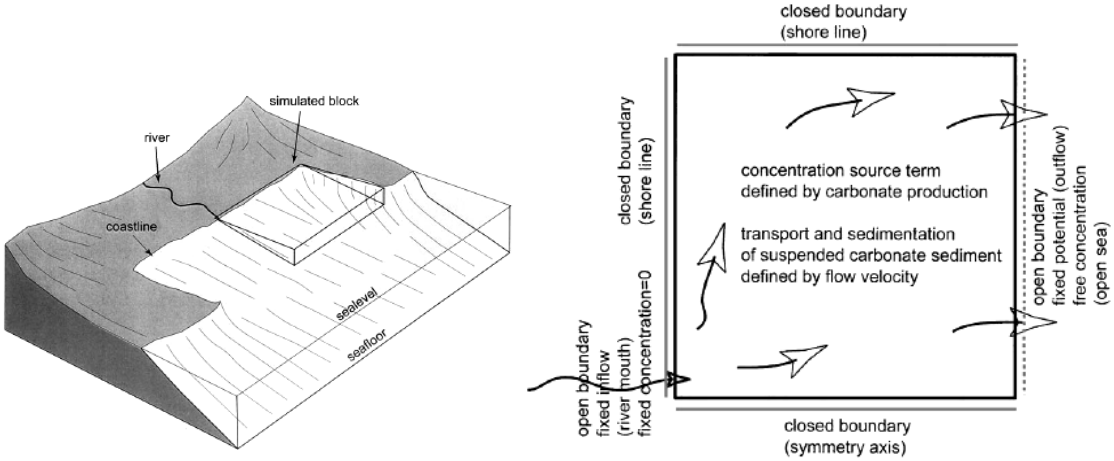

B)

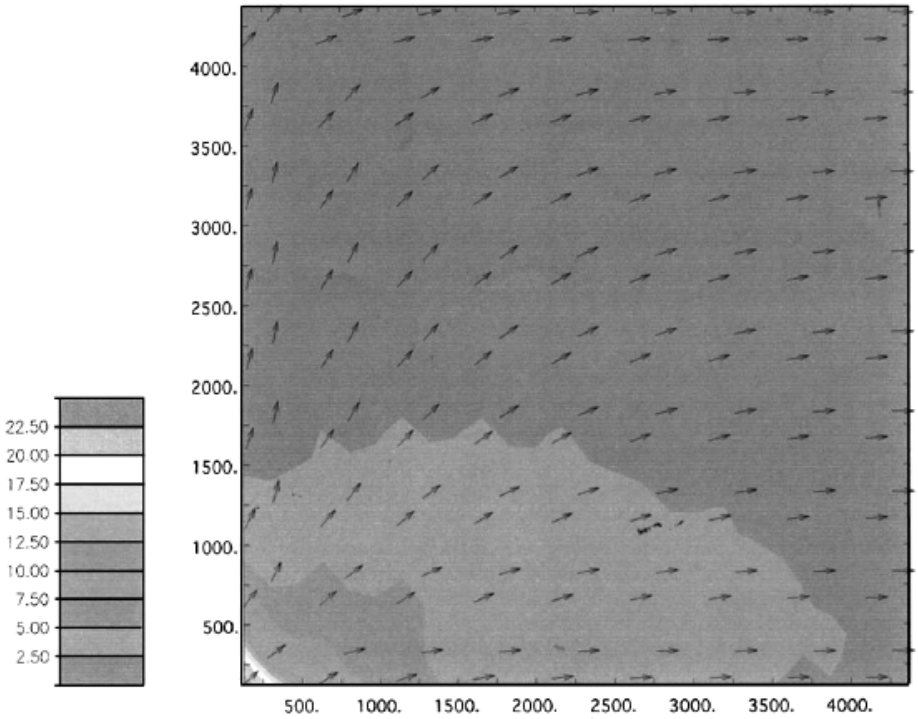

Figure 3.11: Result of the fluid flow algorithm in SIMSAFADIM. A) shows the topography of the study area, along with the boundary conditions used. B) shows the resulting flow field in m/day. Note the input source which simulates a river in the bottom –left corner. After Bitzer and Salas (2002)

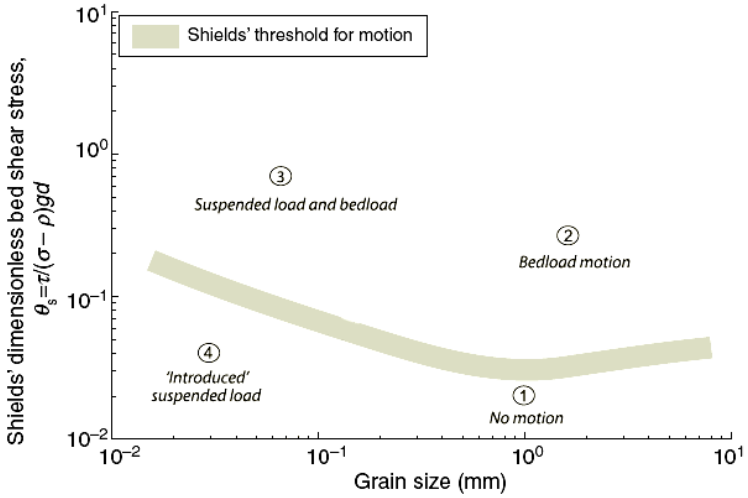

Figure 3.12: Shields Threshold for sediment movement and transport. Modified from Leeder et al., (2005).

3.4 Problems Inherent to Forward Modelling

There are several problems that are inherent to forward modelling, which have to be taken into account when interpreting any results (Watney *et al.*, 1999). The problems relevant to carbonate modelling will be discussed in this section.

The first issue is the boundary conditions: a model must have some kind of boundary applied to the edges of the simulated area. This weakness also exists in physical experimental models, such as when using flume tanks which must have solid sides. Therefore some conditions must be applied at the boundaries of the simulation. Boundary conditions range from closed, and act like a solid wall, to open, where the edge acts as an open edge (Harbaugh and Bonham-Carter, 1970).

Secondly, the representation of continuous data on a digital computer can result in several errors. Rounding errors are a result of a computer not being able to represent floating point numbers precisely. This can be alleviated somewhat by using double precision storage where necessary (Press *et al.*, 1992). Discretisation errors result from representing continuous data as a set of discrete points. Truncation errors result from an iterative numerical algorithm being terminated before the approximate solution being calculated is identical to the exact, analytical solution (Press *et al.*,

1992). These errors can result in instability as they can occur early in the calculation, swamping the true answer (Press *et al.*, 1992).

The third issue is the value of parameters needed for the model. For geological models these parameters are sometimes not well known and have large uncertainties associated with them (Watney *et al.*, 1999). Unlike engineering models for example, which have very accurate measurements of pertinent parameters, it is extremely difficult to obtain accurate data for a geological model (Tetzlaff and Harbaugh, 1989). In addition there is a plethora of used input parameters; over 200 were used in geological models in a survey carried out in 1999 (Watney *et al.*, 1999) and this is certain to have increased since. Data sources for geological models includes modern analogues, empirical observations and even output from other models (Watney *et al.*, 1999). Of course, any computer model is only as good as its input data. This imposes a fundamental limit on how much information can be gleaned from model output.

3.5 Model evaluation

Once a model has been created there are several ways to evaluate it (Watney *et al.*, 1999). Carbonate systems are complex, natural systems with many non-linear interactions (e.g. Burgess and Emery, 2004), which means that models cannot be verified completely for several reasons: including (1) unknown input parameters, (2) non-linearity, (3) errors in assumptions, inferences and input parameters may cancel out each other, masking potential flaws, (4) small errors in input can lead to large changes in output (see Burgess (2004)) and (5) non-uniqueness of the output (Watney *et al.*, 1999). To evaluate a model, it is usually compared to real-world data and observations, but the fact that the model may simulate a real-world area well does not necessarily follow from a correct simulation of these data (Watney *et al.*, 1999). Therefore other comparisons can be made, such as to other models and testing the inner workings of a model separately (Watney *et al.*, 1999). This evaluation is done using validation, verification and calibration. A valid model contains no internal flaws and is internally consistent. This could involve, for example, checking that the output is identical for a range of numerical parameters, for instance the time step. Verifying a model means comparing the model to analytical solutions or real-world data. Finally,

calibration of a model involves manipulating a limited number of unknown parameters to match measured data (Watney *et al.*, 1999).

Most carbonate model authors publish a short validation example when first describing the model. Burgess et al. (2001) demonstrate the validity of their model by running the model with various timesteps and grid resolutions. The number of cycles generated over a fixed time frame and using the same geological parameters was then used a measure of validity. Warrlich et al (2002) took a different approach. The sequence stratigraphy produced by the model was compared qualitatively to conceptual models of atoll formation. Bosscher and Schlager (1992) used a similar technique, comparing model output to stratigraphic sequences of coral formation. Although these tests are by no means comprehensive, they show that the conclusions reached by using current carbonate models are valid, at least within the limitations of the model. The model described in this thesis has been checked for internal consistency, calibrated against real-world data and validated using differences in output between runs that used different timesteps.

The next chapter gives details on the carbonate model developed for this thesis, including the algorithm employed to simulate the effect of supersaturation via residence time on carbonate production. The model is also verified against real data.

Chapter 4

Model description and validation

The carbonate processes described in Chapter 2 and the modelling techniques described in the previous chapter describe the state of the art for deterministic modelling of carbonate sediments. Carbonate GPM advances current models by including the pertinent processes that are also included in other models but adds residence time; a method of modelling the thermodynamic equilibrium dynamics of a carbonate platform. Residence time can be thought of as a proxy to carbonate supersaturation. This chapter describes the processes embodied in Carbonate GPM's algorithms and shows that the output of Carbonate GPM is valid and behaves as expected for test cases. First, the algorithms in Carbonate GPM in conjunction of the carbonate processes they are intended to digitally replicate. As the residence time algorithm is vital to Carbonate GPM's uniqueness, this is covered in detail. The residence time algorithm relies heavily on valid output from the flow algorithm in GPM. I show that the flow algorithm does indeed produce valid flow patterns by testing against real-world data. I finally establish the numerical time step that is stable for the carbonate runs used in the rest of the thesis.

4.1 Introduction

Interactions between the controls on carbonate systems presents a particular challenge to modellers because of both the large range of processes that might interact, and the range of temporal and spatial scales that may be important to such processes. Carbonates are notoriously complex sedimentary systems, often displaying spatially variable facies distributions (Rankey, 2002, 2004) and incomplete successions with abundant hiatuses (Algeo and Wilkinson, 1988; Burgess and Wright, 2003). Not only are carbonate geometries governed by the external forcing mechanisms universal to all sedimentary systems, such as sea-level oscillations, subsidence rates, and local climatic conditions, but carbonate production itself is further controlled by the

interplay of biological, ecological, and physicochemical processes that operate over multiple time scales. As a result, a consensus is now emerging that carbonate systems may be capable of creating apparent complexity that is an emergent property of the processes unique to carbonate production but is independent of any external forcing mechanisms (e.g. Drummond and Wilkinson, 1993a; Wilkinson *et al.*, 1997; Drummond and Dugan, 1999; Wilkinson *et al.*, 1999; Burgess *et al.*, 2001; Burgess and Wright, 2003; Burgess and Emery, 2004). Forward models allow an exploration of the interaction between various subsets of controlling parameters, without complications arising from other confounding factors (Dalmasso *et al.*, 2001). In addition, models can predict the consequences of modelled process and assumptions over geological timescales, which cannot be tested experimentally.

The earliest carbonate numerical models simulated reef growth and non-reef sediment production assuming an exponential decrease of carbonate production with increasing water depth as a proxy for light attenuation (Bosence and Waltham, 1990). These models were later refined to include other sedimentary processes such as sediment transport (Bosscher and Southam, 1992), biological activity and ecological processes (Bitzer and Salas, 2002; Wright and Burgess, 2005), multiple carbonate types (Burgess *et al.*, 2001) and siliciclastic input (Norland, 1999; Griffiths *et al.*, 2001; Warrlich *et al.*, 2002). Other processes incorporated into carbonate models include wave energy (Duan *et al.*, 2000) and carbonate diagenesis (Whitaker *et al.*, 1997). Other controls known to be important in reef growth such as salinity, water temperature, nutrient availability and bioerosion (Graus and Macintyre, 1989; Kleypas *et al.*, 1999b; Kleypas *et al.*, 2001), have not been explicitly modelled in a local or regional forward model to date.

Given the multitude of processes that have been considered in carbonate forward models, it is surprising that one of the most important has not yet been included explicitly. Supersaturation with respect to aragonite and calcite has long been known to be a significant control on the local rate of carbonate precipitation in modern platform systems (e.g. Broecker and Takahashi, 1966; Morse *et al.*, 1984). More recently, supersaturation has proved to be an important factor also in controlling the calcification rates of corals (Gattuso *et al.*, 1998b), the current species diversity of

corals (Ware *et al.*, 1996), and in estimating ancient, current, and predicted rates of global carbonate production (Kleypas *et al.*, 1999b; Gattuso and Buddemeier, 2000; Demicco and Hardie, 2002).

Here a new, deterministic three-dimensional carbonate forward model, Carbonate GPM (Geologic Process Modeler) is presented, which simulates reef growth, reef transport and lagoon development using light penetration, wave energy and predicted carbonate supersaturation as the major controls on carbonate production. The program is designed to be applied within a variety of environments, from fringing and barrier reefs to carbonate ramps and atolls. Carbonate GPM interacts with an existing siliciclastic model, GPM (Tetzlaff and Priddy, 2001), and so inherits the processes of erosion, deposition, wave action, compaction, fault activity, fluctuating sea level, siliciclastic sediment sources and flow regimes from that model. The flow can be set as either steady, i.e. a constant rate through all time, or unsteady, where episodic flow pulses, such as turbidites, occur.

This chapter begins by describing the carbonate production processes embodied in Carbonate GPM and giving details of the algorithms implemented. The transport mechanisms used are then described, including the computation of lagoonal water flow patterns that are required to calculate supersaturation. Particular attention is paid to the residence time algorithm and the methodology behind discovering where to start counting the residence time is described in detail. Finally, a simple timestep analysis is carried out to discover the largest, stable timestep for model scenarios carried out in this thesis.

4.2 General Model Forumulation

The algorithms in Carbonate GPM are designed to simulate the average effect of physical and chemical processes that are involved in generating carbonate stratigraphies. The processes are based on those found in modern reefs and lagoons, but may be applicable to ancient settings by changing parameters, such as maximum carbonate production rates, to match estimations of such parameters in ancient environments.

The model begins with a given topography, then takes time steps from a few years to tens of years, during each of which sediment is produced, eroded, transported and deposited (Figure 4.1). Thus stratigraphies can be created over geological timescales. The spatial scale of the model ranges from a tens of metres to tens of kilometres, and, as such, Carbonate GPM can be used to model a small reef (e.g. an individual reef in the Bahamas) to semi-basin sized reefs, for example, the Belize Barrier Reef.

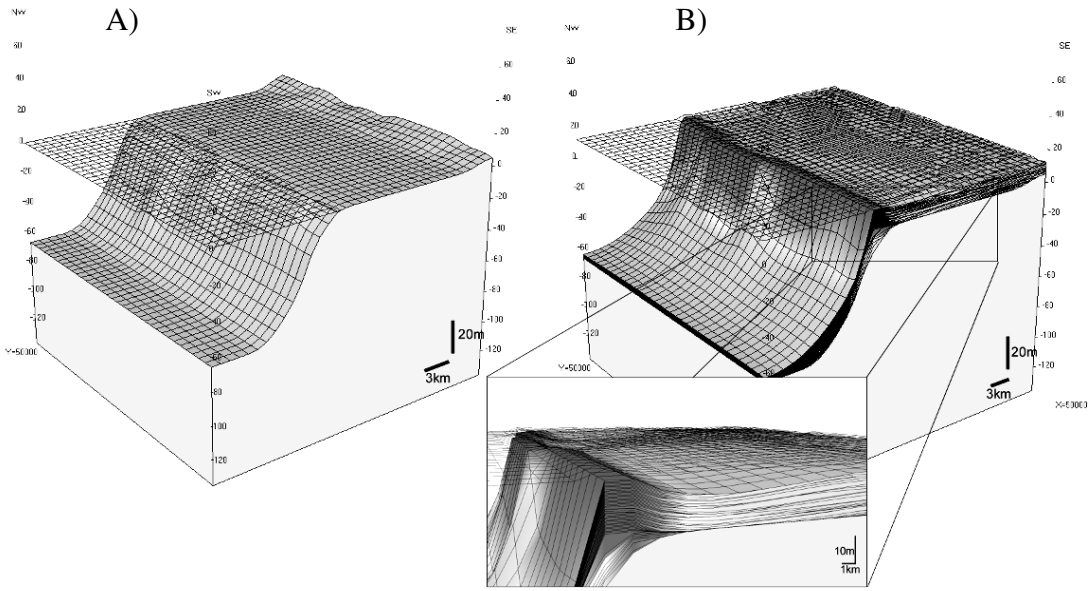

Figure 4.1. A. Example of an initial topography. B. Simulation after 50 display steps (125kyr). The topography has altered due to sediment deposition and a timeline (black lines – see close-up) has been drawn every 2500 years. The shading of sediment indicates the grainsize.

4.2.1 Time Discretisation

GPM contains a number of time discretisation levels (Figure 4.2). A simulation has a start and end time, within which there are several "display steps", as described above. Each display step is further discretised into many time steps. Within each of these discrete time steps, which are user-defined and can vary from fractions of a year to tens of years (which we term the "model timestep") a number of processes are modelled. Firstly, the flow of any water is calculated and assumed to be the same flow for the duration of this timestep. Using the resulting velocity vectors, the residence time (see section 4.3.2) is calculated and again, is assumed to be constant for the duration of this timestep. Finally, any sediment is produced before finally undergoing erosion, transport and re-deposition, based on the flow vectors calculated earlier.

Sediment production, erosion, transport and re-deposition is calculated on the basis of a year as a deposition rate, which is then multiplied by the model timestep gives the amount of sediment deposited at each location over the whole model timestep. Both the flow and residence time algorithms use a separate, smaller time step than the model timestep, which are described in detail in the relevant sections below. Clearly, the assumption of a fixed flow regime and residence time for the duration of the current model timestep assumes that the model timestep is small enough for this assumption to be valid. However, the model timestep should be large enough to finish any model run within a reasonable time.

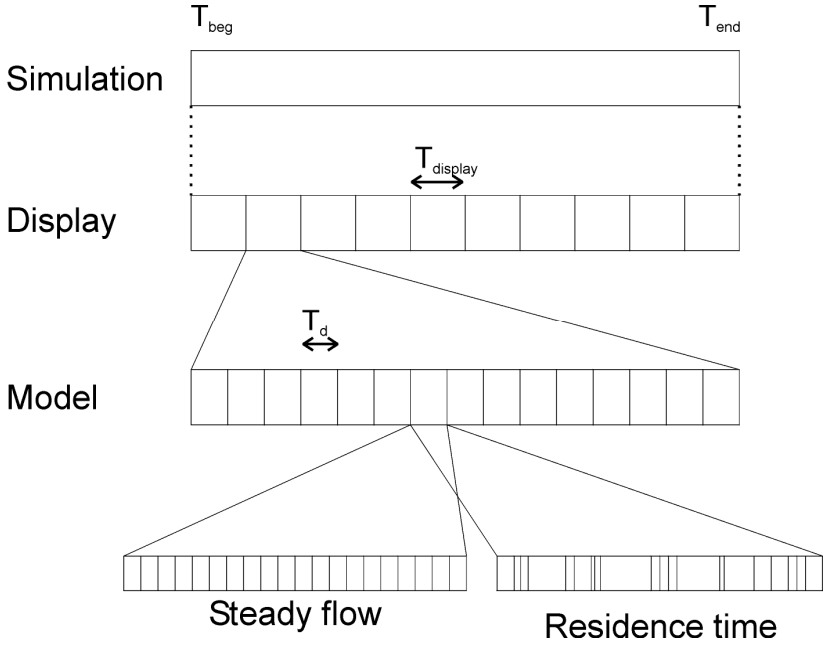

Figure 4.2. The time discretisation scheme used in Carbonate GPM. The simulation starts at T_{beg} and finishes at T_{end} (top). Within that there are several display times (second line) at which output is written to file and a timeline is drawn ($T_{display}$). Within that (third line) there are several model timesteps (T_d). For each model timestep a steady flow is calculated using another time step after which residence time is calculated using a variable time step to minimise errors (bottom). The flow field and residence time are assumed to be constant over that time step.

4.3 Carbonate Production

Marine carbonate production occurs in each time step in Carbonate GPM, and is divided into two sediment types: coral reef and non-reef (which consists of back-reef and lagoonal). Carbonate production is controlled by the user setting a maximum growth rate for the whole reef and another rate for non-reef sediment. In setting these

values, the user can take into account the various carbonate producing species occurring in the area being simulated. At each point in space and in each time step, the actual production rate of each sediment type is a fraction of the maximum rate. The fraction used depends on the particular environmental conditions acting at that point in space and time. This is a similar strategy to other carbonate models (e.g. Hüssner *et al.*, 2001; Bitzer and Salas, 2002; Warrlich *et al.*, 2002).

Modern coral reef production rates are influenced by light energy (Chalker, 1981; Bosscher and Schlager, 1992), wave energy (Roberts, 1974; Chappell, 1980; Kleypas, 1997), water temperature (Kleypas, 1997; Kleypas *et al.*, 1999b), nutrient availability (Kleypas, 1997; Kleypas *et al.*, 1999b) and aragonite supersaturation (Kleypas *et al.*, 1999b). Of these, light energy, wave energy and supersaturation relative to ocean marine waters control reef production explicitly in Carbonate GPM. In setting the maximum growth rates, it is assumed implicitly that the user has accounted for sufficient minimum sea water temperature for coral reef growth (18ºC), minimum required supersaturation with respect to aragonite (3.1 Ω-arag) and maximum nutrient levels (3.0 μmol litre^{-1} NO_3; 2.0 μmol litre^{-1} PO_4) (Kleypas et al. 1999).

Non-reef sediments include all carbonate sediment types excluding reef-building corals. While many of the sediment types included in this category have different responses to environmental conditions to that of reef-building corals, the major controls are water depth and carbonate supersaturation (Demicco and Hardie, 2002).

In both coral reef and non-reef sediments production is calculated at each time using:

$$P(\underline{x},c) = S\left[L(\underline{x}),\Omega(\underline{x}),W(\underline{x}),c\right]P_m(c) \qquad (4.1)$$

Here S is the fraction (between 0 and 1) that defines the efficiency of the production relative to the maximum production rate, P_m (m/yr), $\underline{x}$ is a vector of orthogonal horizontal coordinates (x,y), c is the carbonate type (reef or non-reef), and P is the production rate (m/yr) at each location. We call S the stress function, and details on how this is calculated for each carbonate type are given below. Controlling factors on which the stress function depends are light availability (L), supersaturation (Ω) and wave energy (W), with individual stress functions, S_L, S_Ω and S_W respectively defined below. S[L,Ω,W] is then given by $S = S_L \cdot S_\Omega \cdot S_W$.

4.3.1 Light Availability

Light availability is probably the major control on coral growth (Chalker, 1981; Kleypas, 1997). Increasing water depth decreases the available amount of light exponentially due to absorption. Modern corals in particular grow in a very narrow range of water depths, from the surface to around 50-80 m depth depending on the species and turbidity (Graus and Macintyre, 1989). Water depth can be coupled to the growth rate at any given light level to give a relationship of growth rate with increasing water depth:

$$S_L = \frac{\tanh\left(I_o e^{-kz} / I_k\right)}{\tanh\left(I_0 / I_k\right)} \tag{4.2}$$

(Chalker, 1981; Bosscher and Schlager, 1992). Here S_L is the stress function due to water depth, I_k is the saturating light intensity ($\mu Em^{-2}s^{-1}$) which is the minimum required for growth, I_0 is the light intensity at the surface, z is depth (m), and k is the extinction coefficient (m^{-1}). The denominator normalises S_L to have a maximum value of unity (Figure 4.3).

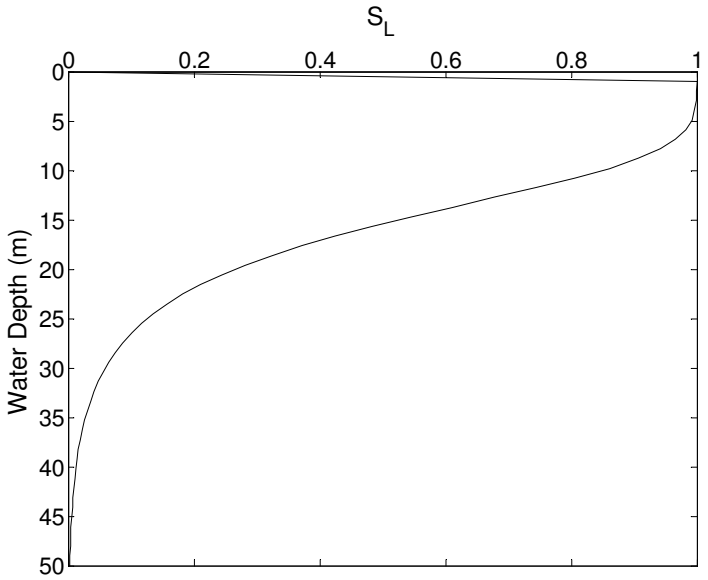

Figure 4.3: Proportion of maximum growth, S_L, due to increasing water depth (equation (4.2)).

4.3.2 Residence Time

Carbonate sediments can only form in seawater that has a sufficiently high carbonate supersaturation level (Kleypas *et al.*, 1999b). Decreasing supersaturation is therefore

of great importance in controlling carbonate production rates in areas where there is a restriction of fluid exchange with the open ocean (Broecker and Takahashi, 1966; Morse *et al.*, 1984). Previous models have used the distance from open marine waters as a control on carbonate production (Warrlich *et al.*, 2002) in order to simulate the effect of restricted circulation. Studies have shown, however, that complex flow patterns are present over reef areas (Kleypas and Burrage, 1994; Wolanski and Spangnol, 2000). This invalidates the assumption of supersaturation decreasing as a function of distance from open marine waters. Instead, we model flow vectors of lagoonal water in space and time explicitly and use these to calculate residence time of water in the lagoon. Since longer residence times should correlate with depleted carbonate supersaturation (Demicco and Hardie 2002), we use the residence time to control carbonate production.

Demicco and Hardie (2002) extended earlier work by Broecker and Takahashi (1966) and Morse et al. (1984) to describe the relationship between residence time and carbonate production rates from the Bahama Banks. They found that carbonate production decreased exponentially with increasing residence time, and ceased completely after around 250 days (Figure 4.4). Carbonate GPM uses this proxy to model supersaturation in areas that have a restricted water flow, i.e. back-reef and lagoonal areas.

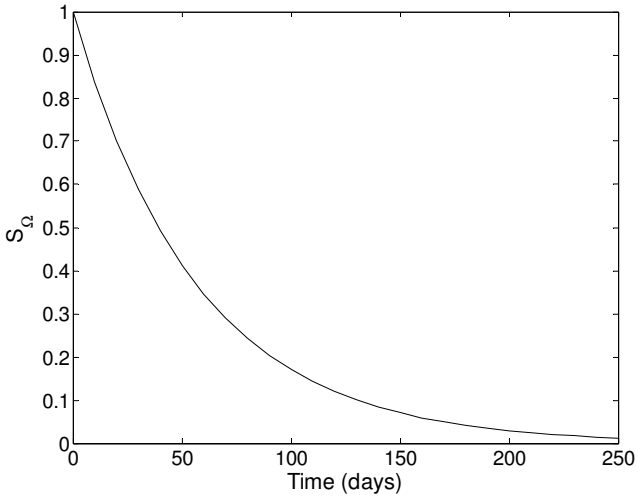

Figure 4.4: Variation in production rate, S_Ω, due to increasing residence time in a lagoon. After Demicco and Hardie (2002).

There are several advantages to this model rather than carrying out a multi-phase flow model which tracks ion concentration within flows. Firstly, it is computationally easier and therefore quicker to carry out, which is important for simulating geological times. Secondly, it can be simulated using modifications of existing algorithms, which speeds development time. Finally, it is relatively easy to test (see section 4.5). There are, however, some weaknesses in this model. It is based on the Bahama Platform and therefore it applicability to other platforms may not be justified. Furthermore, the model presented by Demicco and Hardie (2002) depends on the values of several variables, such a pCO_2 and temperature. Changing these affect the amount of $CaCO_3$ produced by a litre of seawater. The measurements of CaCO3 and residence time by (Broecker and Takahashi, 1966; Morse *et al.*, 1984) do not appear to fit an exponential reduction particularly well. However, even given these difficulties and taking into account the uncertainty in values there is still considerable differences between production rates at the platform margin and interior and there is clearly no relationship between production rates and distance to the platform margin (Demicco and Hardie, 2002), their figure 5. The model presented by Demicco and Hardie (2002) is heavily dependant on platform circulation, which on the Bahaman platform is dependant on tidal flow, winds and storms, as well as the bathymetry. As such this model of carbonate production is somewhat crude, but still a great advance on more simplistic models (Demicco and Hardie, 2002).

In order to predict fluid flow and hence residence time, Carbonate GPM contains an algorithm that models the effect of waves away from any number of wave sources which have an associated wave amplitude and period. The water movement is tracked and the residence time of the water in the lagoon at all horizontal locations is calculated by integrating the time taken for the water to travel between the open marine environment and each location in the restricted environment. Note that, unlike the model proposed by Demicco and Hardie, there are no tides or wind influences on circulation patterns, neither are the effects of storms included. However, if these effects could be included in the production of a flow field, the residence time algorithm presented below would still produce a valid residence time field.

The time the fluid takes to traverse the restricted area is calculated using a particle tracking algorithm. Particle tracking involves tracing the paths of a number of virtual particles within a velocity field. Particles are considered virtual in that they have no mass and do not interact with the environment around them. The algorithm used requires that the velocity field be known everywhere, not just at nodes or cell centres (Press *et al.*, 1992). Carbonate GPM uses a linear interpolation scheme in order to estimate this velocity field. Particles are released (see below for a description of the release mechanism) and their positions are calculated at discrete time steps. Many algorithms exist to calculate the new position, including Euler and Runge-Kutta methods (Glasgow *et al.*, 1996). All of these algorithms need a sufficiently small time step in order for the error to be minimised. Traditional algorithms need a separate error estimate calculation, such as step doubling (Glasgow *et al.*, 1996). Carbonate GPM uses a 5^{th} order Runge-Kutta-Fehlberg scheme, which uses the difference between 4^{th} and 5^{th} order estimates of the position of a particle to provide an estimate of error in the calculated position (Press *et al.*, 1992). The order of a Runge-Kutta method gives the number of sub-steps used to calculate the new position, and higher order methods are usually more accurate. This method allows the new position to be recalculated with a smaller time step if the estimated error is too large. The precise details of the algorithm are given in Press et al. (1992). Carbonate GPM also imposes some additional restrictions on the new position to ensure that particles do not exceed a threshold shift in location, again by reducing the time step.

The algorithm described above has to commence from some arbitrary line where the residence time is zero. This line should be the point where mixing between open oceanic waters, which have a high, constant supersaturation, and restricted waters, which have a supersaturation dependent on residence time. For the purposes of this model this line is the depth contour at which carbonate production commences. This value is specified by the user. The particles are injected into every cell which has a water depth of less than the maximum carbonate production depth and are traced in reverse until they meet the zero residence time line (Figure 4.5). This ensures maximum coverage of particles in every cell. More details on the algorithms used here and how the zero residence time line was determined are given in section 4.5.

Once particle tracking has provided the fluid flow vector field it is integrated spatially to give residence time. Residence time is then related to supersaturation and therefore to carbonate production, using the stress function, S_Ω shown in Figure 4.4.

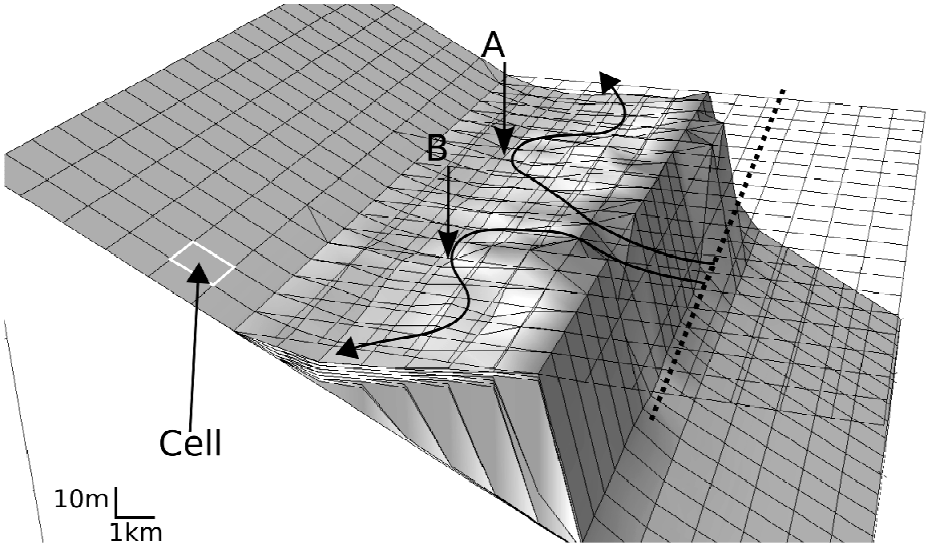

Figure 4.5: 3D view of a hypothetical reef and paths of water parcels over the reef area. Residence time is the time it takes a parcel of water to traverse an area of interest. If residence time commences from zero at the dotted line (see text for a description of this line), then we can track water parcels across the reef as they follow the flow field. To calculate residence time, we inject virtual particles in every cell landward of the zero residence time line and trace them in reverse against the fluid flow. Particles injected in cells A and B will be traced along the black flow line in the opposite direction of the flow until they reach the zero residence time line. The residence time in the cells they traverse can then be calculated. Hundreds of thousands of particles are injected in total to ensure complete coverage of the lagoon area.

4.3.3 Wave Energy

Wave power is known to be a control on both modern coral reef growth rates (Munk and Sargent, 1948; Roberts, 1974) and individual coral morphology (Chappell, 1980). Several studies also use the velocity produced by waves to quantify the effect of energy on reef growth (Graus and Macintyre, 1989; Grigg, 1998; Cruz-Piñón *et al.*, 2003). Terrigenous sediment accompanying waves and currents can also swamp corals as well as clouding the water, reducing the amount of light reaching the sea floor, so further restricting growth if the wave energy is not high enough (McLaughlin *et al.*, 2003). Thus, corals grow on either steep topographies (Kleypas, 1997) or where

the energy (i.e. water velocity) is high enough to remove this sediment (Graus and Macintyre, 1989).

GPM calculates the power dissipated by waves at each node independently of other sedimentary transport processes. These dissipated power values are then used to control reef growth rates. Given the lack of quantitative data on the effect of wave power on reef production, Carbonate GPM uses a simple curve to produce stress function S_W on reef growth due to the action of waves (Figure 4.6). We have assumed that the minimum energy for reef growth is around $2W/m^2$ (Roberts, 1974) after which the growth increases linearly until the wave power reaches $400W/m^2$ (Roberts, 1974). Above this value the growth rate is kept at maximum (given optimum light and supersaturation conditions) until $3000W/m^2$ (Munk and Sargent, 1948; Roberts *et al.*, 1975) is reached, after which the production is zero.

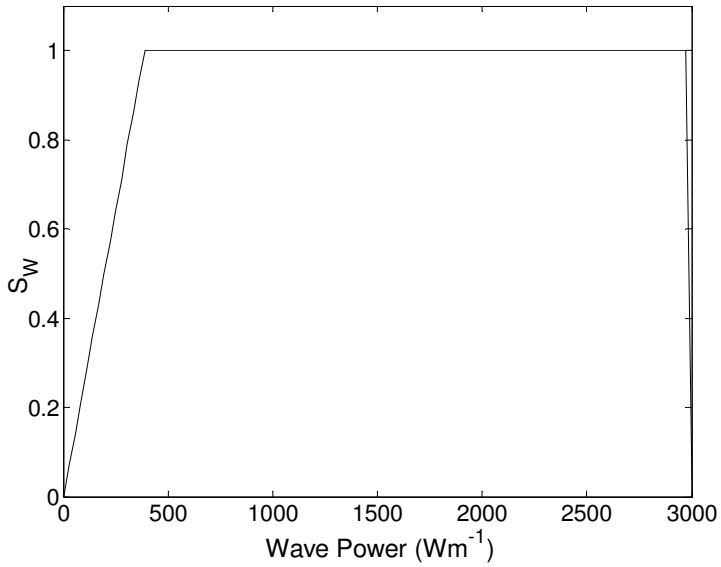

Figure 4.6: Stress function, S_W, which control production using wave power dissipation.

4.4 Erosion, Transport and Deposition

All sediments are subject to three main physical processes: erosion, transport and deposition. Carbonate GPM contains all three processes, utilising the inherited features of GPM.

4.4.1 Waves as a Transport Mechanism

Wave action is modelled independently of other sedimentary transport processes. Waves are crucial to carbonate production as they control coral reef growth and create the velocities used in the supersaturation computation described. However, they also cause longshore drift of both siliciclastic and carbonate sediments. Wave action modelling is based on the wave celerity (speed) equation:

$$c = \sqrt{\frac{g}{\kappa}\tanh(\kappa d)} \tag{4.3}$$

(Pinet, 1992). Here c is the celerity, g is gravitational acceleration, κ is the radian wave number (equal to $2\pi/L$, where L is the wavelength), and d is the water depth. Knowledge of wave celerity and period permits the calculation of trajectory (including refraction and diffraction) to a first approximation for a given set of wave sources and depth distributions. Longshore transport is assumed to be perpendicular to the direction of travel. For useful simulation of sediment transport, however, it is also necessary to model the water movement near the sediment-water interface. The maximum bottom velocity calculated using linear (Airy) wave theory is given by (Tetzlaff, 2005):

$$u_{\max} = \frac{A\eta}{\sinh(\kappa d)} \tag{4.4}$$

Here A is the amplitude, and η is the radian frequency (equal to $2\pi/T$, where T is the period). As waves travel in shallow water, they dissipate power due to friction with the seabed. GPM assumes that power dissipation is proportional to maximum water-bottom velocity, with an additional loss of power when wave breakage occurs, at which time a breakage criterion is employed based on wave height. As wave energy is proportional to wave amplitude squared, this assumption on power dissipation allows the model to calculate the wave amplitude at every point and, through equation 4.4, to calculate the bottom velocity in all locations.

The model uses a finite-difference method to calculate how waves propagate, using wave speeds predicted by equation 4.3. It keeps track of the energy transported by waves, and power dissipation caused by friction. Power dissipation per unit area and wave celerity at every point are the only variables ultimately used to calculate the

effects of waves on sediment transport. More details of the wave algorithm incorporated in GPM along with a validation of the algorithm can be found in Tetzlaff (2005).

4.4.2 Transport and Deposition

GPM contains sediment transport criteria that allow sediment to be eroded, entrained and transported in the direction of the flow, and eventually deposited. Briefly, these criteria are Shields' criterion which specifies the velocity needed to entrain sediment (Shields, 1936), and transport capacity criteria that prescribe the amount of sediment any given flow can transport (Tetzlaff and Harbaugh, 1989). Carbonate GPM can handle various sediment sizes, which when eroded are entrained as bulk sediment, but which are deposited coarsest grains first. Deposition occurs when transport capacity decreases (such as when the flow rate reduces).

Reef sediments are considered in a slightly different manner to that described above. Reefs are by definition immobile but can be eroded to produce sedimentary fragments that are far larger than the 15mm maximum for which the transport algorithms in GPM were designed. In order to simulate the erosional processes of reefs, which shed sediment downslope due to oversteepening, but are not subjected to large amounts of advective erosion, an additional "reef erodibility" parameter has been introduced. This parameter affects advective transport only and effectively extends the range of grain sizes that GPM can erode, entrain and transport advectively. As immobile barriers, reefs are susceptible to oversteepening at the reef front and subsequent collapse, making the dominant direction of transport seawards (Hughes, 1999).

The effect of the reef erodibility parameter is very clear when observing the geometries produced by the model in two runs that are identical apart from one included the reef erodibility parameter, the other did not. If the reef erodibility parameter is not included the reef sediment will initially produce backstepping geometries (Figure 4.7A). These geometries are not the product of reef production moving landward, but of transport of reef sediment onshore. If this were to happen in reality, the reef would drown in its own sediment. In addition, there is no transport of sediment downslope as is observed on modern reefs (Figure 4.7B). This is the result

of the net balance of sediment transport being onshore, as the advective transport onshore is higher than diffusive transport offshore. Although the advective transport coefficient could be reduced in order to mitigate both of these problems, this would result in no sediment transport in the lagoon, producing perfectly horizontal beds with no migrating facies, channels or any of the other features observed in carbonate lagoon settings.

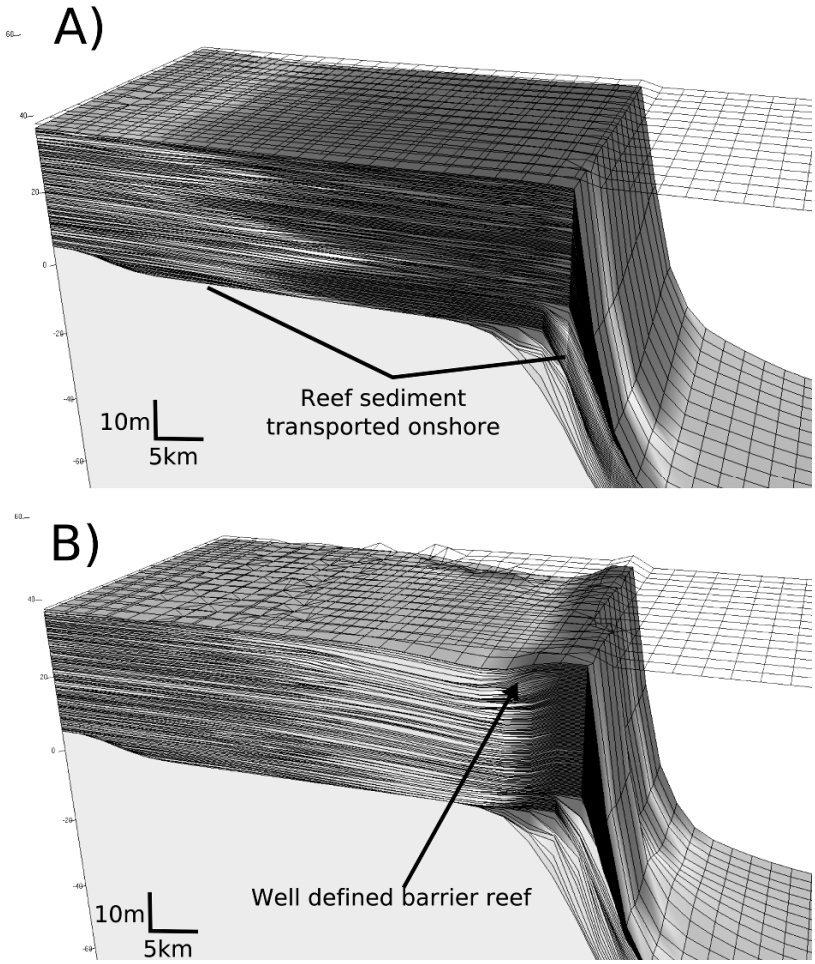

Figure 4.7. The effect of adding an erodibility parameter to reef sediment is to form a well-defined barrier reef. A) shows output when the erodibility factor is not present in the model. Large volumes of reef sediment (dark grey) are transported onshore and produce unrealistic geometries as the reef would "drown" in the sediment it produces. B) shows output with the erodibility parameter enabled. Instead of a large broad reef, a strong barrier reef is produced and the "classic" reef profile is obtained.

4.4.3 Diffusion

One of the algorithms that GPM uses for sediment redistribution is diffusion, a commonly used proxy for the combination of more complex sediment transport

mechanisms. A number of authors have used diffusion to model sediment transport and geomorphologic evolution (e.g. Hanks *et al.*, 1984; Kenyon and Turcotte, 1985; Flemings and Jordan, 1989; Martin, 2000).

Sediment diffusion in the modelling context is the assumption that states that sediment moves downslope at a rate that is proportional to the tangent of the slope angle and to the physical characteristics of the sediment, jointly represented by a diffusion coefficient. In Carbonate GPM, the diffusion coefficient is a function of sediment size, modified by a user-provided water-depth dependent function (Tetzlaff and Harbaugh, 1989). The relation between sediment grain diameter and diffusion coefficient assumes that the latter is proportional to the logarithm of the grain diameter. Diffusion coefficients for different grain sizes and water depth are shown in Figure 4.8.

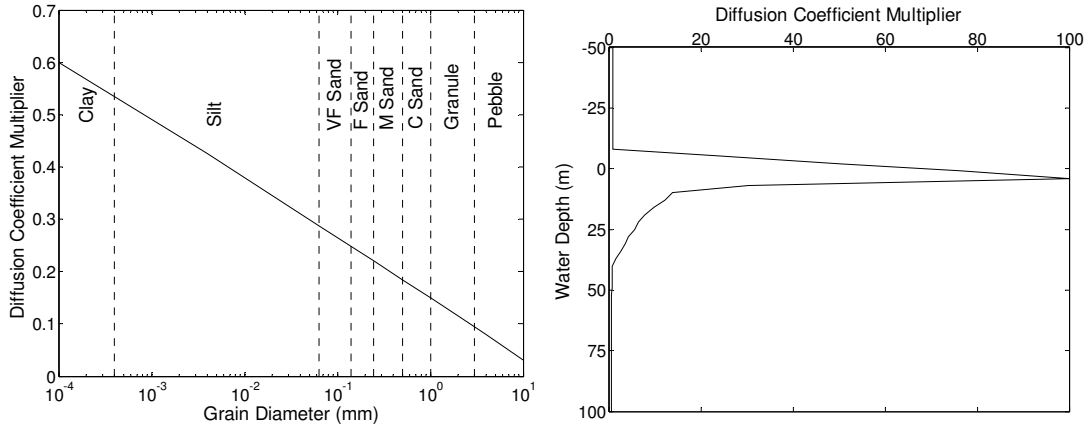

Figure 4.8: Sediment diffusion constant, kd, as a function of grain size (left). VF – very fine; M – medium; C – Coarse. Diffusion also varies with water depth using a multiplication factor (right).

4.5 Numerical Validation of Carbonate GPM's Residence Time Algorithm

Residence time (which is a proxy for supersaturation) is calculated using a particle tracking algorithm in Carbonate GPM as described in section 4.3.2. The point at which residence time starts to increase has varied from study to study. Demicco and Hardie (2002) started calculating residence time at the point where the depth of the Bahaman platform was four metres or less. Other residence time calculations start

from a human decided boundary and apply to a single problem only (e.g. Glasgow *et al.*, 1996; Deleersnijder *et al.*, 1997; Tartinville *et al.*, 1997; Walker, 1998; Andrefouet *et al.*, 2001b; Bellucci *et al.*, 2001).

If residence time is to be calculated automatically at each timestep, the restricted area in which the residence time increases also need to be defined automatically. The restricted area is the region where the supersaturation of carbonate cannot be replenished by interaction with the open water. The definition of this area, in terms of a numerical computation, is crucial in order to get a residence time that is accurate compared to that observed in nature. This section details the steps taken to derive an accurate restricted area and verifies the accuracy of the residence time algorithm itself.

The restricted area has to be defined using parameters available in GPM and without any human interaction. There are four properties that could be used to define the restricted area:

- Water depth (node-centred).
- Wave power dissipated (node-centred).
- Carbonate production from the last iteration (which is a function of water depth, the previous residence time and wave power) (node-centred).
- Water velocity (tie-centred).

As stated earlier the residence time is a proxy for the depletion of carbonate ions from water by precipitation of carbonate. The boundary between the restricted area and the open-ocean is where residence time will start to increase from a value of zero days. The computational version of this boundary therefore needs to be appropriate for these physicochemical changes. In order for the residence time calculation to be accurate, the boundary needs to be well defined, only one cell in width, with no ambiguity in its location. As the particles do not represent anything physical, the direction they travel is immaterial to the residence time calculation. However, the release points of the particles are of great importance to the accuracy of the calculated residence time. If cells do not have particles passing through them, they cannot contain an estimate of residence time and instead the value must be interpolated from neighbouring cells.

The problem of defining a restricted area is made somewhat more challenging due to the fact that several parameters of the particle tracking algorithm can affect how well the particle tracking performs and hence how well the boundary is defined when using the particle paths themselves to define a boundary. For example, more particles can be released in the initial injection, i.e. two particles per cell, rather than a single particle, affecting which cells have particles travelling through them due to the fact that a particle is given a random starting position inside its starting cell. Parameters that could affect the definition of the restricted area are:

- Initial particles per cell.
- Number of iterations for which the simulation runs.
- Whether the particles are traced forwards or backwards.

Running particles in a forward direction means that they are injected into inflow cells (the boundary) and follow the velocity vectors until they either reach an outflow cell or leave the calculation domain (Figure 4.9). They may not necessarily reach every cell, depending on their injection point. This can be countered somewhat by randomising the injection point within a cell and injecting multiple particles per cell.

Particles may also be run backwards from *every* cell in the calculation domain until they leave the simulation by either leaving an "inflow" cell or exiting the calculation domain (Figure 4.9). This ensures that (nearly) every cell has particles passing through them. The only difference between this method and the forward tracking method is that the velocities used are the negative of those that were actually calculated. The only cells that will not have particles passing through are sinks and sources. However, many more particles are needed and much information is duplicated. This increases the computational load and therefore the time taken to make the calculation.

In both cases, once a particle is removed its properties are reset and it is re-injected into the flow. The particle is re-injected into any inflow cell (for the forward running algorithm) or into any restricted area cell (in the backward running algorithm), in a random position inside this cell.

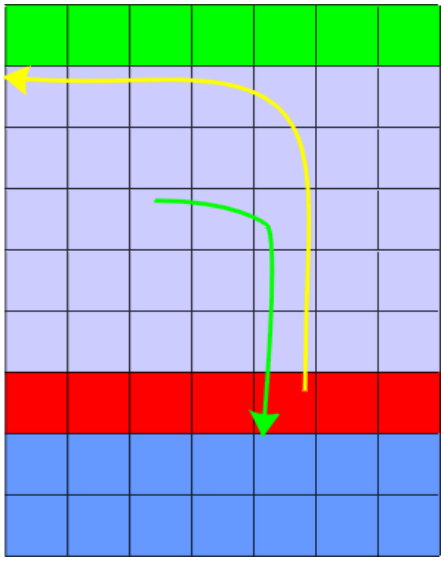

Figure 4.9: Two particle tracking methods used in Carbonate GPM. The yellow path shows a particle that is injected into an inflow cell and is traced until it leaves the calculation domain. This method is forward particle tracking. The green path shows a particle that is injected into an interior cell and is traced to an inflow cell. This is backwards particle tracking. The coloured cells represent land (green), restricted area (light blue), open-ocean (dark blue) and the boundary between (red).

4.5.1 Algorithm Verification

The residence time algorithm was verified by calculating the residence time over a known velocity field. Because the velocity and cell size were known (and simple) the solution could also be calculated analytically. Comparisons were then drawn between the answer supplied by the residence time algorithm and the analytical calculations. For both forward- and backward-tracing residence time algorithms the results agreed well with analytical results, varying only to the fifth or sixth significant figure as a result of numerical rounding.

4.5.2 Methods of Determining Zero Residence Time

4.5.2.1 Method 1 – Using Dissipated Wave Power

This method uses the location of the wave power dissipated to decide the location of the boundary. The logic behind the method was that a restricted area would be bound by some topographic high, which caused a restriction on the interchange of carbonate with the open ocean. This topographic high would, necessarily, cause waves to break and therefore dissipate power.

Algorithm

The interior cells are defined first, using the following conditions:

- Depth > 0 m.
- Carbonate production rates > 0 m/yr.
- Wave power dissipated < 0.1 W/m^2.

Once the cells have been designated as interior using the above criteria, inflow or outflow cells replace interior cells where:

- The cell has wave power dissipated > 1.0 W/m^2.
- The cell has a flow speed > 0 m/s.

The cell is decided as an outflow or inflow based on the direction of the velocity vectors. Once the main restricted area has been defined it is checked for consistency. Any cells that are designated as inflow must have at least one interior cell adjacent. Equally, groups of cells that are designated as interior must have at least one inflow cell adjacent to this group. This is checked by deciding on the landward-seaward direction and making any cells open-ocean until an inflow cell is reached in each row/column.

4.5.2.2 Method 2 – Gradient Tracing

The second method was to use the paths of the particles themselves to define a boundary. The particles were released on the edge of the calculation grid and traced throughout the whole calculation domain. Once the particles have been tracked, their paths are analysed in the reverse direction (i.e. from the location where they are removed from the calculation to their injection cell). The final location in the path of a zero gradient or extremum point (along the particle path) in either the wave power dissipated or carbonate production rate from the previous timestep is then used to define an inflow boundary. An extremum is defined as a change from a positive (or zero) gradient to a negative gradient in the next cell. This gradient can occur in either the present wave power dissipated or carbonate production rates from the previous time step.

This method was also tried with particles being released into every cell and traced backwards to the edge of the calculation grid. Again, tracing against the flow, the last cell in which power dissipated or production rates had a zero gradient or an inflexion point was defined as the boundary.

Algorithm

The starting point for this algorithm was to create an initial set of boundary conditions. The whole grid is defined as interior to the restricted area, apart from the cells on the edge of the calculation domain where the flow is into the domain. Particles are then injected from these cells and traced around until they reach a boundary cell. The path of each particle is then searched from its leaving point to its start point. The inflow cell is the final extremum along the path.

Any cells before this point are now labelled as interior. Any cells after this point are open-ocean. A path may overwrite another paths interior or open-ocean cells, but not an inflow cell. If no boundary is found on a path, the path is ignored and does not contribute towards the boundary definition.

If the particles are traced backwards, the algorithm is identical, except particle paths are examined from their starting point to their leaving point, i.e. still traced against the currents.

4.5.2.3 Method 3 – Modified Gradient Tracing

The modified gradient tracing technique uses the gradient tracing technique as described above, but uses the fact that paths may cross and tries to synthesise this information to produce a more reliable boundary definition.

Algorithm

The algorithm proceeds as in the original gradient tracing technique, whereby the gradient of both power dissipated and carbonate production rates are calculated along a particles path. When a boundary is found on any particular path, any other paths also passing through this cell are analysed. The boundary is then decided on the following rule:

- Use the final inflexion point, unless other paths crossing the same cell found either:
    - No inflexion *and*
    - A previous inflexion (along its path)

4.5.2.4 Method 4 – Using Water Depth as a Limit

This is the simplest of the four methods outlined. The maximum depth of carbonate production is taken to be the edge of the restricted area. Particles are released in every cell and traced to the edge of the restricted area.

Algorithm

The algorithm is the simplest of the four described. Each cell is designated as open-ocean if its depth is greater than the maximum carbonate production depth or interior if its depth is less than or equal to the maximum carbonate production depth. The boundary between interior and open-ocean is then designated as either inflow or outflow, depending on the velocity direction.

4.5.2.5 Test Scenarios

The methods were tested using a small computer program specifically designed to test the residence time algorithm. The input data for this program were generated via GPM or by hand (test 1 only – see below). Data to test each method were generated in three ways:

- Simple test cases with a constant velocity in each cell. Water depth, production and wave power dissipated were varied according to the method being tested. This test was carried out eight times, to ensure that the method worked in all compass directions.
- A barrier reef simulation from data produced by GPM (Figure 4.10).
- The Great Bahama Banks carbonate platform from data produced in GPM (Figure 4.11).

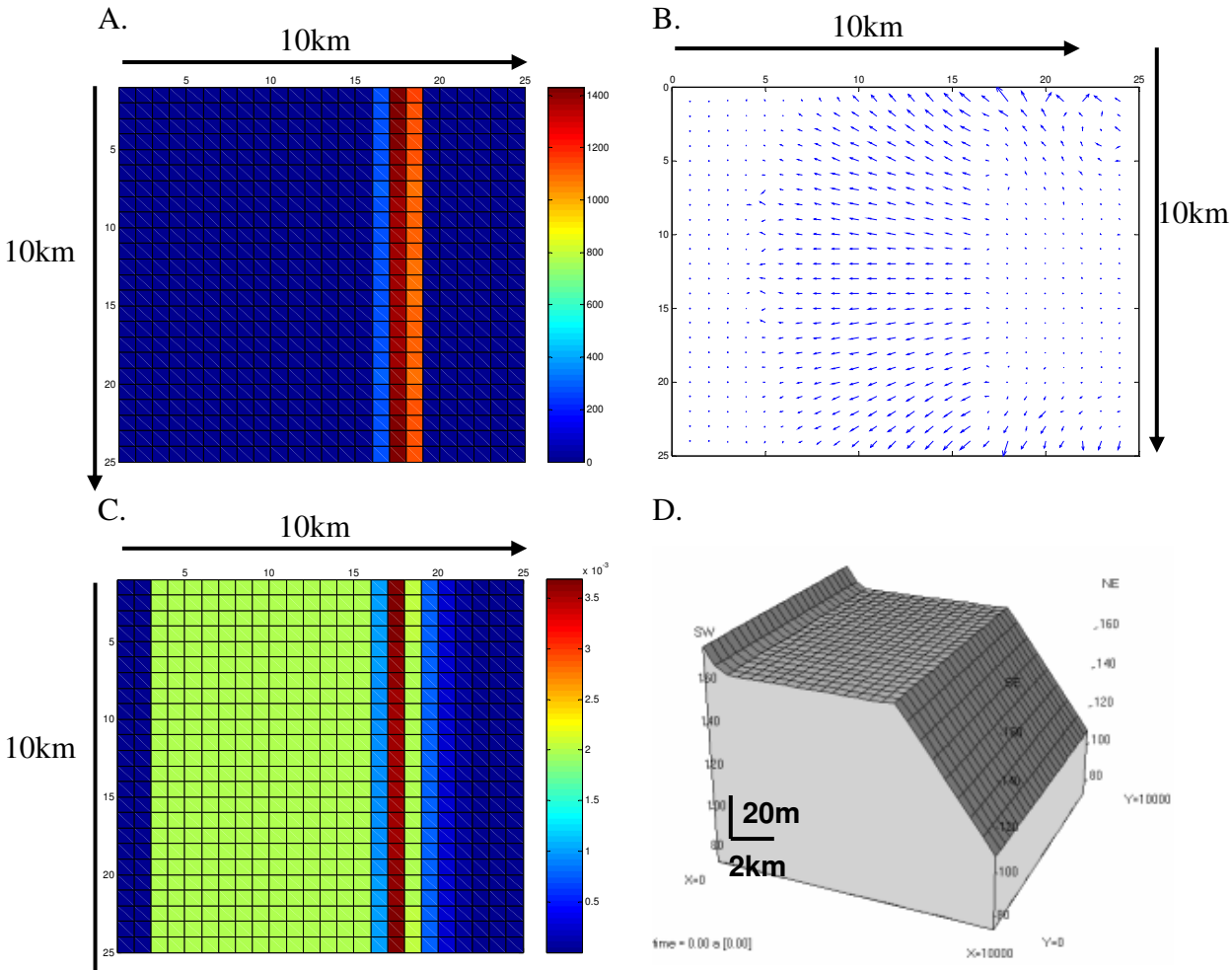

Figure 4.10: The power output (A) in W/m, velocity (B) in m/s, production (C) in m/yr and starting topography (D) of the barrier reef test.

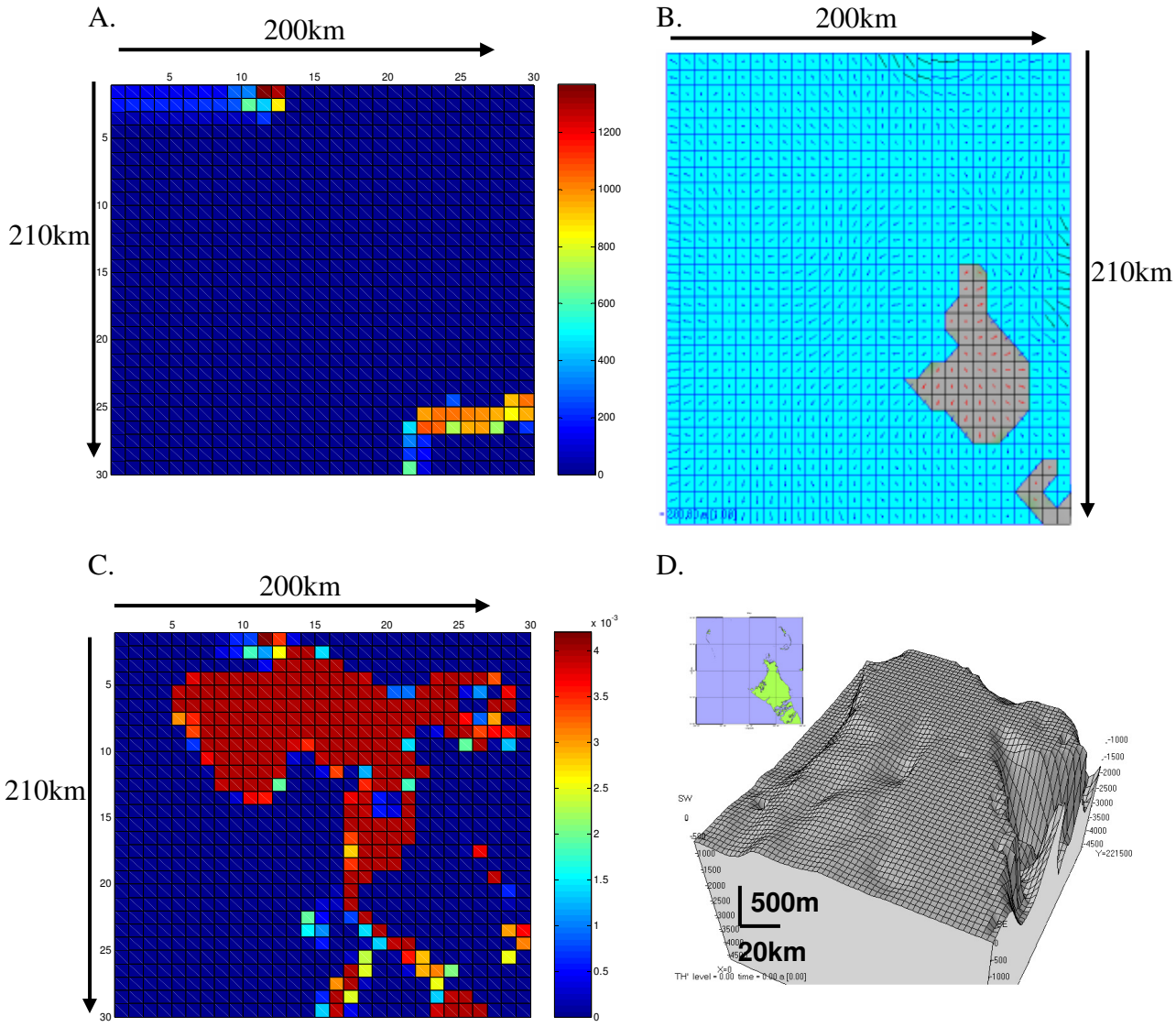

Figure 4.11. The wave power dissipated (A) in W/m, the velocity field (B) in m/s, production rates (C) in m/yr and starting topography (D) of the Bahaman simulation. The inset in D. shows a map of the same region. This view covers approximately 200km east-west and 210 km north-south. The Florida Straits is to the left and the deeper region on the right is the Tongue of Ocean. The actual starting topography used in the test was of lower resolution than shown here to decrease execution times.

4.5.2.6 Results

All methods of defining the restricted area worked using the simple test of using a fixed velocity in each of the eight compass directions. As such, no results from this test will be discussed here.

Method 1 – Using Dissipated wave power

This method produced clear boundary definitions on the barrier reef GPM run. The boundary between open-ocean and the restricted area occurs where the highest gradient of wave power dissipated occurs as is expected (Figure 4.12).

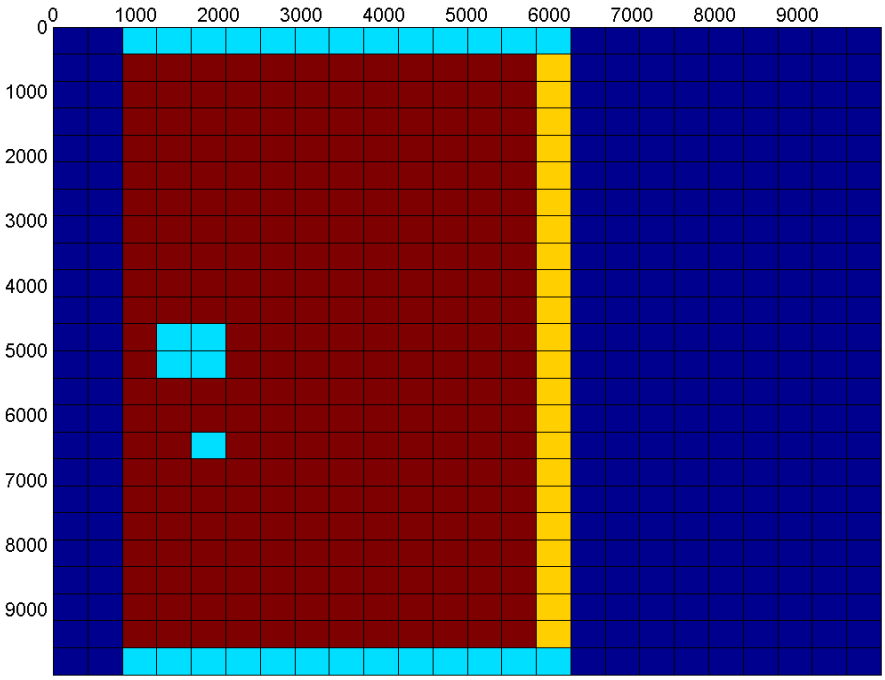

Figure 4.12: The boundary matrix found using the location of wave power dissipated. Yellow cells are inflow cells, light blue are outflow, red are interior and dark blue are open-ocean cells. The five light blue cells in the interior region are sinks where the velocity does not allow particles to leave these cells.

This method did not work on the simulation based on the Bahama Banks as there was no wave power dissipated at the edge of the platform. This effectively stopped any residence time calculations occurring.

Method 2 – Gradient Tracing

The restricted area definition of barrier reef test showed some problems with this method. When particles were released from the edge of the calculation domain they did not reach every cell and hence no boundary was defined. This was caused by the flow being slightly divergent near to the edges of the calculation domain. This is clearly seen in the velocity plot (Figure 4.10B) and prevented a clear boundary definition.

When particles were released from every cell, a boundary could be defined but it was not clear, showing multiple inflow cells being defined in any one row instead (Figure 4.13).

This method was not tested on the Bahaman scenario, but would presumably produce a blurred boundary again as the mechanism responsible for the blurring will act in any situation (see section 4.5.3).

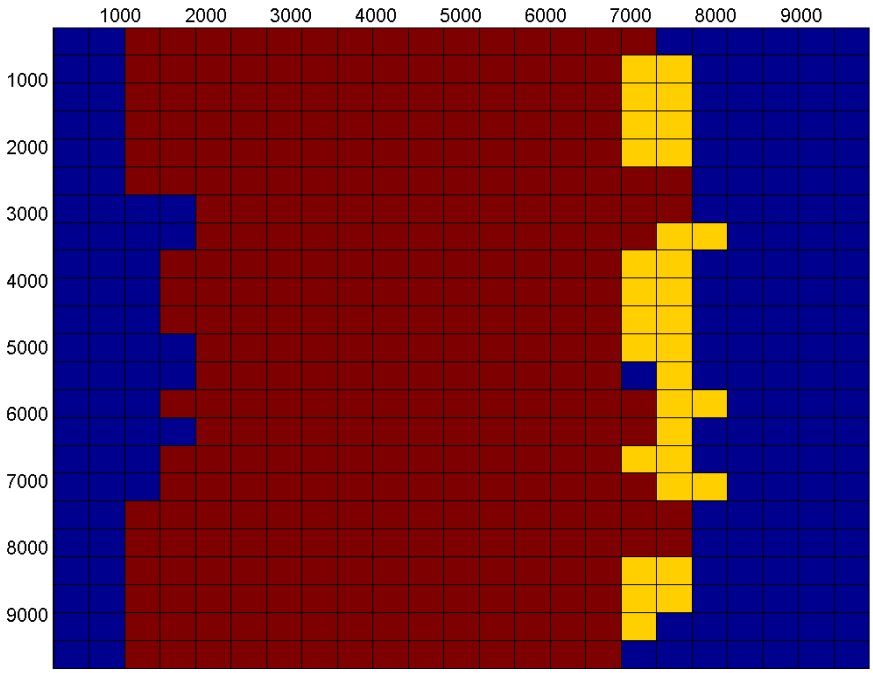

Figure 4.13: Boundary for barrier reef test using the final position of a zero gradient along particle paths. Red represents interior cells, blue empty cells (either land or open marine) and yellow represents the boundary between open and restricted environments. It is clear that the boundary is not well defined, but is in approximately the correct position.

Method 3 – Modified Gradient Tracing

The method responded better than the original gradient tracing method in terms of defining a sharp boundary on the reef test. However, the rules used had an unexpected consequence which resulted in large gaps occurring in the boundary. The reasons for these gaps occurring are covered in section 4.5.3.

As in the original gradient tracing method, this algorithm was not tested on the Bahamas scenario as, again; similar mechanisms would operate producing a boundary with large gaps.

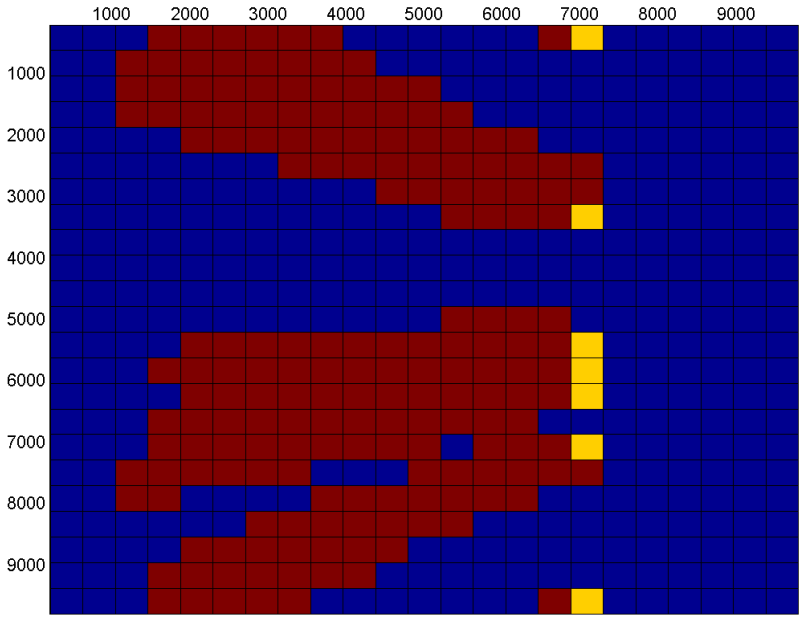

Figure 4.14: Boundary definition for the modified gradient tracing algorithm. Red cells are the restricted areas, blue are open-ocean and yellow is the boundary between.

Method 4 – Using Water Depth as a Limit

Although this method is the simplest it does produce a clear, well defined boundary for both the barrier reef (Figure 4.15) and Bahaman scenarios (Figure 4.16). However, this method does not put the boundary in an ideal location, instead placing it in what could be described as open marine.

The Bahaman simulation also has a few problematic cells (Figure 4.16), mainly due to the discretisation of the topographical data. On a higher resolution the inlets would not be one cell wide, giving an almost perfect boundary.

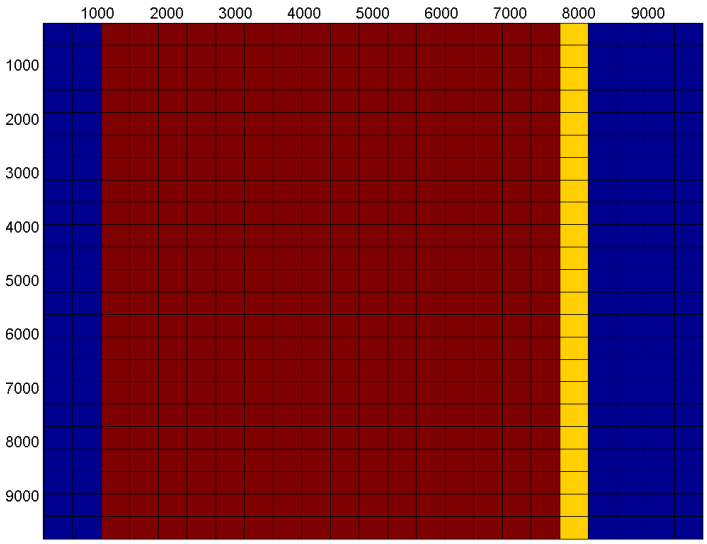

Figure 4.15: The boundary matrix produced using the 25m depth contour as the boundary between open-ocean and restricted marine areas. Red cells represent the restricted area, blue cells are open-ocean or land and yellow cells are the boundary cells.

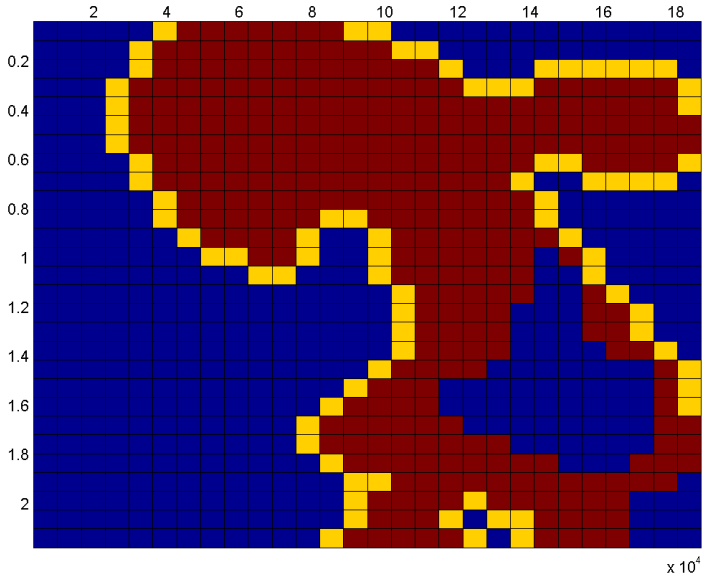

Figure 4.16: The boundary matrix produced for the Bahaman simulation using the 50m water depth contour as the boundary between open-ocean and restricted areas. Blue represents open-ocean or land, red cells are the restricted area and yellow cells are boundary cells.

4.5.3 Discussion

The definition of the restricted area is of crucial importance to the accuracy of the residence time calculation. All methods described in this section produce a boundary in a subset of all possible problems that may be encountered by the algorithm. Using wave power as the delimiter (method 1) between open marine and restricted

environments clearly does not work in every situation. Situations such as the Bahamas where the restricted area is defined by a change in water depth, but no significant waves break in this area, will cause this method to fail. However, this situation could be easily recognised by looking at the wave power dissipated data and then switching to an alternative method.

Using the gradient tracing method fails to produce adequate results on the barrier reef simulation, resulting in a vague boundary between open-ocean and restricted areas. The reason that the boundary appears fuzzy is due to the crossing of paths (Figure 4.17). As each particle experiences slightly different values of wave power dissipated and carbonate production along its path, the position of the final inflexion point may be moved by one cell in either the horizontal or vertical direction. For example, both the green and orange paths start in cell (15,1), but due to their different starting positions, they traverse slightly different cells. Due to the higher value of wave power in cells (16,1) compared to (16,2), the position of the final inflexion point shifts. The green path finds a positive gradient from cell (15,1) to cell (16,1), but a negative gradient from cell (16,1) to cell (16,2). The final inflexion point is therefore placed in cell (16,2). The orange path finds a positive gradient until cell (16,2) and finds a negative gradient in cell (17,2). The final inflexion point is then placed in cell (17,2). This is mainly an artefact of using discrete cells which is, of course, unavoidable in any numerical model.

The results of the modified gradient tracing method show that it does work better than the original gradient tracing method in producing a sharp boundary; however, it also results in large gaps in the boundary. The reason behind these gaps is similar to the original gradient method, in that paths crossing each other may both find the “correct” boundary, yet if one path finds the boundary before it enters the cell in which the paths cross, the cell in which they cross cannot be a boundary. This point is illustrated in Figure 4.18. The “correct” boundary is a linear one found in column 16 and is shown with a dashed green line. The red path finds the last inflexion point in cell (16,7), which is shown in light red. The blue path finds the last inflexion point in cell (16,8), which is shown in light blue. Both are correct. However, when the blue path is cross referenced against paths that cross it in cell (16,8), it finds that the red path has

crossed. The algorithm then searches the red path and finds that the last inflexion point on this path is in cell (16,7), which is *before* cell (16,8) and hence (16,8) cannot be a boundary cell according to the two rules used in this method. This explains the large gaps in the boundary matrix when using this method.

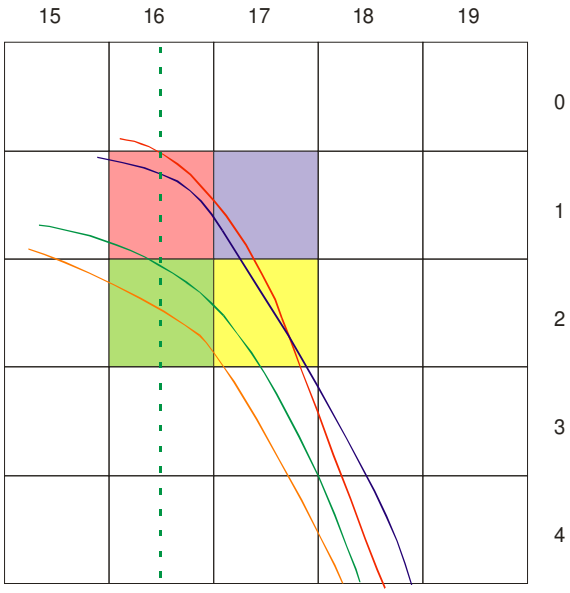

Figure 4.17: Paths of four particles in the gradient tracing method. All four paths start around the same area (cell (15,1) and all four find different boundary cells. Each coloured cell corresponds to the colour of the path that found a boundary in that cell. The green dashed line is where the boundary should be found.

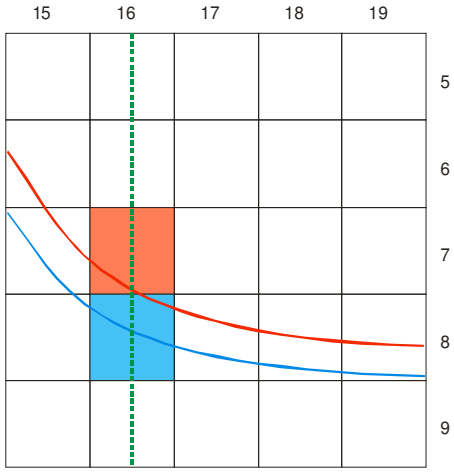

Figure 4.18: The traces of two paths that both find a boundary cell and pass through the same cell at some point (i.e. cross). The actual boundary location is shown with the dashed green line. The red path finds the red boundary cell; the blue path finds the blue boundary cell. As the red path finds the boundary before crossing the blue path, the blue cell cannot be a boundary due to the rules given in section 4.5.2.3.

From the above experiments it would appear that using a depth defined boundary covers a broader range of situations and as such will be used in future versions of Carbonate GPM. The residence time algorithm produces results that agree with analytical solutions and is therefore valid.

4.6 Validation of GPM's Flow Algorithm

GPM's flow algorithm calculates the flow as a depth-averaged value due to the action of waves and external currents. The force exerted by waves (an internal parameter called *vlafact*), which generates the wave-induced current, is a parameter that requires calibration against real-world data. In addition, changes to the boundary conditions were also tried.

To calibrate the flow in GPM, data from Duck, NC, USA was used (Elgar *et al.*, 1995). This dataset consists of three data locations to record the longshore and cross-shore current; a wave meter which records the wave amplitude, period and direction; tidal data, and bathymetric data. As such, it can be used to build up a full GPM scenario in order to calibrate the pushing force of waves on the current.

The data from Duck consists of three months of data recorded at frequent intervals (minutes or hours, depending on the data source). In order to eliminate the effects of tide and to simplify the construction of the GPM scenario, the data used must fulfil the following requirements:

- Be at a suitable point in the tidal cycle in order to reduce the effects of tidal flow.
- The wave direction must be zero degrees; that is, the wave direction is perpendicular to the shoreline. This enables the wave source to be simulated using a line of point sources along the eastern edge of the grid.
- The wave period and amplitude should be such that the waves break near-shore. This is to avoid waves breaking on the wave point-sources due to the limited bathymetric data.
- Bathymetric data should be recorded within a day of the other data used.

4.6.1 Description of Data

Tidal flow often lags behind the tidal changes in water height. The amount of lag can be found by cross-correlating the tidal height with velocity. The minimum tidal flow for Duck occurs approximately three hours after low tide. An appropriate date that fulfils all the above criteria above is the 21st of September at around 4am (day 264.16667). The starting scenario was created using the bathymetric data collected from Duck on the 20th September, 1994. All runs started with the same antecedent topography (Figure 4.19).

All flow, wave and tide data was collected at 4am on 21st September, 1994 (see following tables). The flow data comes from three sets of velocity meters, which are placed at various depths. The figures shown in the table below are an average of all velocities measured, as GPM produces a depth-averaged velocity located at the centre of each cell.

Tide:

Year/Mo/Day	HH:mm:SS	Gage	Tide (m)
1994/09/21	04:00:00	11	-0.030

Wave:

Year/Mo/Day	HH:mm:SS	Amplitude (m)	Period (s)	Direction (°)
194/09/21	4:00:00	0.393	3.717	2

Flow:

Velocity Meter	X-Coord (m)	Y-Coord (m)	Ave. Long (m/s)	Ave. Cross (m/s)
1	190.09	930.09	-0.05175	-0.05275
2	370.15	928.58	0.071166667	0.006166667
3	884.11	915.44	0.224125	-0.0235

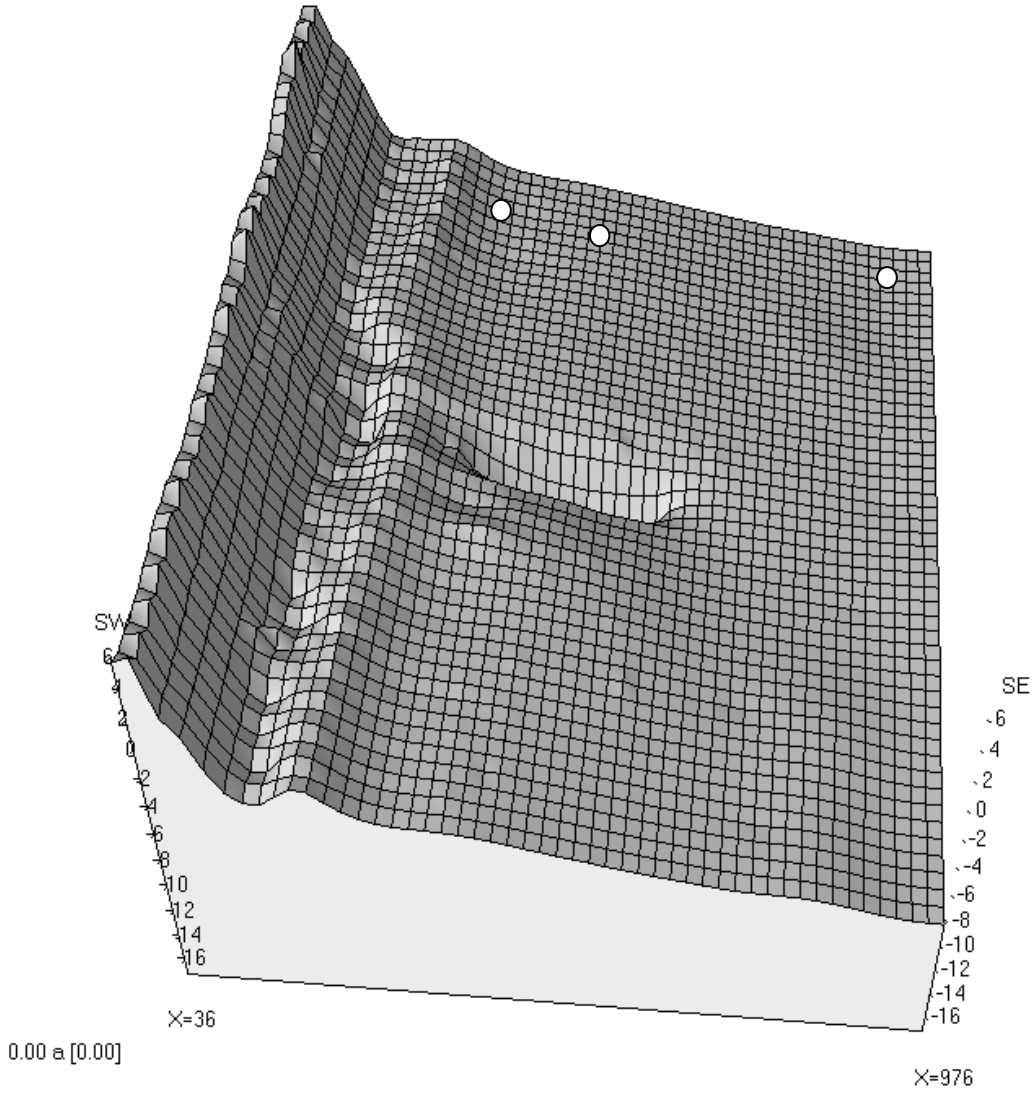

Figure 4.19: Bathymetry from Duck loaded into GPM. The approximate locations of the velocity meters are shown by white circles.

Run	Additional South Boundary Cells	Additional North Boundary Cells	Additional East (source) Boundary Cells	vlafact	Boundary Conditions
1	0	0	0	0.01	Open
2	0	25	25	0.01	Open
3	0	0	25	0.01	Open
4	25	25	25	0.01	open
5	0	50	0	0.01	Open
6	25	25	25	0.01	Leaky, open on source edge
7	25	25	25	0.01	Leaky, closed on source edge
8	25	25	25	0.1	Leaky, closed on source edge
9	25	25	25	0.05	Leaky, closed on source edge

Table 4.1. Details of all parameters used in the calibration and testing of GPM's flow algorithm against data collected at Duck, NC.

4.6.2 Method

The validation was carried out by running the same GPM scenario and varying one of the following parameters: *vlafact*; the north, south and source boundary conditions and location; and the minimum flow depth. A full description of the parameters used can be found in Table 4.1.

Boundary conditions were either closed, fully open or "leaky". Boundary conditions on the north and south edge are not set using velocity, but by setting the flow height in an additional, adjacent cell. A "leaky" boundary sets this flow depth to half the height on the edge cell. The fully open boundary conditions set the flow depth equal to that of the edge cell and the closed boundary sets the flow depth to zero. On the source boundary the flow in the x-direction is set to zero when the boundary is closed or is not set when using fully open boundary conditions and the same boundary conditions as the north and south edges. In addition to changing the boundary conditions the extent of the boundary was also changed. An additional 25 cells were placed on the north, south or source boundary (or combination of these three) in order to reduce the effect the boundary has on the flow patterns as the velocity meters are close to the boundary (Figure 4.19), which is not ideal for any model. *Vlafact* was set at 0.05, 0.01 or 0.1.

Once GPM had produced output, the flow magnitudes in both the x- and y-direction were linearly interpolated to produce an estimate of the depth-averaged velocity at the coordinates of the velocity meters.

4.6.3 Results

The first set compares runs that did not have any additional cells placed on any boundary to those that did (Figure 4.20 and Figure 4.21). It is clear that the boundaries have a large effect on the current calculated at the three meter locations. Adding 25 cells on each boundary gives much better results.

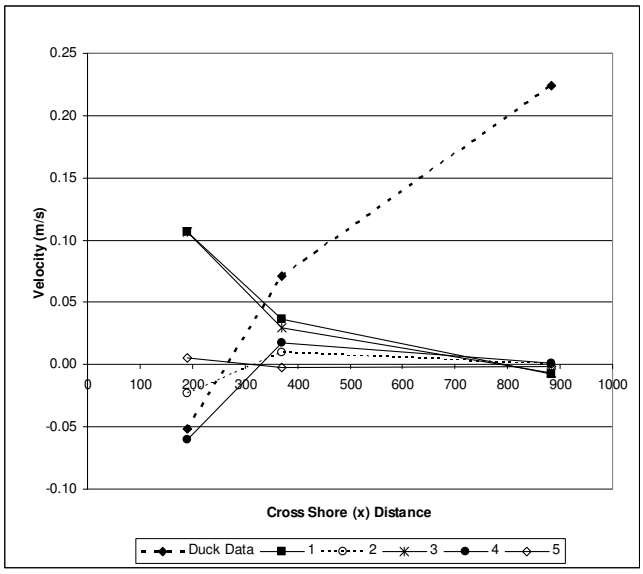

Figure 4.20: Comparisons of longshore flow magnitude between data from Duck (dashed line) to GPM output. See Table 4.1 for a full description of all parameters used.

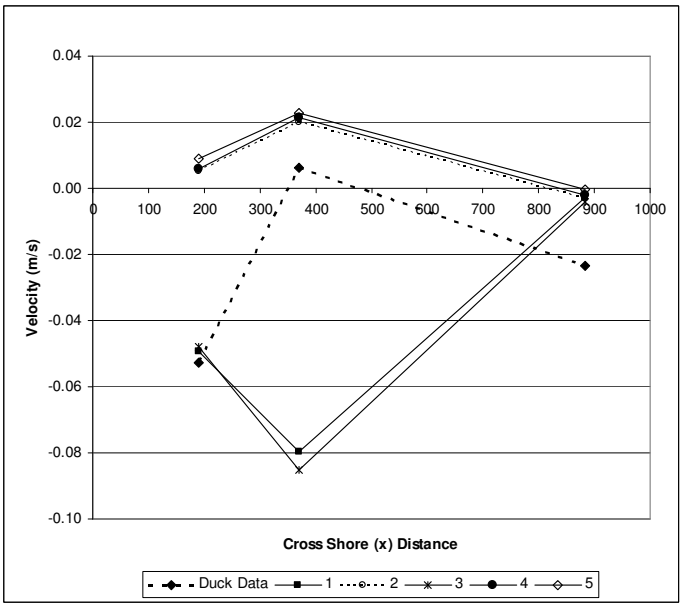

Figure 4.21: Cross-shore current comparison between Duck (dotted line) against GPM runs. See Table 4.1 for a full description of all parameters used.

The second set of runs uses scenarios which have 25 additional cells on the three boundaries (north, south and source) and varies the value of *vlafact* and the type of boundary condition used (Figure 4.22 and Figure 4.23).

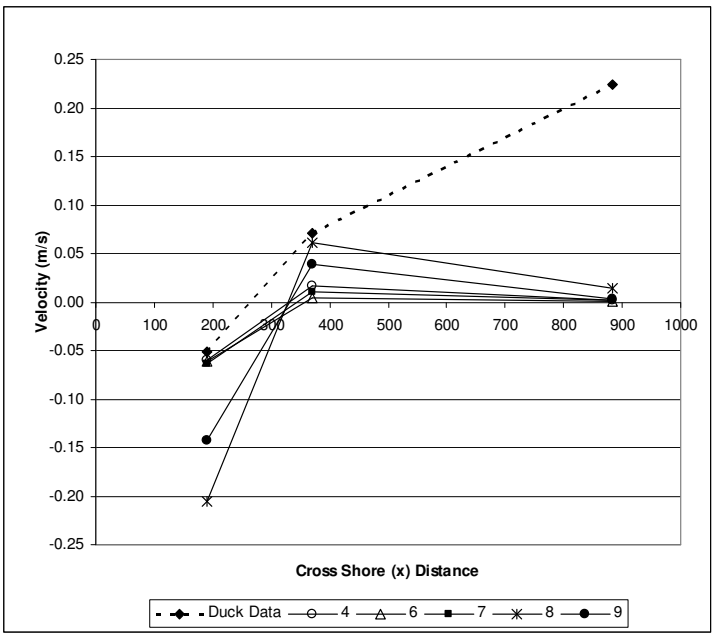

Figure 4.22: Longshore current from Duck (dotted line) and GPM run. See Table 4.1 for a full description of all parameters used.

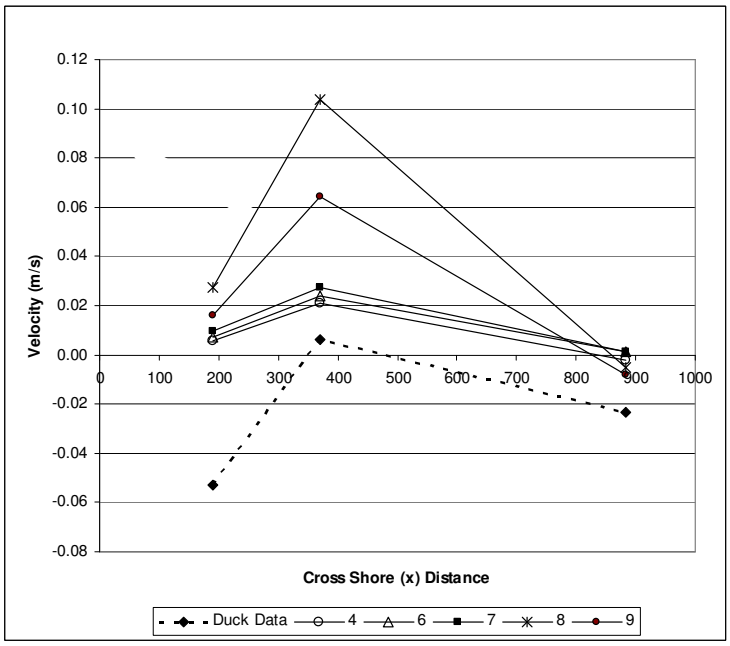

Figure 4.23: Cross-shore velocity magnitude for Duck (dotted blue line) and GPM. See Table 4.1 for details of the run parameters.

The output from GPM shows that the flow is complex, with gyres and rotational features near the shoreline (Figure 4.24).

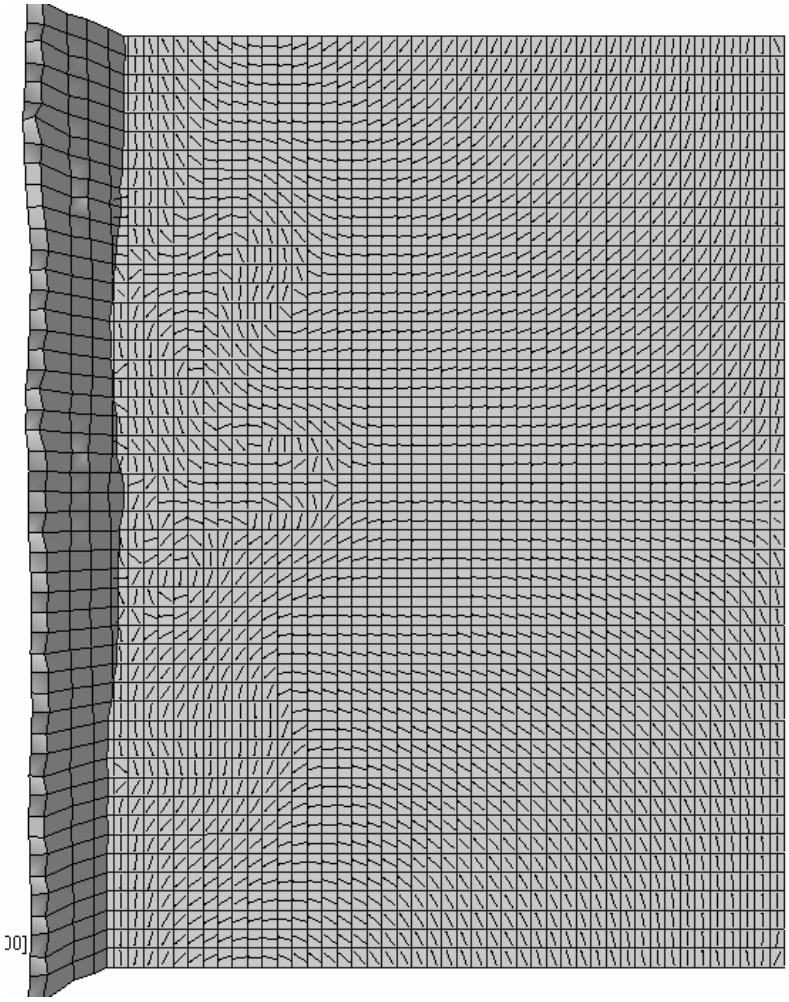

Figure 4.24. GPM output from run 2. Note the complex gyres in the nearshore region. Arrows have been scaled to show the pattern, rather than magnitude.

The wave-induced flow from GPM compares very well to the data recorded from Duck, NC. The boundaries are clearly a problem, as they are in any numerical model. However, extending the boundaries does produce better results. The boundary conditions themselves seem to make little difference to the flow patterns produced, but do alter the magnitude in the three meter locations slightly. A *vlafact* of 0.01 gives results that qualitatively seem reasonable.

There are two reasons for why the velocity will not match the Duck data exactly. Firstly, the gyres need only be out by a cell or two to radically change the velocity (i.e. reverse direction) at the meter locations. Given that GPM's flow algorithm is designed to be computationally efficient, rather than include details such as depth varying flow it is reasonable that it is more important to reproduce the patterns of

velocity change between the meters, rather than the actual values recorded at the meters. Secondly, GPM calculates a depth-averaged flow. This is related to point one, but is perhaps more critical to the velocity in deeper water. The data recorded at Duck was done using a vertical line of velocity meters. In order to carry out the comparison, the values from each vertical array were averaged to produce an estimate of the depth averaged value. However, the meters are not spread equally throughout the water column. Using the meters at location 3 (the meter locality that is closest to the eastern edge) there are two sets of velocity meters close to the surface, two at 1.4m depth, 2 at 2.73m depth and 2 around 7m depth (Table 4.2).

Table 4.2. Values for the velocity as recorded by the meters used at Duck.

Meter	X (m)	Y (m)	D (m)	Longshore Vel (Y)	Cross Shore Vel (X)
u87	884.11	915.44	-7.29	0.036	-0.029
u86	884.11	915.44	-6.92	0.062	-0.043
u80	884.11	915.44	-2.73	0.233	0.06
u83	884.11	915.44	-2.73	0.234	0.06
u82	884.11	915.44	-1.44	0.26	0.001
u89	884.11	915.44	-1.44	0.259	0.001
u81	884.11	915.44	-0.48	0.355	-0.119
u88	884.11	915.44	-0.36	0.354	-0.119

The longshore velocity calculated by GPM at this location is much lower than the average from the Duck data. However, the velocity near the sea bed is two orders of magnitude lower than the flow in the top few metres. Taking an average of these values skews it towards the higher magnitude flows. A better estimate could be arrived at by plotting the flow magnitude against depth and plotting an exponential curve through the data (Figure 4.25). Using this method, the flow at 3.8m (half depth) is around 1.3m/s, much lower than the average of the eight meter readings and closer to the GPM estimate.

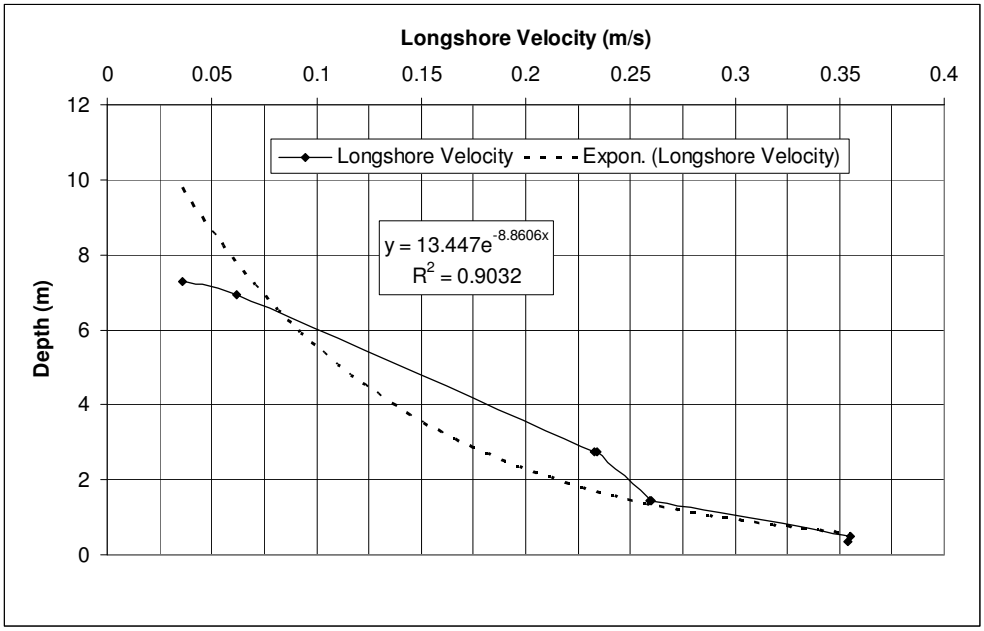

Figure 4.25: Longshore flow against depth for meter 3.The black line shows the best exponential fit for the data.

There could also be other reasons for the discrepancies between the GPM modelled flow and the Duck data in the form of currents not modelled by GPM. Although the effect of tidal currents was minimised by choosing a low tide regime, there could still be some residual tidal currents. In addition there may be current from other sources, such as wind-induced flow or even ocean currents. The data period chosen happens to be just after a particular windy time and is during a period of fairly high wind, suggesting the anomaly could be wind-induced (Figure 4.26). Finally, the wave model in GPM is very simple, containing only one period and amplitude for each source. In reality waves has a spectrum of frequencies and heights. This will make a difference to the modelled velocity but would take too much computational power in order to simulate millions of years.

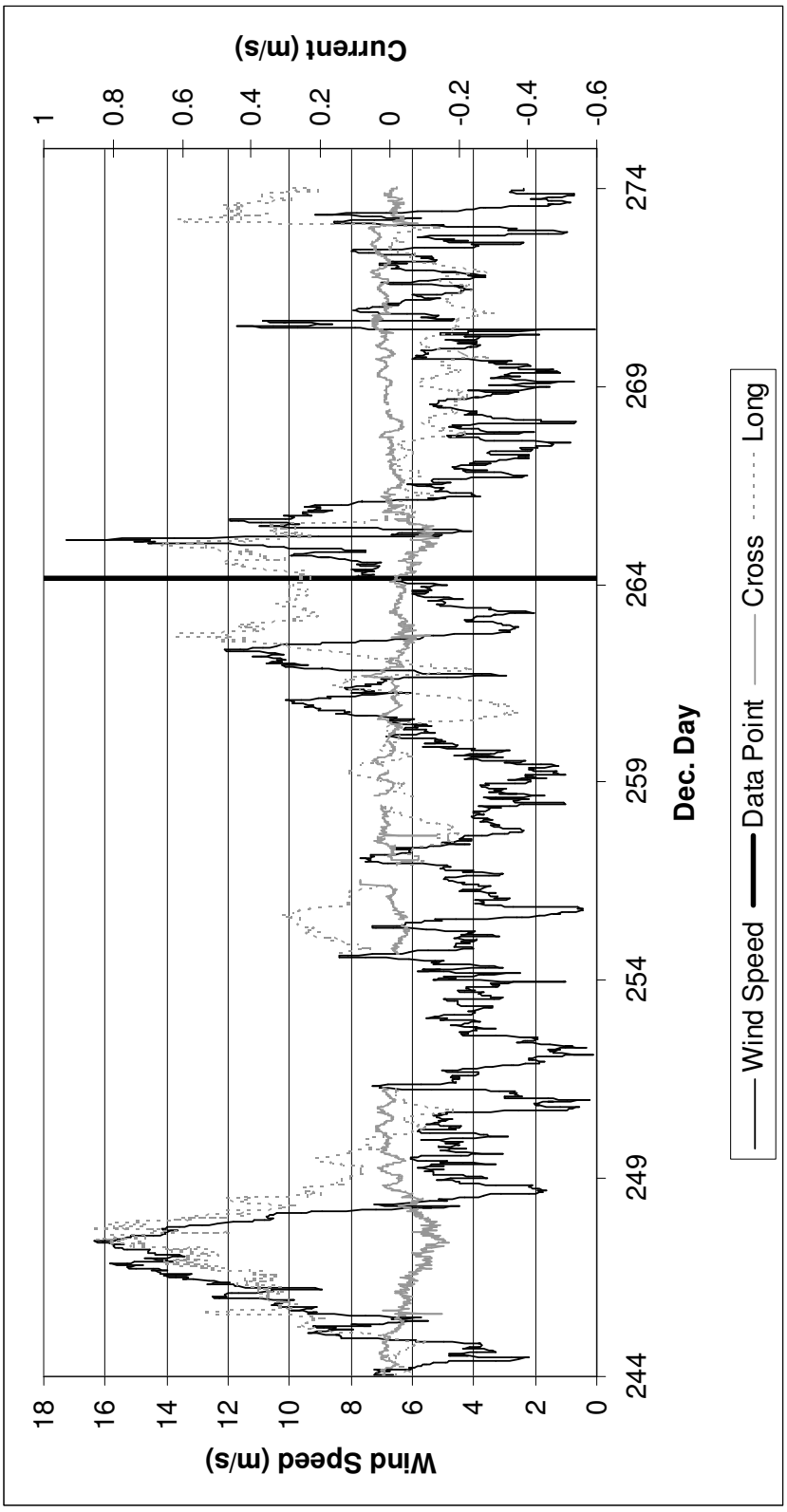

Figure 4.26. Meteorological data on and around the date of interest (dotted black vertical line). Note that there is a peak in longshore velocity around day 264 and a corresponding peak in wind speed.

4.7 Timestep Analysis

To establish a value for the model timestep (see section 4.2.1), several identical runs were carried out with the model, each with a different value for the model timestep. Table 4.3 shows the geological and numerical parameters used for the tests. The models were run for a total of 100kyr with output every 2500 years. To assess the effect of decreasing timestep, the absolute topographic values summed across the whole grid were then calculated for the final output step.

Table 4.3. Parameters used in the stability test of GPM.

Parameter	Value
Display time	2500 years
Diffusion coefficient	7500 m^2/yr
Transport coefficient	20 s/m
Timestep	0.5, 1, 2, 5, 10, 15 or 25 years
Reef sediment grain size	15mm
Non-reef sediment grain size	0.25mm
Maximum reef production rate	3 mm/yr
Maximum non-reef production rate	2 mm/yr
Wave source amplitude	0.25m
Wave source period	3.2s
Wave direction	Perpendicular to shoreline

The results (Figure 4.27) show that as the timestep decreases, the value of the final sum of absolute topography converges to a stable value, as expected. From this, a conservative model timestep of 1 year will be used throughout this thesis, which will ensure stable runs even when making changes to geological parameters, such as eustatic sea level.

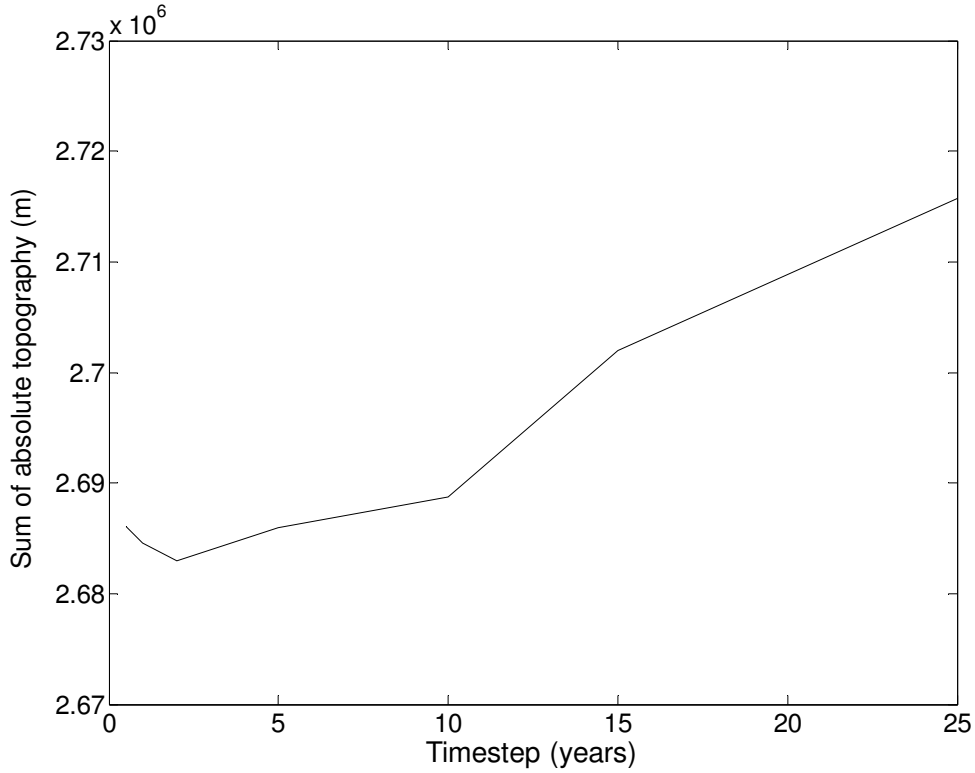

Figure 4.27. Results of the timestep analysis. The vertical axis shows the value of sum of absolute topography (m) from the final output after 100kyr. The horizontal axis shows the value of the model timestep, with higher values to the right. As the model timstep decreases, the sum of topography appears to converge to a stable value. It is estimated that a timestep of around less than 5 years should be used.

4.8 Discussion

This chapter has covered the processes that Carbonate GPM attempts to simulate and details of the algorithms used in order to do this. The key algorithm is the residence time algorithm, which is dependant on the flow produced by GPM. Due to their critical nature, both these algorithms were tested extensively to ensure they produced reasonable results.

The residence time algorithm requires a "start line" from where residence time starts increasing. Determining this proved much more problematic than expected, even using quite sophisticated algorithms. Eventually, the simplest algorithm, using a fixed water depth, proved most effective. This method may also run into problems if the depth, say on a barrier reef, increases to beyond the carbonate production limit

landward of the reef. This would produce two restricted areas, not one as is intended. However, situations like this can be easily recognised and the maximum depth of carbonate production could be increased to counter this problem. This would not affect the carbonate production rates as a series of zero values can be placed in the increased depth range. This may have other consequences, but this would need to be explored further.

The flow algorithm produces a reasonable estimate of the flow measured at Duck, NC, USA, given the limits of Carbonate GPM (it must be able to simulate millions of years in a reasonable amount of time). There are problems with boundary conditions, as occurs with any deterministic model, but these appear rather minimal and should not affect the models use in testing hypothetical premises. However, they would affect the use of Carbonate GPM in any attempt to simulate a real-world carbonate-producing area, in which case periodic boundary conditions (currently no implemented in Carbonate GPM) would be preferable. The flow algorithm is the weakest part of Carbonate GPM. There is no tidal flow, storms or wind influenced currents, mainly due to the difficulty of including these factors in any forward model for simulating geological time periods. The same weakness occurs in every other carbonate forward model.

The timestep analysis of GPM shows that a short model timestep must be used. This is disappointing as runs will take a relatively long time to run to completion (an estimated week of CPU time (3.2GHz P4 processor) per 250kyr). Further changes to the flow algorithm in the future may improve this, which is responsible for the majority of this runtime.

Chapter 5

Modelling of carbonate reefs and platforms with equilibrium thermodynamics

Having established that Carbonate GPM produced numerically valid output for a given timestep, the effect of the new process that Carbonate GPM includes, supersaturation, can now be demonstrated.

5.1 Introduction

Shallow, tropical carbonate production, that is the ability of a platform to produce carbonate sands and grains, has long been thought to be a function of either water depth (e.g. Bosscher and Southam, 1992) or distance from platform the margin (e.g. Bosence and Waltham, 1990). This paradigm has been challenged recently by Demicco and Hardie (2002) who found that residence time - that is the amount of time a parcel of water spends within a region - together with depth can be used to accurately calculate carbonate production of the Great Bahamas Bank. These authors conclude that forward models based on depth-dependent carbonate production alone without reference to circulation and hence residence times across large platforms are therefore invalid.

The biology of carbonate production appears to be ultimately controlled by physicochemical factors (e.g. Kleypas, 1997; Kleypas *et al.*, 1999b). For example, the latitudinal range of carbonate-producing species today is largely governed by temperature and carbonate supersaturation (Opdyke and Wilkinson, 1993). Corals are particularly sensitive to low levels of supersaturation, with production rates increasing three-fold for a four-fold increase in carbonate saturation (Gattuso *et al.*, 1998b). This suggests that it might not be necessary to explicitly include biological processes such a species competition within a model of shallow water carbonate production in order to obtain realistic stratigraphic geometries, such as autocycles, and indeed many

studies show long range (either temporal or spatial) interactions between supersaturation and production rates (Hautmann, 2004).

The chapter follows on from the previous chapter by using Carbonate GPM to simulate a hypothetical carbonate platform to assess the effect of residence time has on carbonate stratigraphy. This is done by comparing two outputs; one with the residence time control turned on, the other without. I show that the inclusion of residence time as a fundamental control could explain several complex phenomena with simple underlying physics and chemistry, such as autocycles, which are currently explained by evocation of a lag time (via various mechanisms) in carbonate deposition post flooding.

5.2 Methods

Two runs are needed to demonstrate the effect of residence time on carbonate stratigraphy. The runs are identical apart from the addition of the residence time algorithm in one of the runs. The parameters used for the runs are those shown in Table 5.1. Both runs used the same parameters (apart from the inclusion of residence time) and a linear relative sea-level curve, simulating a steady subsidence rate of 0.1m/kyr with no eustatic sea-level oscillations. In addition, both runs started with the same antecedent topography (Figure 5.1).

5.3 Results

Having established that Carbonate GPM produces a numerically valid output for a one year modelling time step (chapter 4), the effect of residence time considerations on carbonate stratigraphy can be assessed. Two separate model runs were used in this study. The first used residence time as a controlling parameter on sediment production, the second run did not. All runs used the same parameters (Table 5.1), apart from those indicated in the text, the same starting topography (Figure 5.1) and a linearly increasing relative sea-level curve, simulating steady subsidence of $0.1 m kyr^{-1}$ with no eustatic sea-level oscillations.

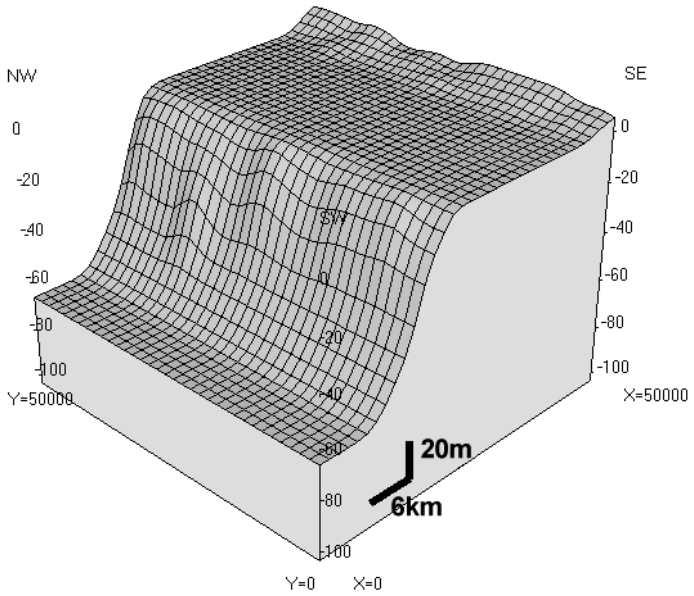

Figure 5.1. Initial topography used for both runs.

Table 5.1. Parameters used in the runs demonstrating the effect of supersaturation and reef transport. Production of carbonate is modified from the maximum values using the functions shown in Figures 4.1, 4.2 and 4.4.

Parameter	**Value**
Display time	2500 years
Diffusion coefficient	1000 m^2/yr (varying with depth)
Transport coefficient	10 s/m
Timestep	1 yr
Reef sediment grain size	15mm
Non-reef sediment grain size	0.25mm
Maximum reef production rate	3 mm/yr
Maximum non-reef production rate	2 mm/yr
Wave source amplitude	0.25m
Wave source period	3.2s
Wave direction	Perpendicular to shore
Cell Dimensions	1470.6 x 1470.6 m
Model size	50 x 50 km (35 x 35 cells)

Overall the model behaves as one would expect given the parameters used. The reef builds along the edge of the antecedent topographic high due to high power dissipation from waves breaking. The reef progrades rapidly to begin with before

aggradation for the duration of the model run (Figure 5.2). In addition, the irregularities in the antecendant topography also produce lateral progradation from the centre of the reef (Figure 5.2A). The model produces occasional patch reefs in the lagoon, which occur due to wave power dissipating in that area (recall that reef growth is dependent on wave power and is zero where wave power dissipated is less than 2W/m^2). Wave power dissipates shoreward of the reef due to erosion (and/or non-deposition coupled with subsidence) creating deeper water behind the reef, allowing waves to propagate from the reef shoreward. Patch reef development occurs in both models runs used here (Figure 5.2B).

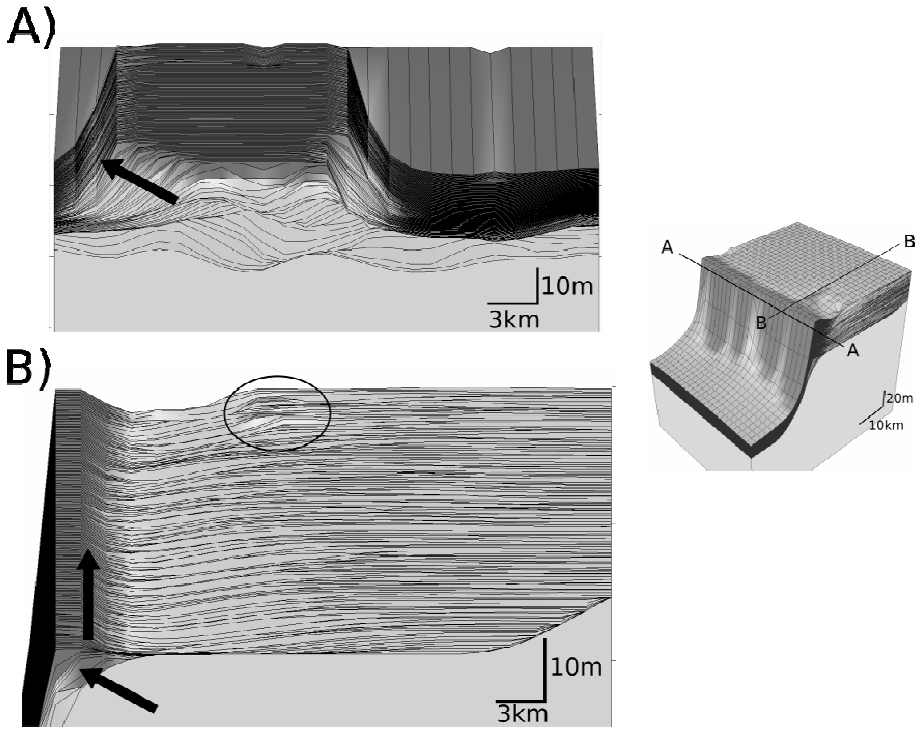

Figure 5.2. Cross-sections of the output from the supersaturation run after 400kyr. Reef sediment is shown in dark grey, non-reef in lighter shades. Section A) shows a section along strike of the reef and highlights the extensive lateral progradation of the reef structure (arrow). Section B) shows a shore-sea section. There is clear initial progradation followed by aggradation of the reef (black arrows) which is controlled by antecedent topography. Also shown is a patch reef that develops in the lagoon area (circled) due to deeper water developing just behind the reef which allows wave power to be dissipated in the lagoon area.

The effect of residence time is best seen in the lagoon, near to the shoreline. Residence time times varied from fractions of a day around the reef to nearly 1000 days. Areas of highest residence time formed in areas near the shoreline where gyres

formed, effectively sequestering the water for prolonged periods of time. The main feature of the residence time in this model is that it is entirely dependant on water flow around the model. Although flow direction and magnitude are both dependant on bathymetry they do not follow bathymetric change exclusively. Hence, residence time changes also do not echo bathymetric changes exactly. The effect of residence time is to suppress carbonate production where residence time is high. As areas of high residence time can vary in size, the areas of low or zero carbonate production also vary in size. This produces "patchy" production, which when combined with steady subsidence produces sea-level oscillations that are local to a particular area. The oscillations arise due to increases in accommodation where production rates are less than subsidence rates, which results in an increase in water depth. This is usually followed by a decrease in residence time, due to less restricted flow, which in turn increases production rates and hence decreases water depth. Therefore plotting water depth changes at any location produces oscillations in water depth (Figure 5.3). When residence time is not used as a control on carbonate production, these oscillation in water depths are not seen (Figure 5.3). Using this set of parameters the model produces water depth oscillations which have a magnitude of around 1m and a periodicity of tens of thousands of year. Of course, these changes in water depth could be a result of non-deposition or erosion (or indeed both). However, given that these water depth oscillations only occur when carbonate production is dependant on residence time and occur adjacent to the shoreline, where flow is weakest, some (if not most) are most certainly caused by shifting of locus of deposition, not by erosion. In areas of high advective transport and low residence time, such as immediately behind the reef, such water depth oscillations are caused by erosion and subsequent filling.

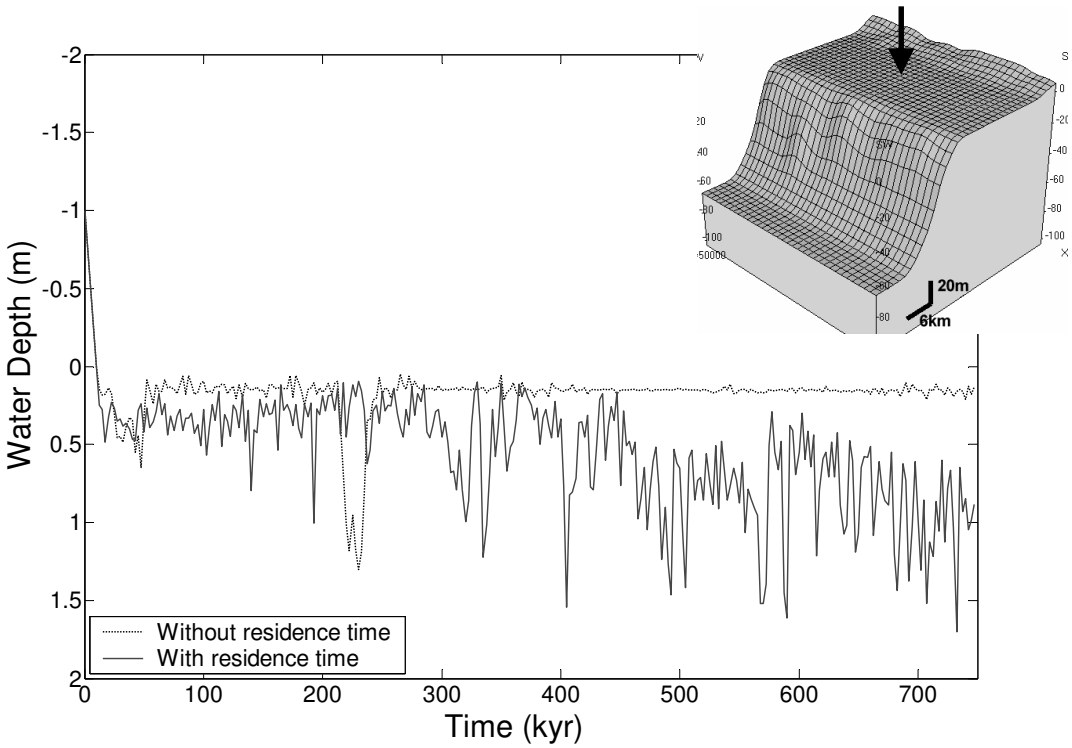

Figure 5.3. Water depth history of a single cell in the lagoon area (see arrow on initial topography insert for location). The dashed line shows the output when not using residence time as a control on carbonate production. The water depth stays at around 0.2m depth for the duration of the run apart from an increase to 1.5m depth at 232.5Kyr. This is cause by erosion rates increasing above production rates for a short period of time. In contrast the output with residence time (solid line) shows repeated fluctuations of water depth on the order of a metre in amplitude. This is caused by production rates being rapidly altered due to the interplay of water flow around the lagoon and residence time.

Due to the suppression of sediment production occurring on both temporal and spatial scales neighbouring localities have different sediment production histories. From observing the model output as it progresses in time, one can see how sediment is produced in one area until either accommodation is filled, or, due to the changing topography, flow patterns changes, moving residence time highs around the lagoon. This switching of production location produces hiatus horizons that are discontinuous spatially. Defining a cycle as the sediment deposited between two hiatus events, one can interpret GPM's output as cycles which occur with no eustatic sea-level oscillatory forcing – autocycles. In other words, including residence time in a computer model has caused the occurrence of autocycles, which manifest themselves as rapid changes in water depth due to two-dimensional differences in sediment

production over the lagoon. Without residence time, the sediment production fills available accommodation and is near uniform across the lagoon area. Any differences are entirely due to sediment transport and re-deposition.

The scales of this patchy production vary in spatial size from a few square kilometres to (very occasionally) the whole of the modelled lagoon (around 1200km^2). The patches of production tend to have a fairly short lifespan, often lasting up to only 10,000 years. However, the lower limit on this resolution is the model display step, 2500 years, limiting the lower value. Patches of production can also be seen to move across the lagoon, moving both laterally and ocean-ward (Figure 5.4 and 5.5). If this sediment is not eroded, this movement manifests as progradation in the stratigraphy. Given the subsidence rate of 0.1m/kyr any sediment accumulation above this rate must be proceeded by a period of erosion or non-deposition in order to create the necessary accommodation. This is exactly what is observed in the model output; rapid deposition nearly always immediately follows erosion.

5.4 Discussion

The two key differences of Carbonate GPM and previous carbonate models are the inclusion of supersaturation-related production via lagoonal water residence time and the explicit differentiation of reef transport from that of other sediments. These two features generate notable differences in the output produced by the model. The experiments outlined above are not intended to replicate a particular real-world locality in any way. The relative sea-level increased linearly throughout, simulating linear subsidence and no eustatic sea-level changes; clearly something that does not occur over long periods of time in the geological record. However, useful insight can be derived between the output generated and carbonate settings, both modern and ancient.

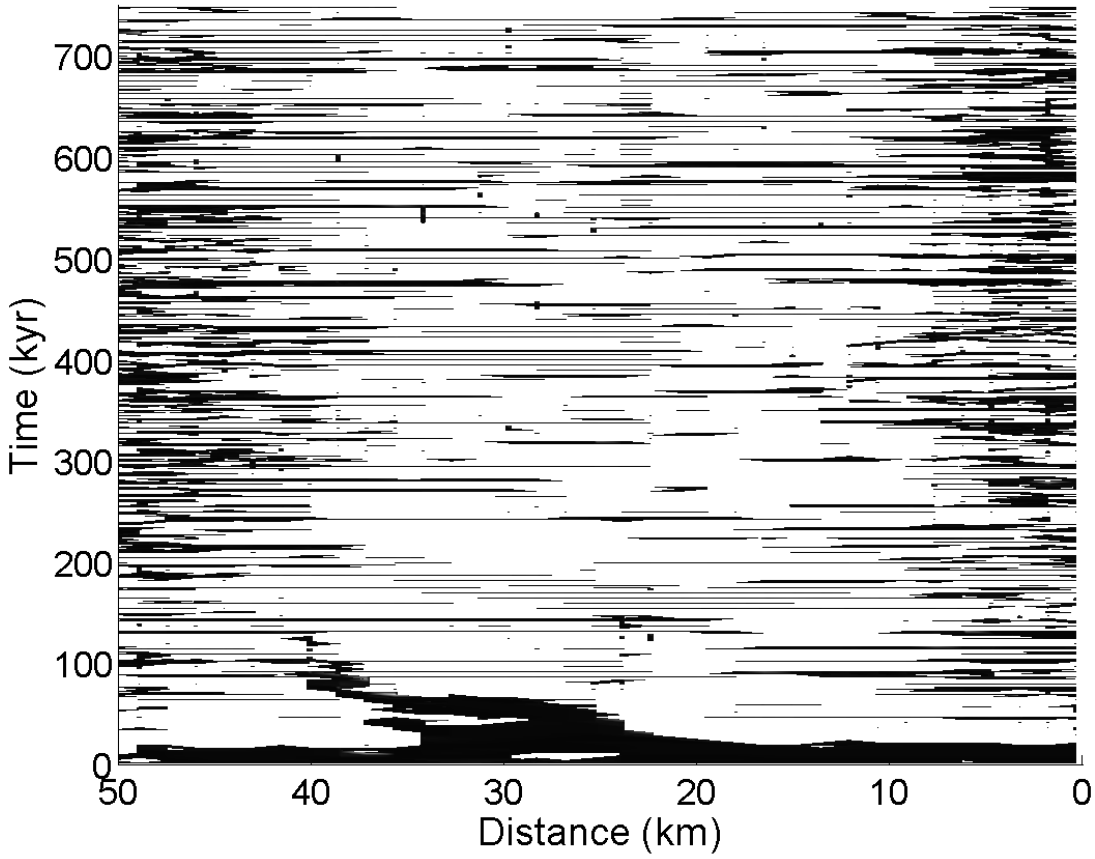

Figure 5.4. View of a 3D volume from an edge which shows temporal and spatial scales of deposition. The view is from the shoreline towards the open-ocean edge, with time increasing from 0 years at the base of the y-axis to 750kyrs at the top. The dark areas represent areas and times where deposition was above 0.6m/kyr. The initial reef growth can be clearly between 40 and 20km along the x-axis and lasts some 100kyr. There is also clear lateral progradtion of the reef. The rest of the production is largely in the lagoon and is generally short in duration covering a variable-sized area. Areas of lateral progradation can be identified. A similar view perpendicular to this figure (Figure 5.5) shows some progradation reefward in the lagoon also.

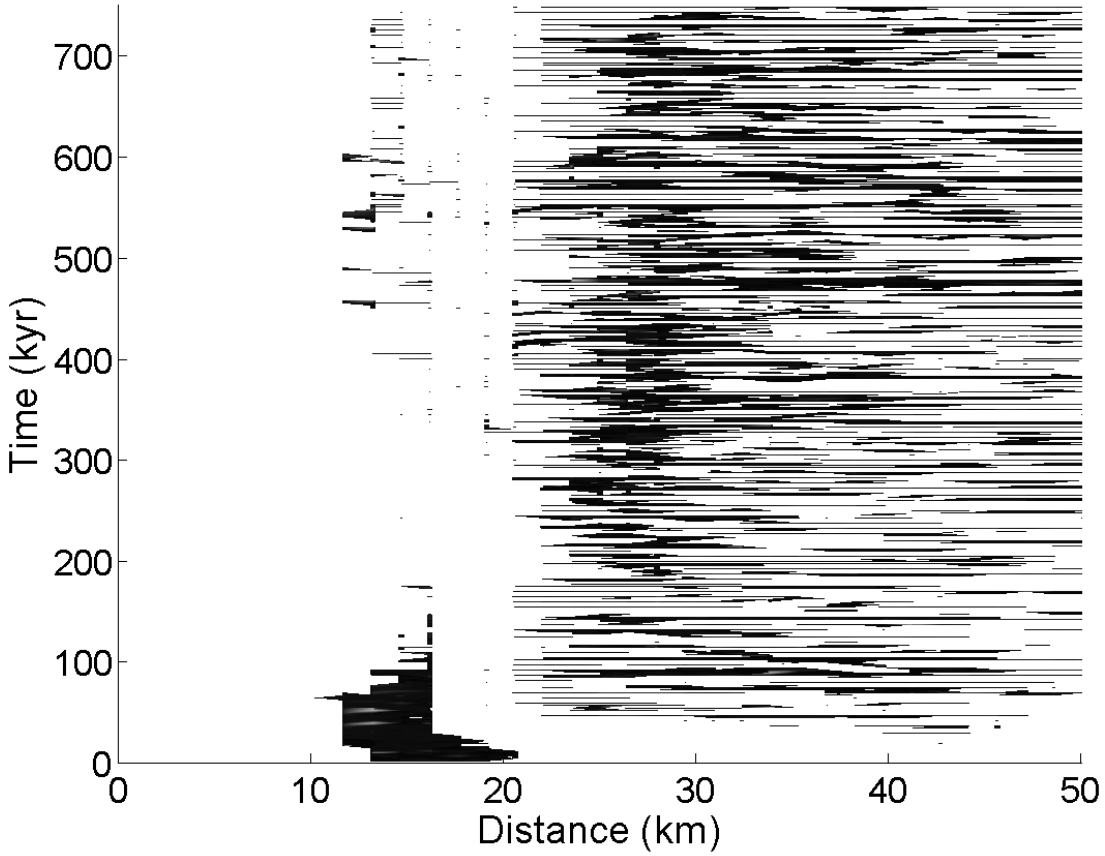

Figure 5.5. Perpendicular view to Figure 5.4 showing sediment production. The left-hand side is the open ocean, the right-hand side is the shoreline. Again, the reef growth is clearly visible between 10 and 20km on the x-axis. Most depositions occurs between 5 and 20km from the reef and there a many periods of time where deposition is greater than the 06.m/kyr threshold deposition near the shoreline.

The residence time process encapsulated within GPM is clearly the key process. Given that this process depends heavily on flow it is important to ensure that accumulation rates produced via this mechanism are representative of the flux, which determines recharge rates of carbonate ions. Essentially, one needs to ensure that the production due to residence time fluctuations is "mass balanced"; the mass entering the system (via fluid movement) should dictate the mass of carbonate produced. The flux has already been tested against real-world data (previous chapter) and compares favourably to it. The "mass balance" can be tested quite simply in GPM by considering the case of a simple "canal", with a known cross sectional area, and measuring the amount of carbonate deposited given a known flux. Only the residence time process was enabled; depth-dependant and waver power dependant production

were disabled. A fixed flux was applied to the fluid flow and the amount of carbonate produced (in metres, summed over the whole canal) recorded. A total of seven runs were carried out, each with a different flux. The length of the canal was such that the highest flux (i.e. fastest flow) still resulted in residence times above the maximum residence time for any production to occur (250 days) at the far end of the canal. The results of this show an unambiguous linear relationship between flux and carbonate produced, showing that for a given volume of flux we produce an amount of carbonate that is consistent with this flux.

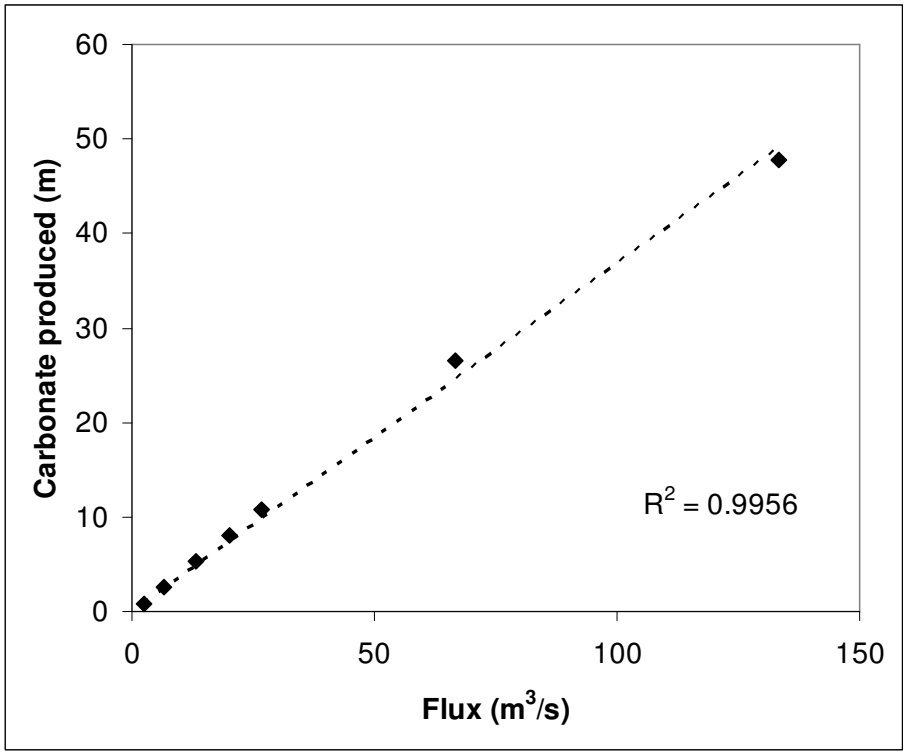

Figure 5.6. Relationship between carbonate produced and flux. There is a clear linear relationship here, showing that the carbonate produced is representative of the flow of water.

The transport algorithm in Carbonate GPM is based on fundamental physical processes. While other models use a more simplistic model of transport that is only dependant on depth (Burgess, 2001; Burgess *et al.*, 2001; Burgess and Wright, 2003; Burgess and Emery, 2004; Burgess, 2006), the flow in GPM wanes as you approach the shoreline, reducing transport accordingly. Comparing Carbonate GPM to other models, such as that by Burgess and Emery (2004) contain a transport profile such that advective transport is controlled by water depth only (Figure 5.7 and equations

5.1 and 5.2 from Burgess and Emery (2004)), clearly shows this reduction in flow due to depth.

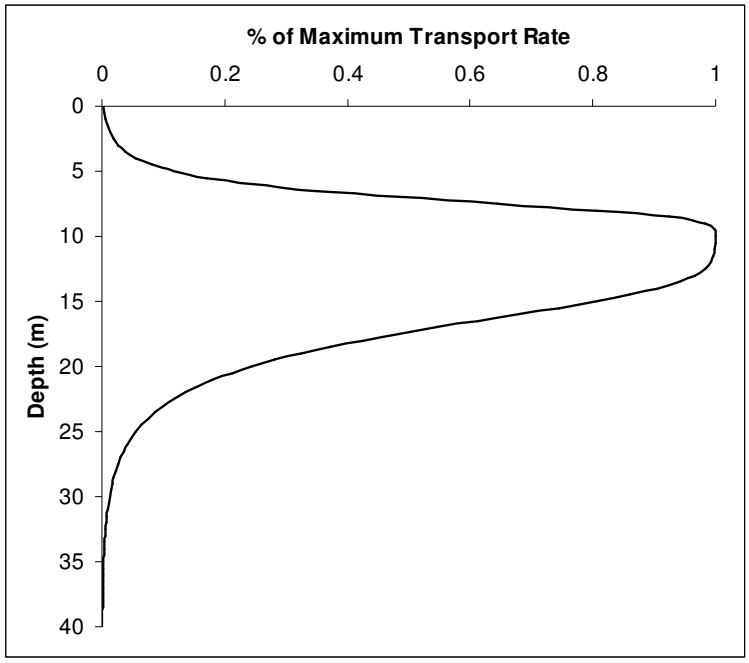

Figure 5.7. Transport profile used by Burgess and Emery (2004).

$$e_{xy}\left(z_{xy} > 10\right) = e_{\max} \cdot \tanh(5 \cdot \exp(-0.75 \cdot (z_{xy} - z_{t\max}))) \cdot \ell \qquad (5.1)$$

$$e_{xy}\left(z_{xy} \le 10\right) = e_{\max} \cdot \tanh(5 \cdot \exp(-0.30 \cdot (z_{t\max} - z_{xy}))) \cdot \ell \qquad (5.2)$$

This curve is justified in the text (Burgess and Emery, 2004):

> *"Erosion and entrainment increases with water depth to a maximum at 10m in response to increasing wave energy with decreasing friction due to decreasing bottom contact, and then decreases with depth in response to decreasing wave orbital motion."*

The form of the curve shown in Figure 5.7 is commonly used as a proxy to transport rates and can be justified by considering a sloping bathymetry onto which waves of many different wavelengths (and height) are impacting. These waves cover the range of periods and height from short period fair-weather waves to very high, long wavelength storm waves. The short waves will carry almost all of their energy into the shallowest water. The storm waves will break in deeper water, but will dissipate much more energy and so comparatively less energy reaches shallow water. Overall, the highest energy and therefore sediment transport is therefore found in deeper water.

The problem with the "profile" approach is that it assumes that there is no lateral variation and depends heavily on the bathymetric profile. This profile may not be valid on a bathymetry that includes a very steep drop, such as a reef-edged platform.

However, Carbonate GPM explicitly models wave energy dissipated and wave induced currents and therefore should generate a profile similar to that in Figure 5.7, but with significant variations in transport rates as the flow wanes towards the shoreline. The profile may not be an exact match to that occurring in reality as Carbonate GPM only contains a single wave period and amplitude, rather than a full spectrum, but should be very similar to Figure 5.7.

Using the same bathymetry as shown in Figure 5.1, the transport rate (magnitude of the transport vector) was output from each node throughout a run. This was then plotted against depth to produce a depth-dependent transport profile. The profile is remarkably similar to that shown in Figure 5.7 when considering the maximum transport at each depth. However, the profile shows much more variation of transport rates at each depth, showing that Carbonate GPM includes a more detailed, but still theoretically accurate, transport algorithm.

The effect of this waning flow can be further shown by considering the transport rates at a single timestep. Similarly to above, the magnitude of velocity (which is proportional to transport rate) can be plotted across the simulation (Figure 5.9). The flow is highest across the reef, as expected. The flow then wanes as it approaches the shoreline. This explains why sediment is not transported all the way to the shore to produce prograding islands as in other models, despite Carbonate GPM containing all the necessary processes. However, this may only be true for this set of parameters and more investigation is required.

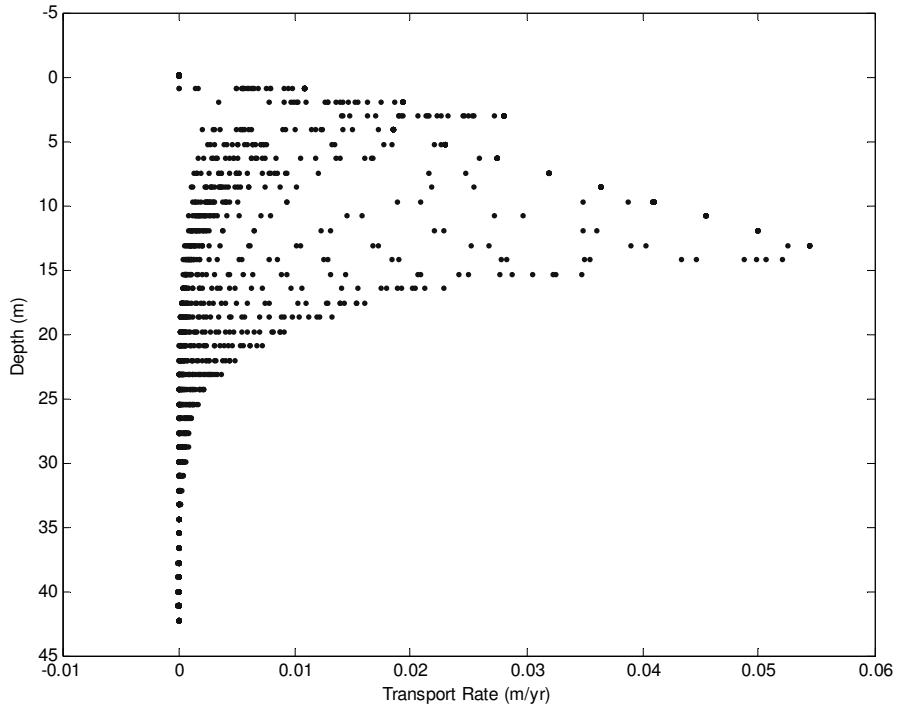

Figure 5.8. Transport profile generated in GPM. Note the similarity in shape to Figure 5.7 and the variability at each depth as the flow wanes towards the shoreline.

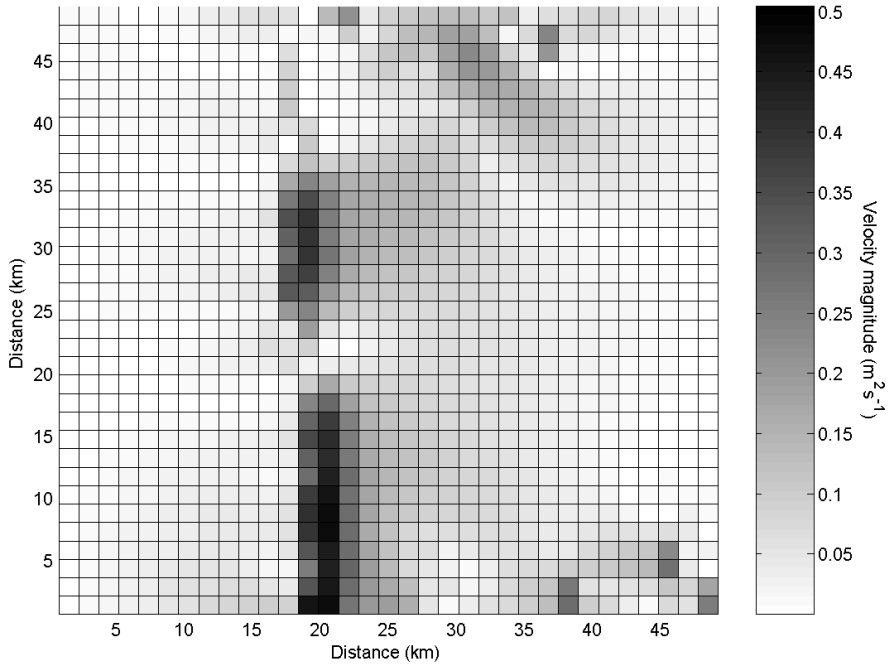

Figure 5.9. Plot of velocity magnitude at every point in the run at 250kyr. The reef is highlighted by a region of high transport (dark colours), which wanes as the shoreline is approached.

The results from this experiment described here highlights an important phenomenon often included in carbonate models: namely the "lag" phenomenon, which is observed on many ancient platforms (Enos, 1991). Carbonate GPM simulates this effect without having it explicitly encoded into the model, as with previous models (e.g. Bosence and Waltham, 1990; Warrlich *et al.*, 2002). The formative cause of this phenomenon is the switching of deposition locus as the flow regime shifts within the lagoon area. The shifting of this locus is due to the complicated feedback and interaction between all of the processes embodied in the model – all processes included have an effect on one or more of the other processes. In addition, the non-linearity of the embodied processes can cause, what is otherwise a steady-state model, to exhibit large and seemingly sudden events. The only other models that are able to simulate this behaviour without an explicit lag are those of Tipper (1997) and Burgess and Emery (2004), both of which use cellular automata algorithms to simulate the colonisation effect of biology.

5.5 Conclusions

A new carbonate forward model, Carbonate GPM, was used to support the argument put forward by Demicco and Hardie (2002) that using a simple proxy for supersaturation by incorporating distance from the open marine settings is inadequate to simulate carbonate production. Instead, proper consideration for the circulation of fluid on the platform is required to predict areas of higher residence time and hence of lower production rates. Carbonate GPM incorporates sediment transport and erosion, wave action, water depth-related carbonate production and residence time, and is based on mathematical representations of sedimentological and stratigraphic processes. Carbonate GPM therefore confirms the conclusion of Demicco and Hardie (2002) that circulation patterns on the platform are crucial to predicting carbonate accumulation rates and previous models that incorporate a production vs. "distance to open marine sources" relationship are invalid.

The residence time algorithm embodied in Carbonate GPM behaves well producing a very clear relationship between fluid flux entering the system and carbonate deposited. The flow algorithm which determines this flux also explains why sediment is not transported to the shoreline to produce so-called "prograding islands". The flow

rates fall, and hence transport rates also fall, as the shoreline is approached. This is a much more detailed algorithm than used in previous models. It remains unclear if Carbonate GPM *could* simulate prograding islands and more work will be needed to test this.

Despite the lack of prograding islands, abundant cycles form in lagoon areas due to horizontal movement of the locus of maximum sedimentation as water currents and hence the supersaturation distribution changes with time. Cycles form even in the absence of high-frequency sea-level oscillations and are therefore unequivocal autocycles. The effect of residence time is to cause a natural lag phenomenon without any appeal to biological processes such as colonisation of areas (Tipper, 1997; Burgess and Emery, 2004).

Chapter 6

Complexity in Carbonate Deposition

Carbonate sediments are often highly heterogeneous due to the numerous factors that control deposition. Several of these processes are non-linear, so that depositional stratigraphies may consequently form complicated, perhaps even chaotic, geometries. Forward modelling can help to elucidate the interactions between the various processes involved. Here, a deterministic three-dimensional forward model of carbonate production and deposition (Carbonate GPM) is used, which is specifically designed to test the interactions between the three main depositional controls: light intensity, wave power and carbonate supersaturation, the latter of which is unique to this model. The results of this analysis suggest that it may be impossible to predict in detail the stratigraphy of carbonate deposits due to its super-sensitivity to initial conditions or controlling parameters. Results from two model runs which are identical apart from a one metre change in initial conditions at one location are broadly similar but differ in detail. This reinforces the conclusions reached using previous process models. However, unlike previous models, this model does not explicitly include non-linear biological interactions as a control. Instead it shows that similar sensitive behaviour may originate from physicochemical processes alone.

6.1 Introduction

Carbonates form notoriously complex sedimentary systems, often displaying spatially variable facies distributions (Rankey, 2002; Wilkinson and Drummond, 2004) and incomplete successions with abundant hiatuses (Algeo and Wilkinson, 1988; Burgess and Wright, 2003). Not only are carbonate geometries governed by the external forcing mechanisms universal to all sedimentary systems, such as sea-level oscillations and local climatic conditions, but carbonate production itself is further controlled by the interplay of biological and physicochemical processes that operate over multiple time scales. As a result, a consensus is now emerging that carbonate

systems may be capable of creating apparent complexity that is an emergent property of the processes unique to carbonate production but independent of any external forcing mechanisms (e.g. Drummond and Wilkinson, 1993a; Wilkinson *et al.*, 1999; Burgess, 2001; Burgess and Emery, 2004).

Several processes involved in carbonate production are non-linear in the sense that their response is not directly proportional to changes in controlling parameters or conditions. Interactions between non-linear processes can lead to chaotic behaviour (Nicolis and Nicolis, 1991) and a key feature of chaotic systems is their sensitivity to initial conditions. Chaotic behaviour in carbonates has recently been sought by Burgess and Emery (2004) using a forward model that included interactions between biological communities. Burgess and Emery found that, although complicated, the water depth changes at a single point through time were not chaotically dependent on initial conditions. Burgess and Emery's model produced cyclical, quasi-periodic shallowing upwards stratigraphy, without any sea level oscillations, clearly demonstrating the non-linear effect of internal controls on carbonate production. However, a significant component of the nonlinearity in Burgess and Emery's model is derived from a matrix of competing biological communities with controlling parameters that are currently poorly known in carbonate systems.

This chapter describes the initial starting parameters used for the two model runs used in this study. The results from the two cases where the starting topography differed by only one metre at one location are then described. The differences between the two models are highlighted as are any similarities. The water depth history and autocyclic thickness record at a single location is used to assess whether the output from the model is chaotic. The chapter concludes with a discussion section.

6.2 Methods

The experiment carried out is based on that described in detail by Burgess and Emery (2004). Two model runs were produced which used identical parameters, including a relative sea level curve that included subsidence only (Figure 6.1). The only difference between the two runs is a one metre change of topography at one node, henceforth referred to as the α-node (Figure 6.1). The two runs were then run forward

for 750 kyr and data were output every 2500 years, producing 300 data points in total. All other parameters are described in Table 6.1.

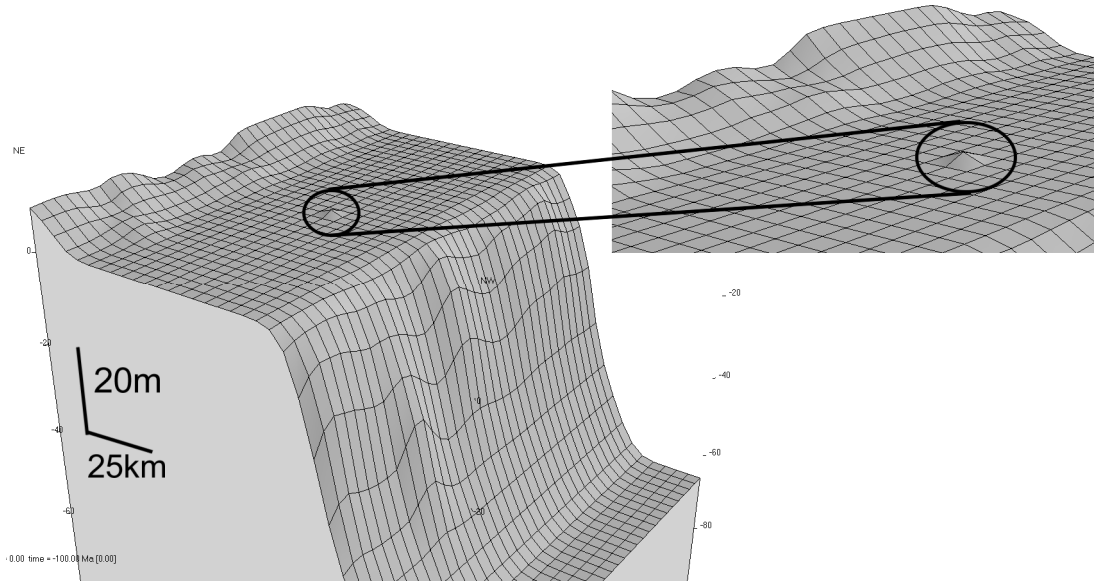

Figure 6.1. The starting topographies for the two experimental runs. The node at which the topography was raised by one metre is highlighted on the top-centre plot. Note that there is a 450x vertical exaggeration in order to show the one metre difference.

Table 6.1. Parameters used in both runs described in this chapter.

Parameter	Value
Display time	2500 years
Diffusion coefficient	7500 m^2/yr
Transport coefficient	20 s/m
Timestep	1 year
Reef sediment grain size	15mm
Non-reef sediment grain size	0.25mm
Maximum reef production rate	3 mm/yr
Maximum non-reef production rate	2 mm/yr
Wave source amplitude	0.25m
Wave source period	3.2s
Wave direction	Perpendicular to shore

6.3 Results from Model Experiments

Both runs typically show similarities in their overall final stratigraphic geometries. In each run cycles are formed by areas of subdued sedimentation rates across the back-lagoon area. This is due to the effect of supersaturation calculated via residence time, which as described in the previous chapter interacts with the flow and topography to produce quite complex feedback mechanisms (Figure 6.2). The intricate relationships between residence time (which is the proxy for supersaturation), water depth, flow, and sedimentation rates is allows the small one metre difference in starting topography to change the details of sedimentation over the 750 kyr simulation time.

The statistical properties of the cycles produced by the two runs are useful to demonstrate how complicated patterns of sediment deposition can be formed from internal forcings alone. One of the most striking things about models that produce autocycles is that there is no order to the cycle thicknesses generated (Burgess and Emery, 2004). The simplest way of representing this is to plot the thickness of one cycle (n) against the thickness of the proceeding cycle (n+1). Analysing the data in this manner produced no visible patterns at any location around the reef or lagoon (Figure 6.3).

The relationship between cycles can be further analysed using the Durbin-Watson test (Durbin and Watson, 1950, 1951), which tests if the null hypothesis of no correlation between adjacent values can be rejected. The cycles produced at the α-node were analysed and produced a value of 0.7028 (the critical value is 1.26 for an uncertainty of 0.01). This means the null hypothesis can be rejected and hence the cycle thickness at any one time may be dependent on the previous cycle thickness. Other cells analysed confirm this result, meaning that cycle thicknesses in a single vertical section may show some predictable patterns, but this may not apply to the formation as a whole as adjacent cells produce different cycle thicknesses and even different numbers of cycles.

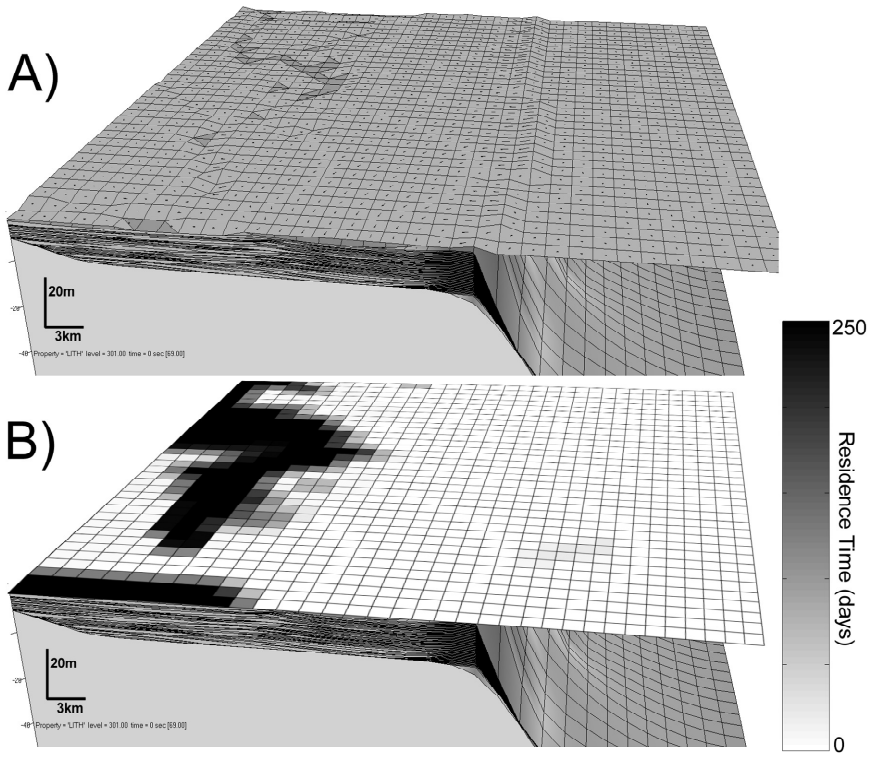

Figure 6.2. The effect of islands on the residence time. A snapshot of the Carbonate GPM output after 160 kyr with arrows showing the direction and magnitude of the wave induced flow (A). Islands can be seen in the lagoon that causes the flow to refract around them. This then causes local changes in the residence time in the vicinity of the islands (B). The scale in B shows the residence time in days.

In addition to the cycle thickness variation with time, the distribution of cycle thicknesses highlights the differences between the two model runs. A histogram of cycle thickness distribution in the back-lagoon area shows that both runs produce a near-exponential cycle thickness distribution, which matches well to those distributions found in ancient settings (Wilkinson *et al.*, 1998; Wilkinson *et al.*, 1999). However, the mean cycle thickness and the number of cycles produced differ for both runs, highlighting that a minor change in a single starting parameter can change the final stratigraphy.

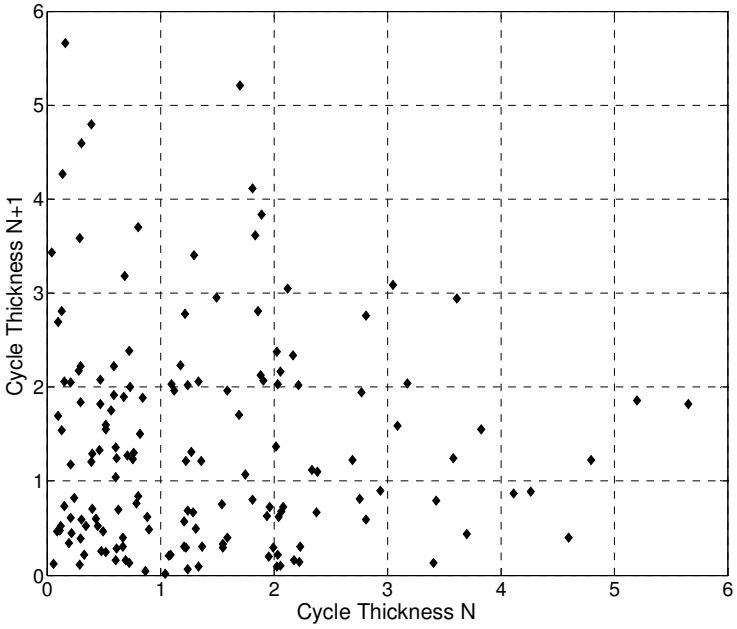

Figure 6.3. Thickness of cycle n plotted against thickness of cycle n+1 for a small cluster of four cells. There are no discernable patterns apart from smaller cycles generally following thicker cycles and vice versa.

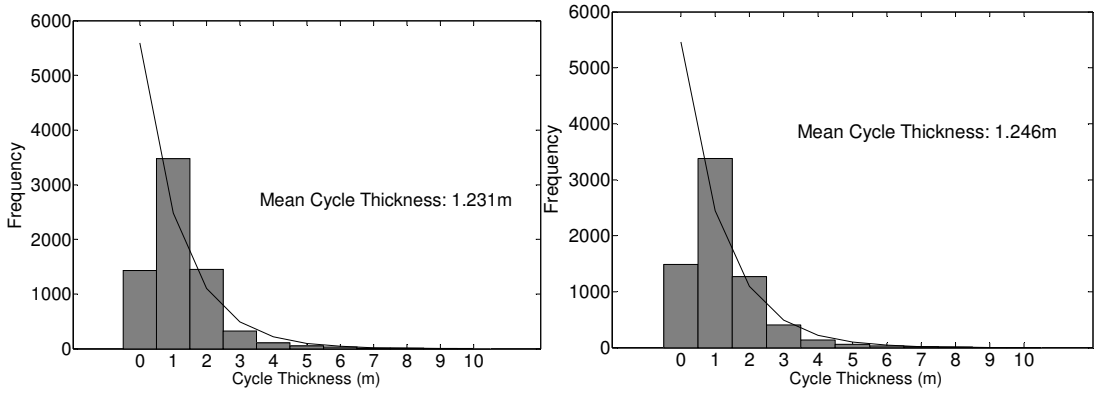

Figure 6.4. Cycle thickness distributions for Run 1 (left plot) and Run 2 (right plot). Both show similar distributions and appear to be similar to a Poisson distribution (black line) as found on many ancient peritidal carbonates (see next chapter for more detail on this).

6.4 Complicated or Chaotic?

In seeking indications of chaotic behaviour, water depth changes at any one point through time can be analysed (Figure 6.5). The first step is to create a power spectrum of the data, which will show if there is any periodicity to the system. A chaotic time series will have a spectrum with no obvious periodicities (Williams, 1997). The power spectrum of the water depth changes at the α-node from Run 1 shows there are some

dominant periodicities present in the time series (Figure 6.6). The peaks correspond to approximately 640 kyr, 32 kyr and a small peak at 14 kyr. A second cell, 3km away, shows peaks at 106 kyr, 16.4 kyr and 12.5 kyr. Note that these values are remarkably close to some Milankovitch frequencies (19, 23, 41 and 100 kyr) (Hinnov, 2000) which confirms that autocyclic processes may present Milankovitch-like signals from ancient deposits. Given that the water depth history shows a clear periodic signal, the system cannot be chaotic, but is not clearly predictable.

A.

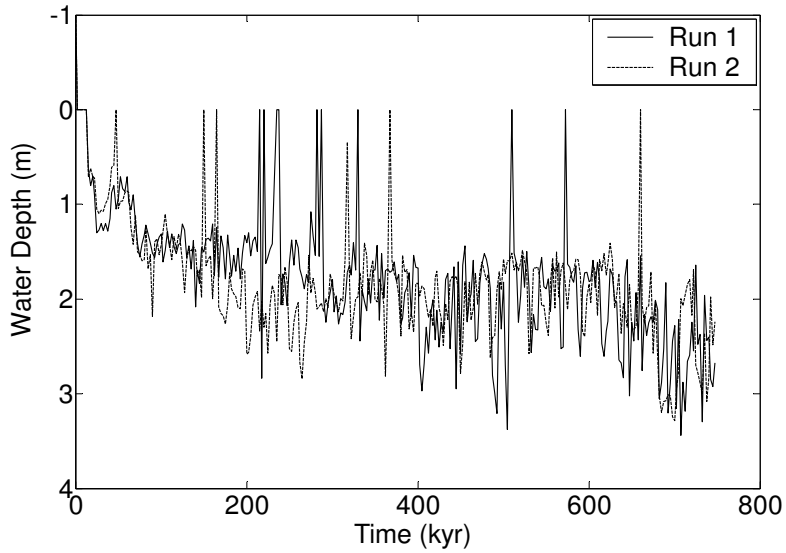

B.

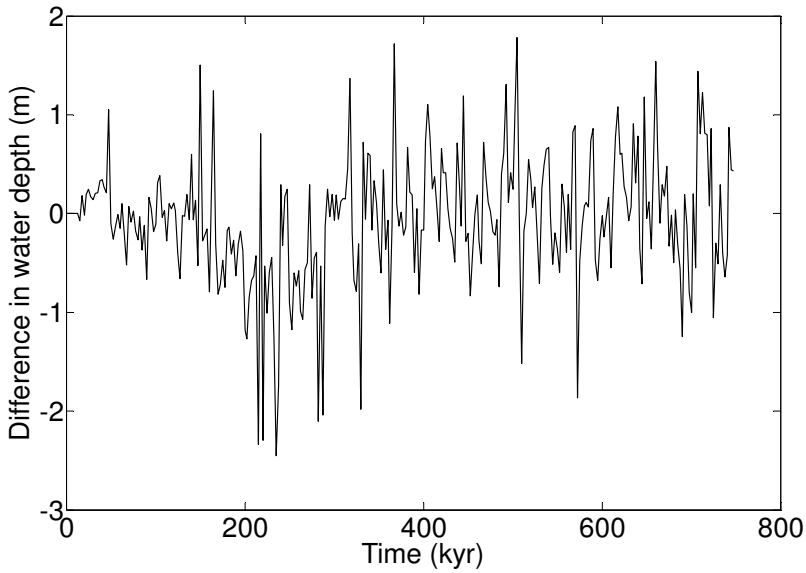

Figure 6.5. Comparison of the water depth histories of the two runs (A). Panel B. shows the difference between the curves in A.

Are the peaks in the power spectrum in Figure 6.6 significant? To test this, a random model white-noise model was used. The mean depth from the standard run from a location in the centre of the lagoon was used as a starting value. Then, a random value was added at each display step. Three different models were tried, each with different amplitudes of random oscillations; 0.5m, 1m and an amplitude equal to the variance of the water depth history of the cell (0.46m). The most pessimistic (i.e. random processes dominate) of these models, therefore, is the 1m random oscillation model. For each model 1000 realisations were carried out and the power spectrum calculated each time. The maximum peak for each realisation was recorded.

The results (Figure 6.6 show that even using the 1m amplitude model, there are still peaks in the water depth power spectrum that are significantly greater than the 99% of the greatest peak value from the random model. The three highest peaks are at 106.67kyr, 12.55kyr and 16.41kyr for the first point and 640.2kyr, 32kyr and 16kyr for the second point. Recall that these points are only 3km away from each other, yet show a difference in the highest peaks. This is overlap in some peaks however.

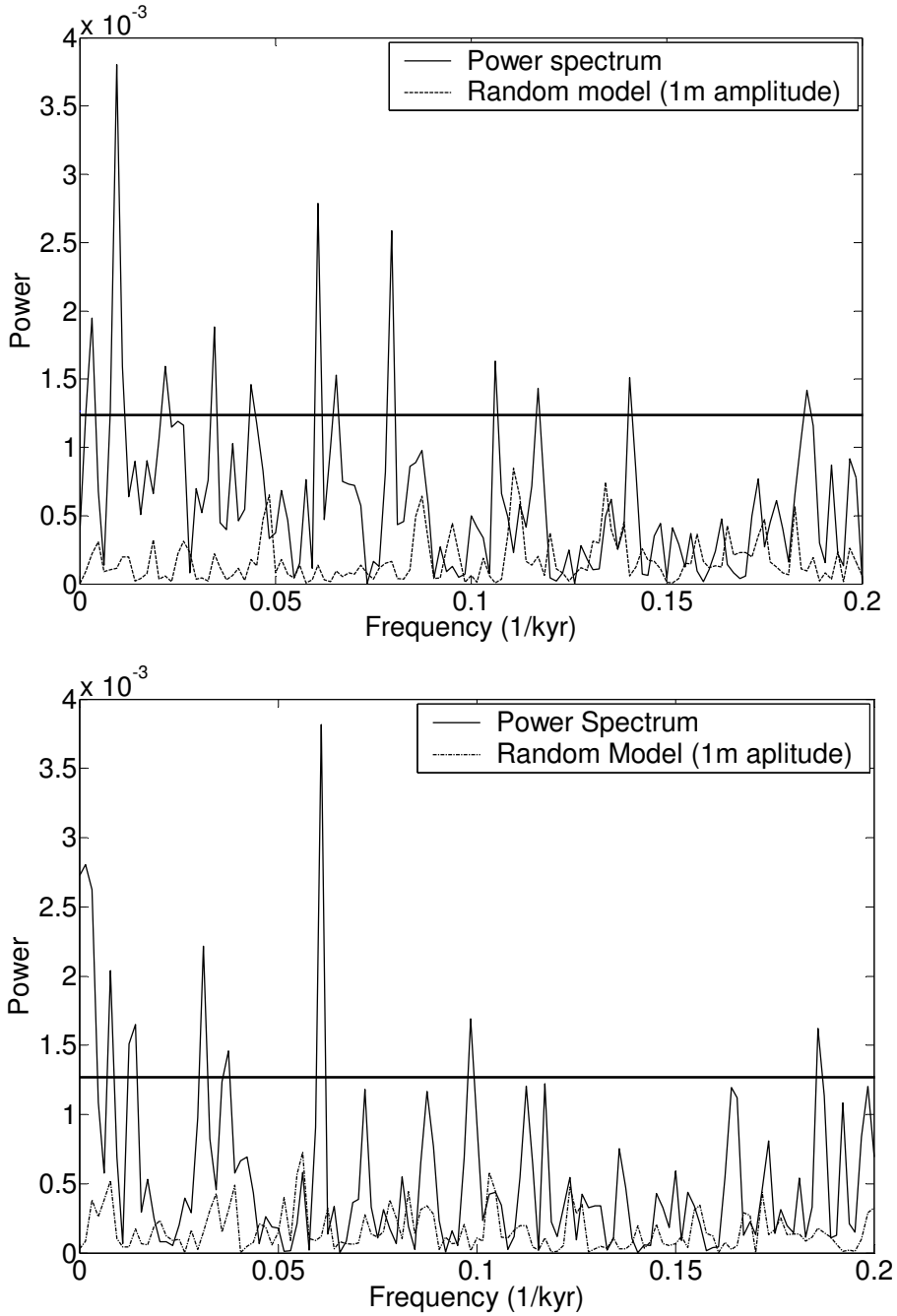

Figure 6.5. Power spectrum calculated using the water depth changes at the altered node from Run 1(top) and a node just 3km away (bottom). There are clear differences in where the main peak occurs and subsequent peaks. The other power spectra show a single realisation of the three random models tried. The black horizontal line shows the value of the 95% percentile of the most pessimistic model: the 1m amplitude model. There are four peaks that are clearly greater than this value.

6.5 Discussion and Conclusions

The numerical forward model presented here includes three major processes controlling carbonate production, which together with transport and erosion of deposited sediment has shown behaviour that is sensitive to initial conditions. Other carbonate models have also shown this type of behaviour (Burgess and Emery, 2004). Carbonate GPM does not produce chaotic behaviour when taking information from a single location through time and the data suggest that it may be possible to derive a statistical model of cycle distribution for a vertical section based on a smaller data sample in the same locality. However, this does not apply laterally. If one were to base a model of cycles derived for a vertical section, that model could not be applied to a nearby locality as they give a different power spectrum (Figure 6.5), water depth history and cycle history even within the same formation. Overall, this suggests that for a single, vertical section carbonate stratigraphy may be statistically predictable, but any lateral movement invalidates a model derived from one locality and applied to a nearby vertical section

The results of this work indicate that such complicated stratigraphies may be an inherent property of a shallow-marine carbonate system. Including biological activity, such as that of Burgess and Emery (2004), may increase the complexity of the stratigraphy. This raises the possibility that it may be impossible to predict the stratigraphy of a carbonate formation in detail. Instead statistical descriptions must be used. The effect that external controls have on the carbonate system is uncertain and is discussed in the next chapter. However, it was found that they do not entirely overwhelm the effect of internal controls used in this model and do not produce ordered successions.

Chapter 7

The Origins of Peritidal Carbonate Cyclicity

The production of carbonate sediments may be controlled by the interaction of several non-linear, internal processes. However, carbonates are also subjected to the external controls that are universal to all sedimentary systems, such as sea-level oscillations. One of the current debates in carbonate research is over what is the main controls governing the production of peritidal carbonate metre-scale cycles. Two hypotheses have been proposed: extrinsic controls dominate and the cycles are therefore allocycles or intrinsic controls dominate and the cycles are therefore autocycles. Many studies have been carried out in the past using computer models in an attempt to elucidate these hypotheses. However, no model to date has used supersaturation as a control on carbonate production and tested the effect of sea-level changes as an external forcing mechanism. This study uses a forward carbonate model, Carbonate GPM, which is capable of generating autocycles with a range of relative sea-level curves that include three different periodicities and amplitudes. The tests performed here include three different periodicities and amplitudes reflecting current accepted opinion about sea level fluctuations of 3^{rd}, 4^{th} and 5^{th} order oscillations. The results show that using eustatic sea-level changes described as 3^{rd} and 4^{th} order oscillations produce clear changes in the stratigraphy generated when compared to autocyclic mechanisms alone, showing that the effect of such oscillations is significant compared to the effect of autocyclic mechanisms. However, 5^{th} order sea-level changes in conjunction with intrinsic controls produce stratigraphy that is indistinguishable from that produced by intrinsic controls only. In addition, the cycles generated without any external controls correspond well with the thickness distributions found on many ancient deposits.

7.1 Introduction

The repetition of metre-scale carbonate units is common in many ancient deposits, but particularly in peritidal deposits. These units are often interpreted as shallowing-upwards cycles, representing changes in glacio-eustatic sea-level as shown by the changes in facies. Glacio-eustatic sea-level changes are short-lived transgressive events which are driven by orbital forcing: Milankovitch cycles (Tucker and Wright, 1990). The premise behind these cycles is that changes in precession (periodicity of 23,000 and 19,000 years), obliquity (41,000 years) and eccentricity (100,000 years) gives rise to insolation changes and that these variations cause fluctuations in the polar ice-caps, which in turn are the underlying cause for the required sea-level fluctuations (Hinnov, 2000). Data from Pleistocene deep sea cores show that the 100,000 year cycle is the major influence and that sea-level rises were much more rapid than the sea-level falls (Pillans *et al.*, 1998). The significance of glacio-eustatic forcing is not just a desire to understand the underlying forcing mechanisms. If cyclic accumulations of these sediments is driven by sea-level fluctuations a high resolution, temporal framework exists within ancient deposits, that would allow for the measurement of sediment accumulation rates, biological evolution and correlation in unprecedented detail (Drummond and Wilkinson, 1993b).

The utility of interpreting carbonate stratigraphy in this manner stems from the recognition of a heirachaical set of finer-scale units nested within larger-scale units (Lehrmann and Goldhammer, 1999). This arrangement is thought to arise due to carbonate sedimentation being strongly controlled by water depth or accommodation, which in turn is driven by hierarchical fluctuations in sea-level (Goldhammer *et al.*, 1990). It is therefore convenient that the carbonate stratigraphic record can be discussed in the temporal terms of these sea-level fluctuations, which are second order (10-100my, third order (1-10my), fourth order (0.1-1my) and fifth order (0.01-0.1my) (Goldhammer *et al.*, 1993). In terms of geologic record, fourth and fifth order are expressed as parasequences, parasequence sets, and high-frequency sequences, recognised at outcrop, core and well log level. Third and second order changes are represented as sequences and composite sequences as large-scale outcrop and seismic level (Lehrmann and Goldhammer, 1999). Lehrmann and Goldhammer (1999) define

five types of stratigraphic units based on which orders are preserved and form the lower-order sequences (Figure 7.1):

1. Fifth-order parasequences grouped into fourth-order parasequences sets, which form the system tracts of the third-order sequences
2. Forth- or fifth-order, high frequency sequences grouped into sequence sets of third-order composite sequences
3. Combination of fourth-order parasequence sets and high-frequency sequences forming the system tracts of third-order composite sequences
4. Fifth-order parasequences forming the system tracts of third-order sequences without development of distinct parasequence sets
5. Facies assemblages, lacking cyclicity or with poorly-developed cyclicity, forming the system tracts of third-order sequences.

The components of all five sequences sets above are the parasequences. Parasequences are defined as a conformable succession of genetically related beds bounded by a marine flooding-surface (Van Wagoner *et al.*, 1998). The formation of these parasequences can be driven by external or internal forcings (and hence be allo- or auto-cycles). As with larger stratigraphic units, Lehrman and Goldhammer also classify parasequences based on the facies changes within them (Figure 7.2).

There is no method of determining if a cycle was formed via allo- or auto-cyclic processes, except in the case where there is an unambiguous sea-level fall resulting in the exposure of subtidal facies: a so-called *abnormal exposure* (Lehrmann and Goldhammer, 1999). In contrast a *normal exposure* is exposure of supra- or inter-tidal deposits which could occur by either a sea-level fall or normal sedimentary processes and hence does not unambiguously record a relative sea-level fall.

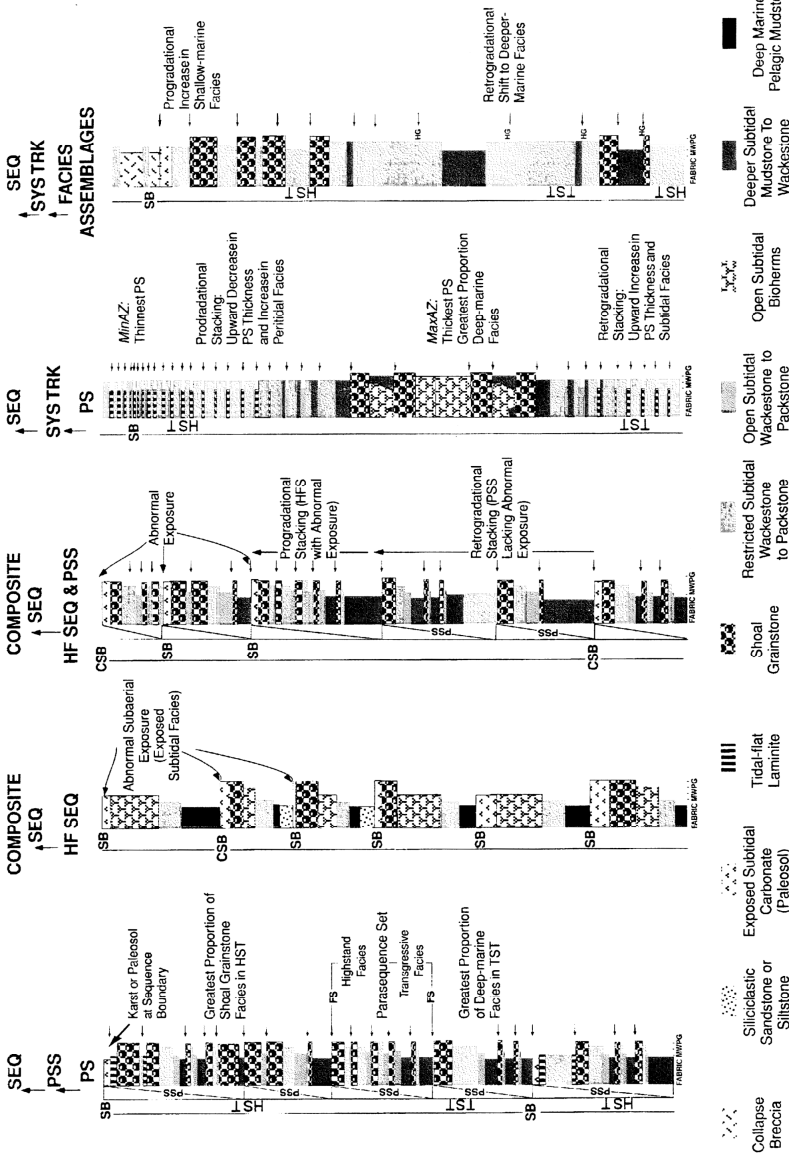

Figure 7.1. different styles of hierarchical stacking patterns of platoform carbonates. SB – sequence boundary, CSB – composite sequence boundary, MinAZ – minimum accommodation zone, HFS – high frequency sequence, PSS – parasequence set, PS – parasequence, SEQ – depositional sequence, HG – hardground, FS – flooding surface, M – mudstone, W – wackestone, P – packstone, G – grainstone, ↞ - Parasequence boundary. From (Lehrmann and Goldhammer, 1999)

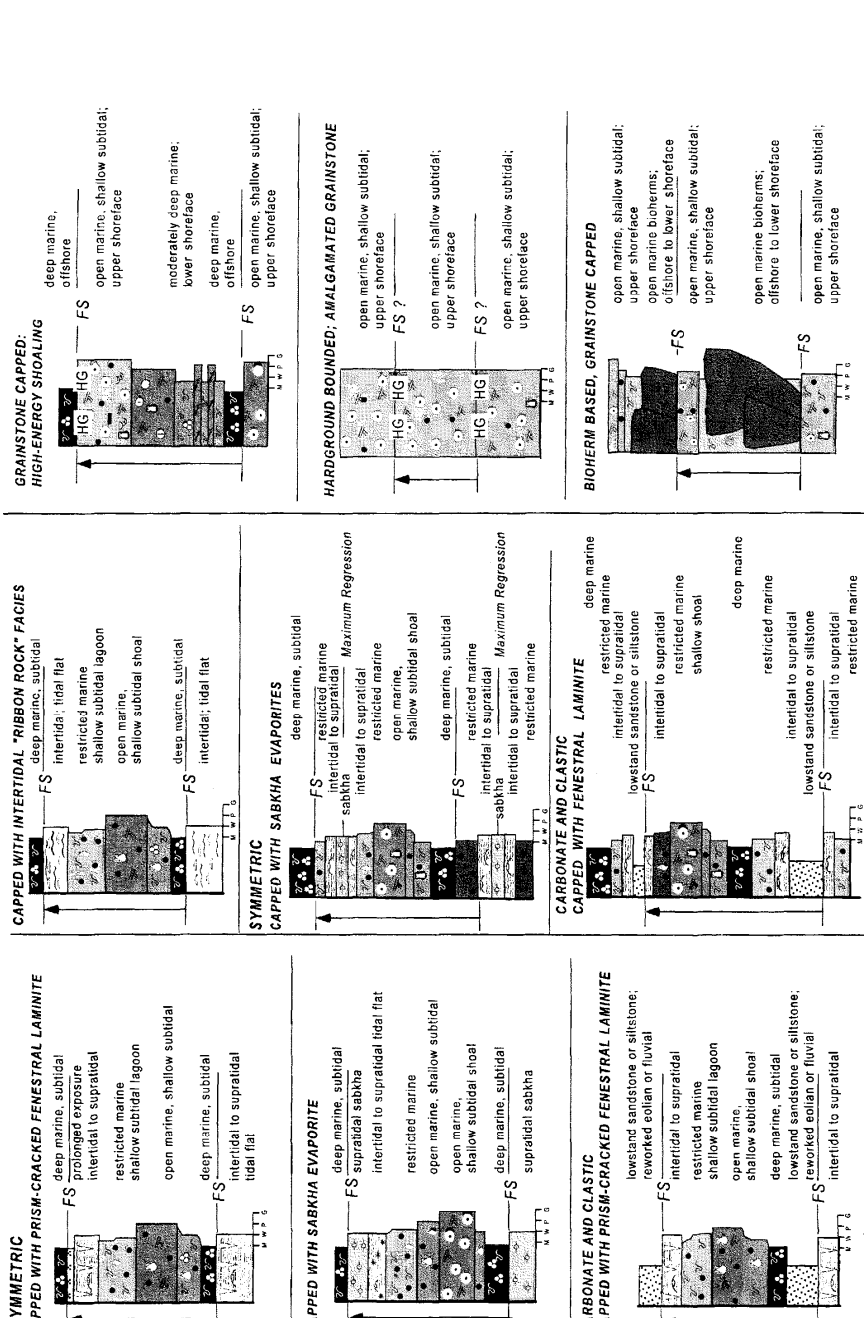

Figure 7.2. Types of parasequences found on carbonate platforms. Pertidal sequences are capped by inter- and supra-tidal facies (Left and middle columns). Subtidal parasequences shallow upwards from deeper-subtidal facies to shallow-subtidal or shoal facies (rightmost columns). From (Lehrmann and Goldhammer, 1999)

Proponents of orbital forcing as an underlying cause have stated three main features to imply that this is the case. The first is that the periodicity of individual cycles falls within the same band of values as anticipated for Milankovitch-band (20-400kyr) frequencies. However, given typical subsidence rates in passive-margin and cratonic settings, cycle thicknesses between 0.3 and 18 metres, analysed as a time series, fall within this band (Algeo and Wilkinson, 1988), meaning that any processes forming cycles of this thickness range could be interpreted as orbitally forced in origin. The second characteristic is the lateral continuity of accumulations such as the Rocknest cycles of northwest Canada for more than 200km along strike and 120km across strike (Grotzinger, 1986). However, this continuity is not seen on all platforms (Pratt and James, 1986). Finally, the cycles observed can be arranged hierarchically and a pattern of cycle thicknesses are repeated throughout a sequence and can be interpreted as evidence for orbital forcing (e.g. Goldhammer *et al.*, 1987, 1990; Osleger and Read, 1991). The argument here is that each cycle records a single sea-level excursion and that the patterns of stacking record long-term sea-level changes and hence Milankovitch cycles. This stacking pattern is the basis for Fischer Plots from which sea-level changes can be derived (Fischer, 1964; Read and Goldhammer, 1988). However, the use of Fischer plots to infer sea-level oscillations has been called into question as they do not accurately represent the sea-level changes recorded on the Bahaman Platform during the Holocene transgressive event (Boss and Rasmussen, 1995). Moreover, the Fischer plots created from ancient deposits are virtually indistinguishable from those created using random cycles thicknesses (Drummond and Wilkinson, 1993c).

However, the arguments outlined above for a glacio-eustatic forcing have been challenged. Firstly, carbonate cycles have been recorded during the Cretaceous, a greenhouse climate, where no ice-caps were present (Mayer, 1993; Lehmann *et al.*, 1998), but glacio-eustatic forcing is still interpreted to be the underlying cause in some studies (e.g. Dargenio *et al.*, 1997; Lehmann *et al.*, 1998; Altiner *et al.*, 1999; Raspini, 2001; Sandulli and Raspini, 2004). The eustatic forcing is, in these cases, thought to have derived from thermal expansion and contraction of ocean water, waxing and waning of small ice-caps and alpine glaciers, and changes in the storage capacity of aquifers and lakes (Lehmann *et al.*, 1998). However, there may have been

ice caps present during some of these studies (Miller *et al.*, 2003; Miller *et al.*, 2005). Secondly, studies have shown that the cycle thicknesses recorded show no difference from cycle sequences assembled from random cycle thickness distributions (Wilkinson *et al.*, 1998). This may be a result of the facies not recording the water depth of deposition. This has been shown to be the case on a modern carbonate platform (Rankey, 2004). The cycles also show no ordering, i.e. the thickness of one cycle does not depend on previous cycles. Furthermore, the distribution of cycle thicknesses shows an exponential distribution (Figure 7.3). This combined with the lack of order means that the cycle thicknesses are consistent with a Poisson process where the cycle thickness is picked at random from a Poisson distribution.

Studies on the modern Bahaman and Florida platforms have called into question the very idea of a shallowing upward cycle in shallow carbonate environments. It has been found that sedimentary facies in shallow marine environments do not correspond to water depth and in fact formed a fractal distribution due to the interaction of non-linear processes (Rankey, 2002, 2004). This implies that one cannot determine when a cycle starts as this requires some knowledge of water depth, which is derived from facies type. Other studies have found that facies mosaics across an area in the Persian Gulf were random, again questioning if a water-depth can be derived from facies alone (Wilkinson and Drummond, 2004). The cycles seen in ancient settings may therefore be a fractal or random distribution of facies meandering across the lagoon floor over time and may not be related to any changes in relative sea level, whether eustatically or internally forced. There is still difficulty relating these changes to the geological record due to the lack of preservation potential for many of these sediments, which has been estimated to be as low as 10-20% (Sadler, 1981).

The studies highlighted here question whether eustatic sea level is the driving force for cycle formation; instead suggesting that cycles are formed by the interaction of internal processes. Although there have been some questions asked of the exact mechanisms involved, autocycles have been simulated in numerous computer models, confirming that at least theoretically, autocycles could be a formative mechanism (e.g. Demicco, 1998; Burgess, 2001; Burgess *et al.*, 2001; Burgess and Wright, 2003; Burgess and Emery, 2004). In addition, the computer models show that the

stratigraphies formed may be chaotic, due to the non-linear nature of the interacting processes (Burgess and Emery, 2004).

This chapter aims to look at the possible driving forces for the preservation of these cycles by using forward modelling. A sedimentary forward model, Carbonate GPM, is used which can generate autocyclic sedimentation patterns with or without an oscillating eustatic sea-level curve. The chapter describes the methods used in this study and the results obtained from running the model with a variety of different relative sea-level curves. The chapter concludes by discussing the implications of this work.

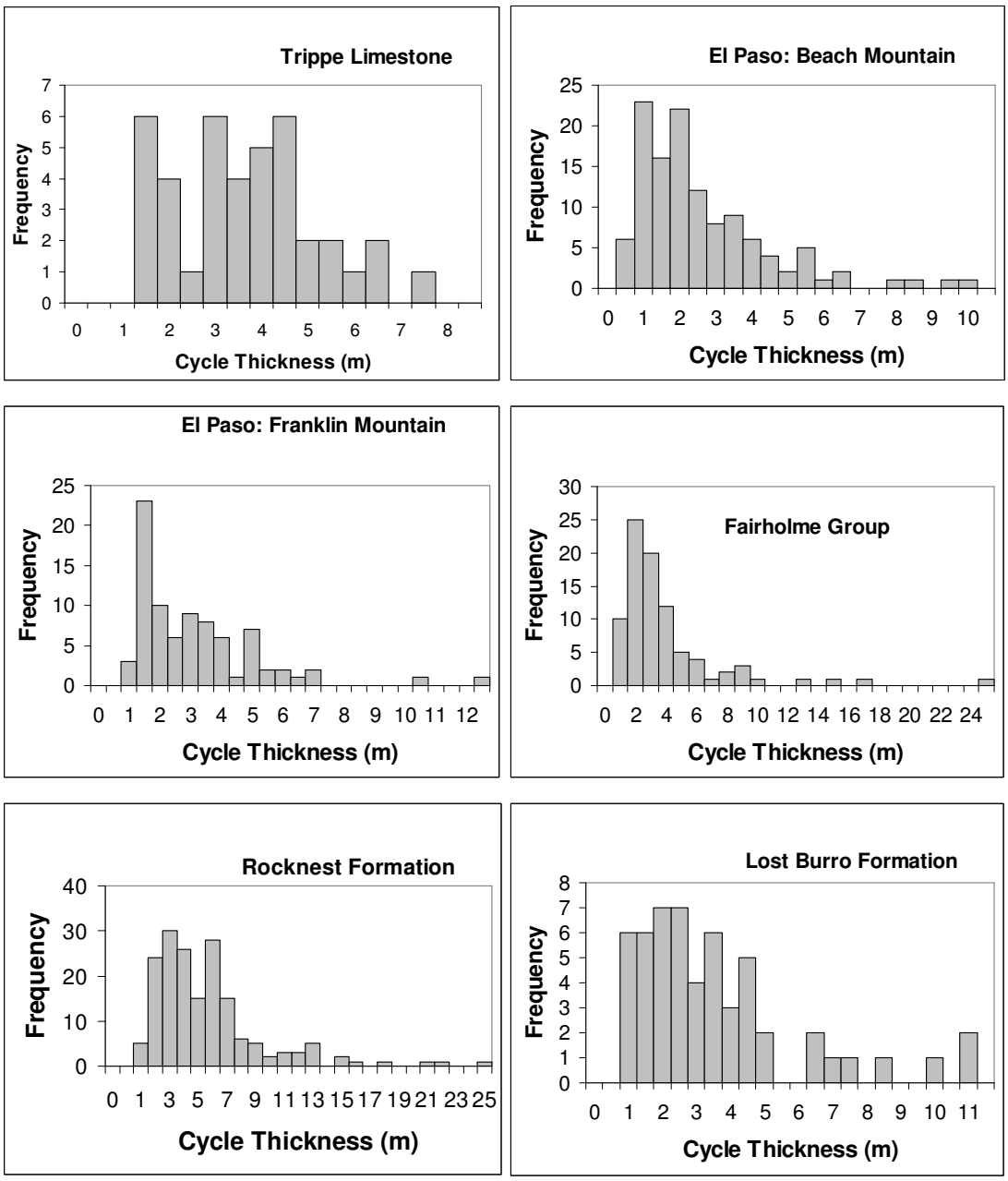

Figure 7.3. Frequency distributions of cycle and bed thicknesses from several localities: the Proterozoic Rocknest Formation, Canada; the Cambrian Trippe Limestone, USA; the Ordovician El Paso Group, USA; and the Upper Devonian Lost Burro Formation, USA and Fairholm Group, Canada. Each formation or group shows an exponential-like distribution of cycles thicknesses, largely consistent with a Poisson process of formation. After Wilkinson et al. (1996).

7.2 Methods

Carbonate GPM is capable of producing metre-scale shallowing upwards carbonate autocycles as described in chapters 5 and 6. The aim of this work is to impose a realistic eustatic change onto a constant subsidence rate. The sea level curves used included three different amplitudes and periodicities, which for the purpose of this chapter, are defined to correspond to 5^{th} order changes (periodicity of 25,000 years, amplitude 1m), 4^{th} order changes (100,000 years, 5m) and 3^{rd} order changes (1,000,000 years, 50m). The following combinations of sea-level oscillations were tried (Figure 7.4):

1. 5^{th} order changes only
2. 4^{th} order changes only
3. 3^{rd} order changes only
4. 4^{th} and 5^{th} order changes
5. 3^{rd}, 4^{th} and 5^{th} order changes
6. No eustatic sea-level oscillations

Each run commenced with a simple platform as an antecedent topography (Figure 7.5) and all other run parameters were kept identical, as described in Table 7.1.

A.

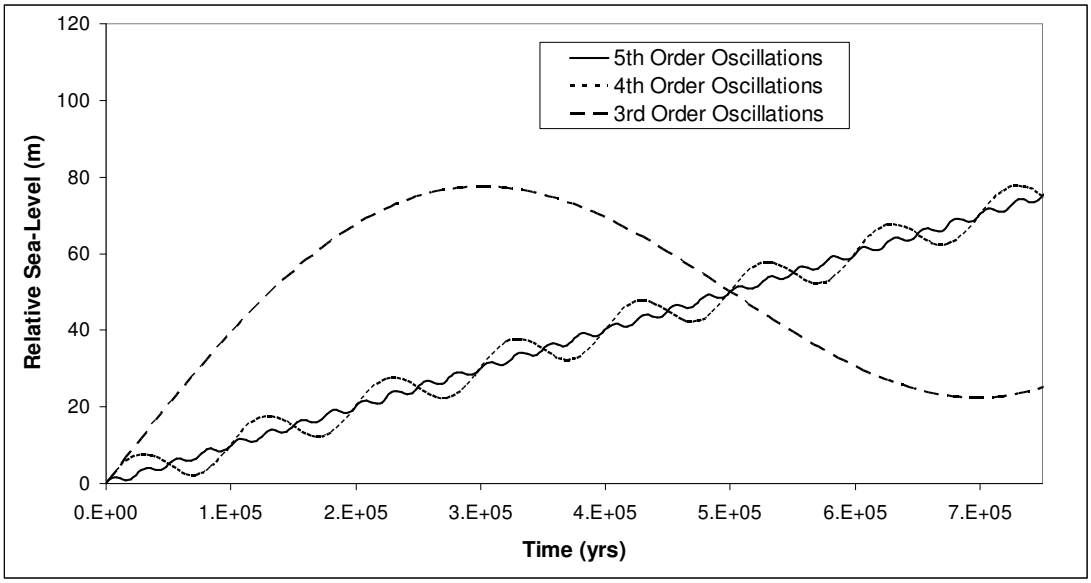

B.

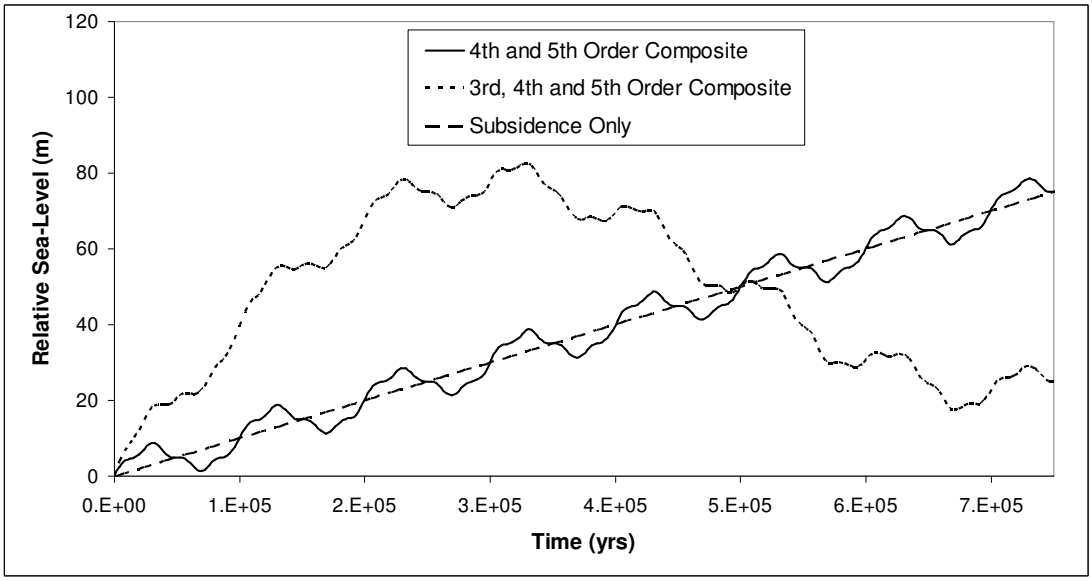

Figure 7.4. Relative sea-level curves that include a constant subsidence rate of 0.025m/yr used in this study. Panel A. shows the three base curves (3rd, 4th and 5th order oscillations). Panel B. shows the two composite curves (3rd, 4th and 5th order and 4th and 5th order oscillations only) and the relative curve with subsidence only.

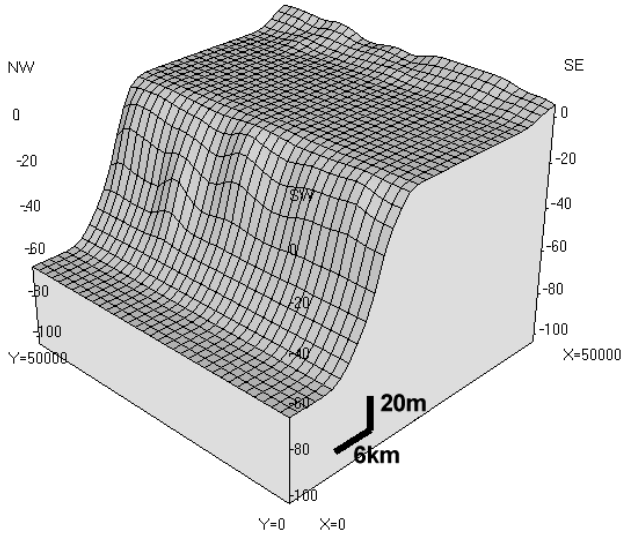

Figure 7.5. Antecedent topography used in this study. The platform is 50x50km and has 35 cells on each side. The basin is around 70m below that platform.

Table 7.1. Parameters used in all runs described in this paper.

Parameter	Value
Display time	2500 years
Diffusion coefficient	7500 m^2/yr
Transport coefficient	20 s/m
Timestep	1 year
Reef sediment grain size	15mm
Non-reef sediment grain size	0.25mm
Maximum reef production rate	3 mm/yr
Maximum non-reef production rate	2 mm/yr
Wave source amplitude	0.25m
Wave source period	3.2s
Wave direction	Perpendicular to shore

7.3 Results

The results show distinct differences in stratigraphy caused by the sea-level oscillations which are superimposed onto the autocycles generated by the model (as described in chapter 4). Using high-frequency 5th order sea-level oscillations (Run 1) shows great similarities with the subsidence only run (Run 6). Looking at longshore

stratigraphy reveals many similarities, including discontinuous horizons, bunching of timelines and rapid deposition following a hiatus event (Figure 7.6). In both runs, cycles are a result of normal exposure and non-deposition of sediment in the supra- and inter-tidal range (i.e. less than 1m). A higher amplitude 5th-order forcing would also produce occasional abnormal exposure cycles.

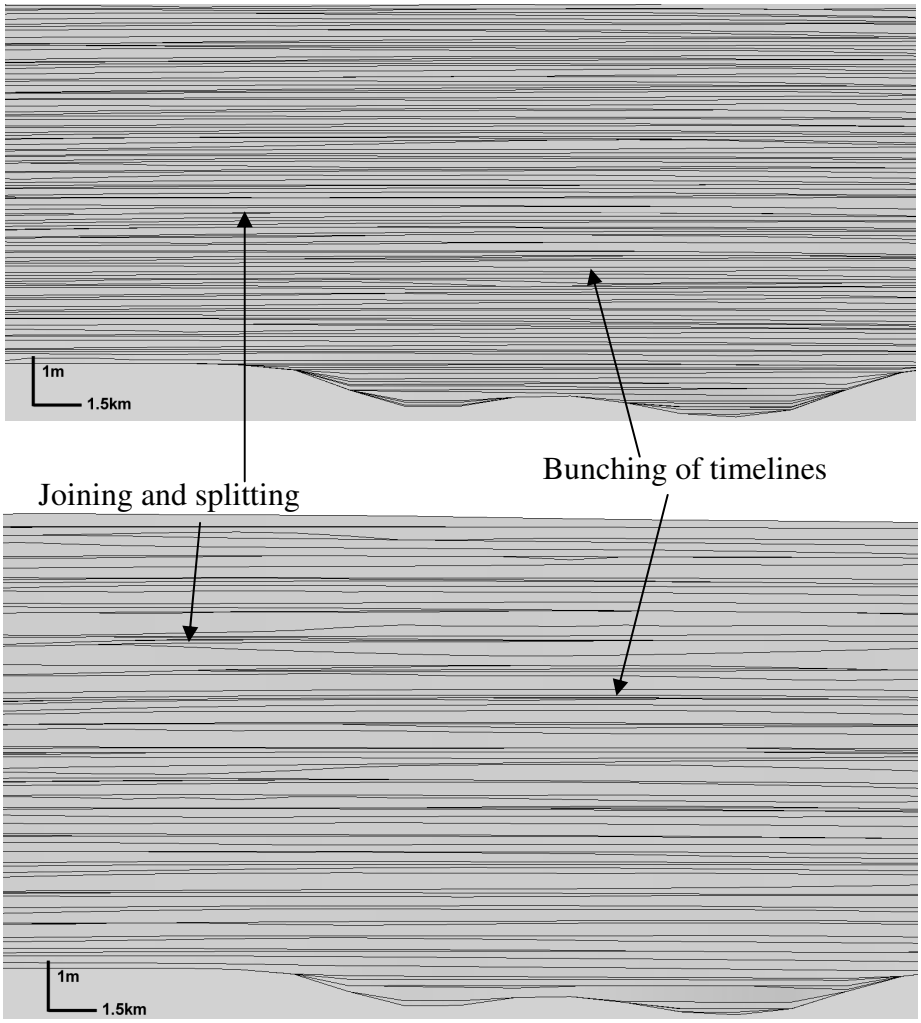

Figure 7.6. Longshore sections from the subsidence only run (upper panel) and the run with 5th order external forcings (lower panel). Similarities exist between both outputs, but it is difficult to translate the timeline stratigraphy to stratigraphies seen in the field.

Low and mid frequency changes (3rd and 4th order) cause a noticeable change in stratigraphy (Runs 2 to 5). This is largely caused by the rapid increase in accommodation during the Highstand Systems Tract and Transgressive System Tract. The increase in accommodation in the shoreward part of the lagoon does not allow a barrier to build up. This prevents residence times increasing in the shoreward part of the lagoon and instead carbonate production keeps pace with the sea-level rise.

However, the absence of a barrier allows waves to travel further inland causing the formation of abundant patch reefs during the time of fastest sea-level rise (Figure 7.7). These patch reefs quickly prograde seaward as the rate of sea-level rise slows. Cycles still form in these runs, but are almost exclusively caused via abnormal exposure.

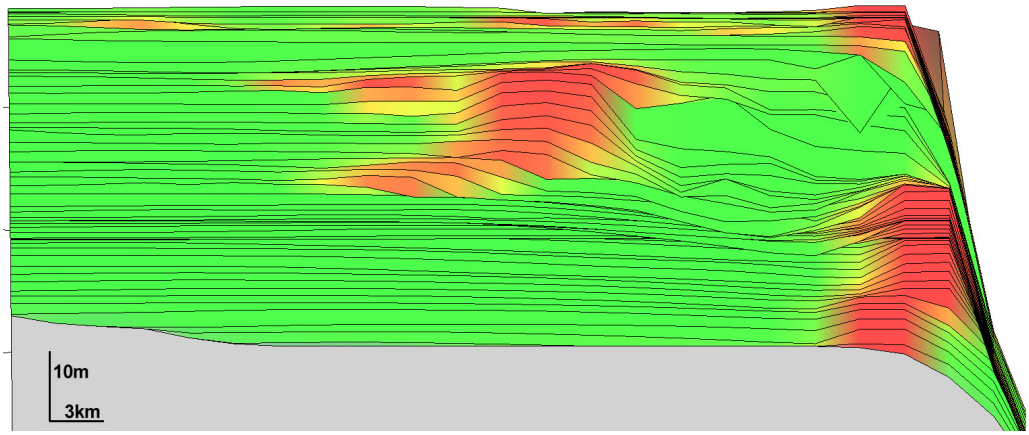

Figure 7.7. Cross-shore section through Run 5 at 175kyr. The reef sediment (red) backsteps during a period of rapid sea-level rise and then progrades rapidly as the rate of sea-level rise slows. The reef is discontinuous laterally (in and out of the page) and the formation is a function of the rate of sea-level rise and the existence of a seaward barrier.

All runs show distinctive lateral variations in stratigraphy in the longshore direction, demonstrating the three-dimensional nature of the processes occurring. This could make the interpretation of cycles not straight forward, as the exposure being recorded is two-dimensional. The toe-of-slope deposits produced in Run 6 show a classic example of this difficulty. Constructing water depth curves of this locality show the shallowest water occurring at around 60 to 100 kyr into the simulation. However, the exact time of this event varies laterally across the slope. This is due to a change in the locus of deposition (lobe switching), which is a function of the deposition on the reef and reef slope, and the topography on the distal part of the slope. This finding is significant but not surprising, as when only 2-dimensional surfaces are available in outcrop, the peak in the water depth history could be wrongly interpreted as a cycle, showing that three dimensional geometries are key to correctly understanding sedimentary sequences.

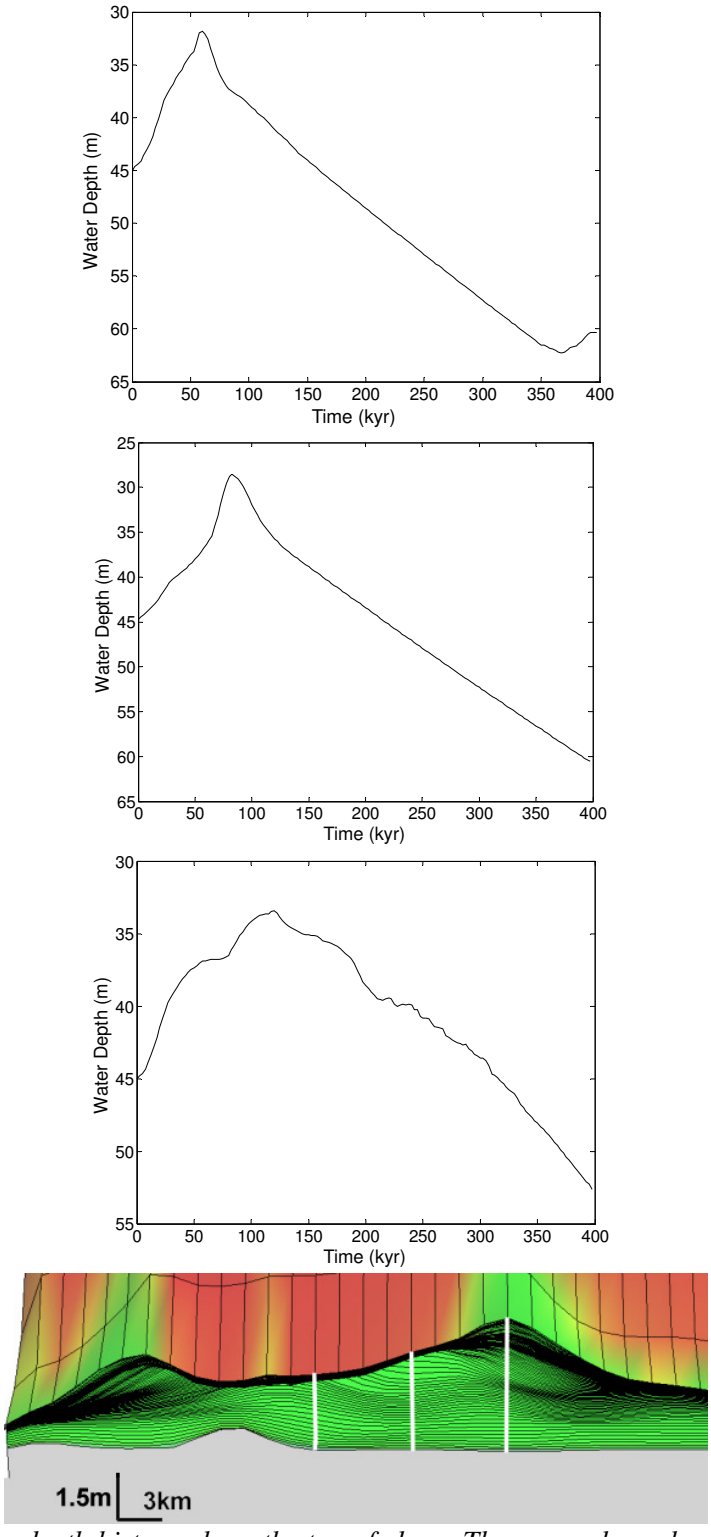

Figure 7.8. Water depth history along the toe-of-slope. There are clear changes longshore in this region. The three white lines on the cross-section (bottom right) show the location of the water depth curves from bottom-left to top-right. The curves are taken approximately just 6km apart from each other.

Fischer plots provide a good method of visualising the difference between the six runs carried out (Figure 7.9). A Fischer plot is constructed using the deviation from mean cycle thickness plotted against cycle number (Sadler *et al.*, 1993). Although their use to derive sea-level data from carbonate cycles has been called into question (Boss and Rasmussen, 1995), they do provide a useful way to visualise the changes in cycle thickness through a succession. However, in order for a Fischer plot to be useful, it must contain at least 40 individual cycles (Sadler *et al.*, 1993). Runs 1 and 6 both produced an adequate number of cycles for visualisation in this manner. Both produced runs that contained positive and negative runs of accumulation, just as cycles recorded from field studies do (e.g. (Read and Goldhammer, 1988)The definition of cycle within Carbonate GPM deserves some discussion. From the rock record, high frequency sequences are defined between two flooding surfaces (Lehrmann and Goldhammer, 1999). The ultimate cause of the flooding surface is an increase in water depth at that location, but this increase could be caused by one of two things. Firstly, there could a relative sea-level rise. Secondly, there could be emergence of the sediment and subsequent flooding due to the transport of sediment. There are closely allied to the normal and abnormal exposure mechanisms outline in section 7.2. Using Carbonate GPM, a total of three definitions of cycles can be used to generate a Fischer plot. The start of a cycle could be defined to be at the same time as an increase in water depth (by any mechanism), flooding following a period of subaerial exposure, or after a hiatus event (a time of non-deposition). From analysis of all runs and methods of delineating cycles, using hiatus events appears to give cycles that match the stratigraphic geometries present in the run output; that is they match the bunching and splitting of timelines and as discussed previously. Periods of non-deposition are closely linked to residence times, which in turn shows most effect in shallow (~1m) water and hence, these sediments would be in the supra-, inter- and the top of the sub-tidal facies ranges. These are therefore considered to be cycles formed by normal exposure. The run that produced the most cycles was Run 6 (subsidence only). Assuming all six cycles generated in this run prograded the whole distance from shoreline to reef gives progradation rates of around 1.5 m per year. However, it is clear that not all cycles prograded the whole distance across the lagoon area, depending upon the interplay between accumulation rates, erosion rates and subsidence rate.

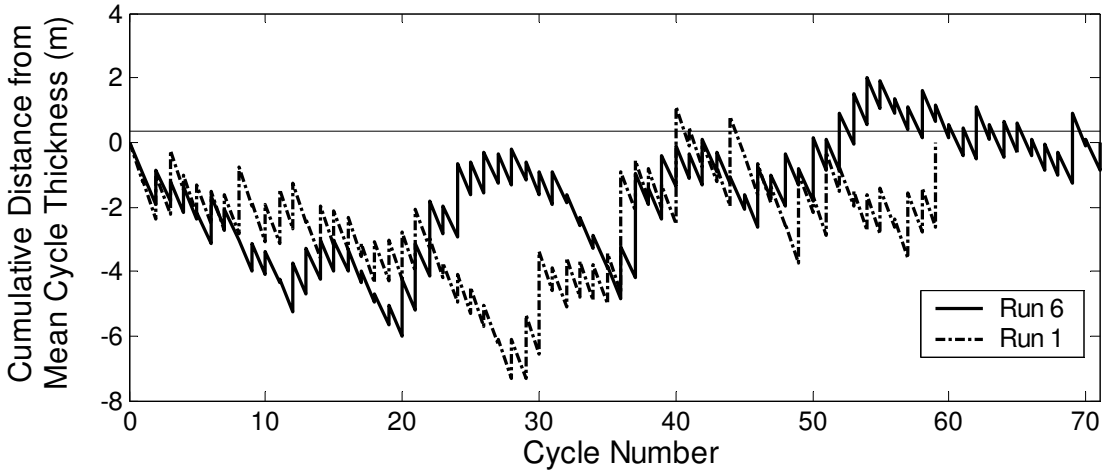

Figure 7.9. Fischer plots derived from the two of the size runs; Runs 1 and 6. These were the only two runs that produced sufficient cycles to create a Fischer Plot (Sadler et al., 1993). Both could be interpreted as showing 3rd-order sea level changes, although neither, of course, contained this level of forcing, with runs of negative accumulation followed by positive.

7.4 Discussion

The debate about the causative factors of shallowing-upward meter-scale carbonate cycles has arrived at two competing hypotheses. The first is that eustatic sea-level changes are the main driving cause of cycle formation which are therefore allocycles. The second is that cycles form due to interaction of non-linear processes and are therefore autocycles. Undoubtedly these are end-points in a continuous spectrum as it is clear that carbonate sediments are generated by a number of non-linear, interacting processes that are capable of not only producing cycles, but may be capable of producing chaotic behaviour (see previous chapter and Burgess and Emery (2004)).

However, glacio-eustatic sea-level oscillations have been recorded in a number of sediment types and using numerous techniques (Hinnov, 2000). The recording of such signals from sedimentary deposits assumes the absence of several confounding factors that could affect the signal recorded, such as times of non-deposition, erosion, changes in sedimentation rates, and of course, autocyclic processes. One of the main methods of detecting an orbitally forced signal is the use of spectral methods. In theory one should be able to detect the various Milankovitch signals that could have influence over changes in sedimentation. Using Carbonate GPM, which is capable of generating autocycles and imposing eustatic sea-level changes onto them, a power

spectrum can be generated from various parameters, such as water depth or sedimentation rates. Constructing power spectra of the water depth history shows a clear periodic signal in each run, but the peaks occur at various frequencies (Figure 7.10). All five runs with external forcing mechanisms show peaks at the frequency of the forcing. However, it would be difficult to differentiate the peaks produced via autocyclic mechanisms and those from external processes without prior knowledge of the external processes. This task is made even more difficult by the fact that facies changes in shallow water may not be related to water depth, so obtaining a water depth signal from a stratigraphic section may well be difficult, if not impossible (Rankey, 2004).

Studies on ancient cycle deposits show an exponential decrease in frequency with increasing cycle thickness (Wilkinson *et al.*, 1996; Wilkinson *et al.*, 1999). This coupled with sequences indistinguishable from random sequences of cycle thicknesses suggest that cycles are consistent with a Poisson process (Wilkinson *et al.*, 1998; Wilkinson *et al.*, 1999). Lithological thicknesses resulting from a Poisson process would have an exponential distribution that followed:

$$F(t) = B\frac{N^2}{L}e^{-t(N/L)} \qquad (7.1)$$

Here, the sequence length is *L*, which is divided into *N* units and then placed into bins of size *B* (Wilkinson *et al.*, 1999).

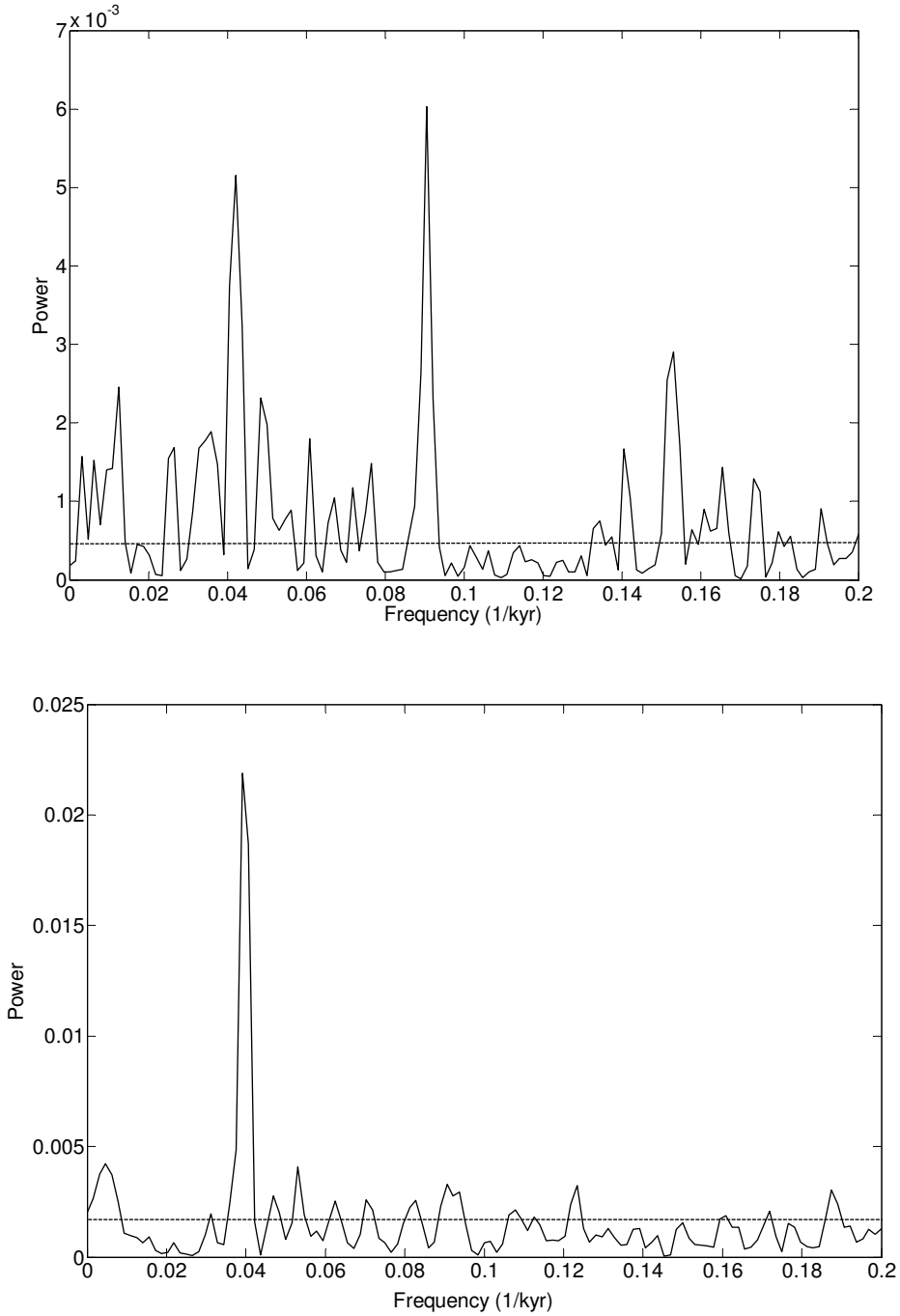

Figure 7.10. Power spectra produced using water depth histories in the centre of the lagoon. The lower spectrum is taken from Run 1 and shows a clear signal at 25 kyr. The upper spectrum is taken from Run 6 and shows numerous clear signals. The dashed line in each is the result of a random model (see Chapter 5). Note that Run 6 (no forcings) also produces a clear peak at 25kyr. Without prior knowledge of the external signals it would be difficult to say which water depth history has experience external forcing.

The cycle thickness distributions from the six runs carried out in this study show that all runs are not compatible with an exponential distribution of cycle thicknesses, based on the Kolmogorov-Smirnoff test, which compares a distribution to a theoretical one (Figure 7.11 and equation 7.1). However, these are not that dissimilar to those generated from field data (Figure 7.3) and show R^2 values of 0.7 to 0.8, whereas the field data distributions show a R^2 of >0.9 (Wilkinson *et al.*, 1999). However, here we are equating cycles (i.e. a succession of lithological units delimited by a flooding surface) from the model to lithofacies units (based on horizons of lithologic change (Wilkinson *et al.*, 1999)). The two are probably related, but are not the same measurement and as Carbonate GPM does not model facies a more robust comparison cannot be drawn. Cycle thicknesses were taken from an area five-by-five grid cells in size from the centre of the lagoon. Only runs with 3rd order changes (Runs 3 and 5) show any large discrepancies, as they produce relatively thick cycles. This is due to the presence of a number of cycles greater than ten metres thickness with some as large as 20 m thick. These two runs are also the only runs to produce sufficient numbers of very thin cycles (<1m) to either match or exceed the predicted frequency of occurrence. All other runs produce too few thin cycles. Examining Figure 7.3 shows that this phenomenon also exists from records of field deposits. Drummond and Wilkinson (1996) suggest that the lack of very thin beds is due to them being placed within other beds or grouped together to form larger beds. In the model, however, the lack of thin beds is due to a lack of temporal output, not due to difficulties in the recognition of thin beds.

In the case of Carbonate GPM there are no random processes occurring and the model is fully deterministic. It still, however, generates cycle thickness distributions that are largely compatible with those collected from field localities, if not a Poisson process. It may, therefore, be the case that the inherent complexities in carbonate formation are not random but still form an exponential-like distribution. Clearly, more work is required here.

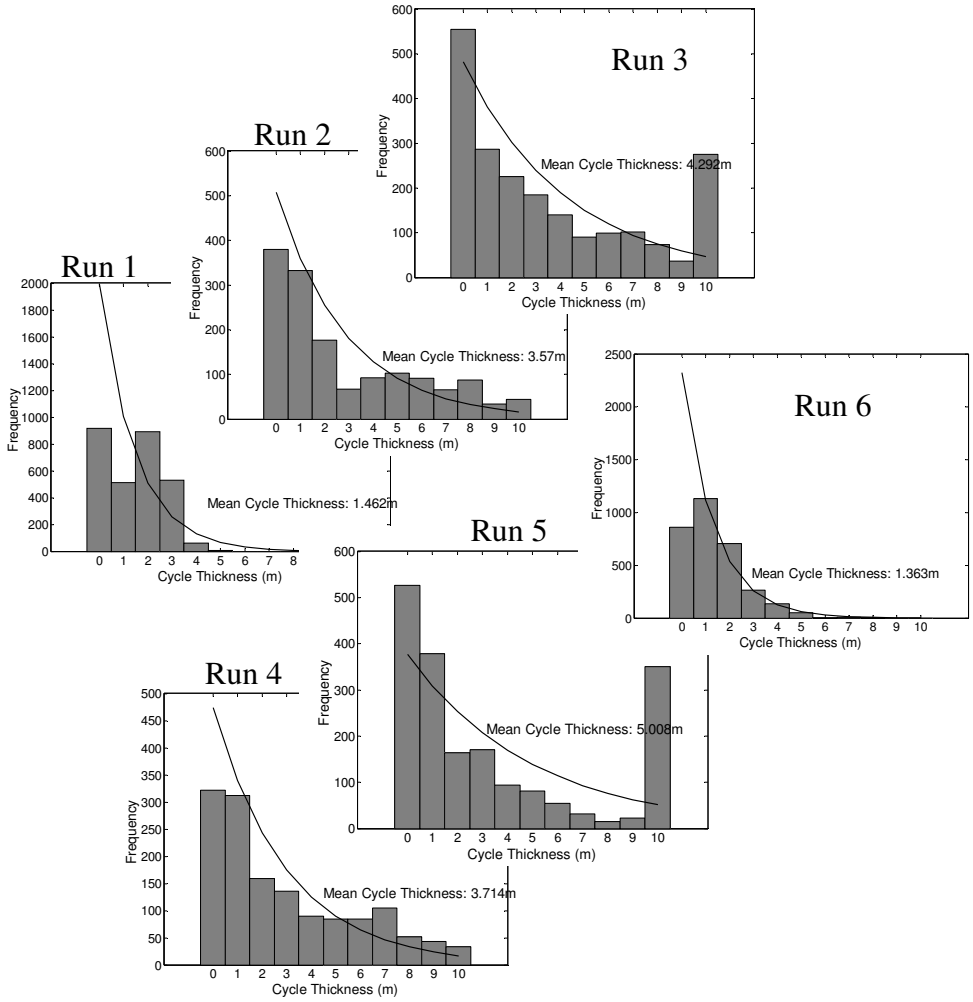

Figure 7.11. Cycle thickness distribution for all six runs presented in this chapter. All are compatible with an exponential distribution (compare to Figure 7.3) apart from when 3rd order changes are imposed (runs 3 and 5) when too many thick cycles (10m or more) are produced.

7.5 Conclusion

Forward modelling of autocyclic sequences coupled with eustatic sea-level changes can give meaningful insight into the formation of shallowing-upward peritidal carbonate cycles that are common throughout the Palaeozoic. Carbonate GPM is a forward model that can generate autocyclic sequences and impose eustatic sea-level changes on those, which make it an ideal "virtual laboratory" to study the phenomenon.

All runs produced cycle thickness distributions that are similar to those derived from lithofacies changes on ancient platforms. The fact that these distributions agree with

those from field studies (which show an exponential distribution and are used as an argument for random cycle formation via a Poisson process), even when no random processes are included in Carbonate GPM, questions whether carbonate cycle thicknesses are truly random, regardless of whether they are largely auto- or allocyclic in nature. However, given that Carbonate GPM does not produce lithofacies, but sediment delimited by timelines, more work is required here.

In addition, care must be taken when inferring the presence of cycles from two-dimensional sections as the three dimensional geometry can cause cycle-like changes in stratigraphy that are due to switching of the locus of sediment deposition.

This study has found that differences do occur in the stratigraphy produced when a sea-level curve is used as a driving mechanism, particularly when 3rd order sea-level changes are introduced. The effect of 5th order sea-level oscillations is similar to autocyclic mechanisms alone and the results shown here, even though some of the parameters examined would not be available from a field study, may be indistinguishable without prior knowledge of the forcing frequencies. It is therefore concluded that external processes do not dominate the internal processes when the external processes is low amplitude and high-frequency. However, high amplitude changes clearly overwhelm the internal processes embodied in Carbonate GPM.

Chapter 8

Discussion and Conclusions

8.1 Introduction

The aim of this thesis was to understand the interacting processes that affect and control carbonate production and deposition using forward modelling of the carbonate sedimentary system. The model used for this study, Carbonate GPM, includes the controlling effects of light penetration, wave energy and particularly supersaturation (via the proxy of residence time) on carbonate production and deposition. This chapter gives a brief summary of the main findings of this study by assessing the hypotheses outlined in chapter 1 and summarising the main conclusions of the study. It concludes with suggestions for future work.

8.2 Hypotheses

Hypothesis 1: Supersaturation is not a major factor in producing carbonate complexity.

The effect of residence time as a proxy supersaturation is to produce "patchy" production of carbonates, in effect the locus of deposition meanders around the platform. Without the effect of supersaturation (or some other processes, such as biological processes) there are no migrating peritidal deposits as no natural "lag effect" occurs (see Chapter 2). More rudimentary algorithms used to simulate the effect of supersaturation do not include the complexities arising from changes in flow regimes: there is not a simple relationship between supersaturation state and distance from open marine waters as is assumed in those models. The carbonate supersaturation is therefore likely to be a significant controlling factor on the carbonate stratigraphy observed in shallow marine settings, agreeing with previous observations (Demicco and Hardie, 2002).

Hypothesis 2: Transport of reefal sediment does not need to be differentiated from other sediments in shallow marine carbonate systems.

The effect of advective transport of reefs is obvious in the initial stages of platform development. Reef sediment is subject to binding of components and can consist of large blocks. As such, the assumption that underlies sediment transport in many forward models (including GPM) that grains are spherical and have a fixed density, does not apply to reef sediments. In order to account of the phenomenon of binding and larger "grains", an additional parameter – a cohesivity parameter – is required to reduce the advective transport of reefal sediment. However, one can simply not reduce the erosion and transport rates of reefal sediment as other types of erosion and transport, such as roackfalls and other downslope movement occurs. Therefore, in this model, only advective transport included the cohesivity parameter. Diffusion transport is not affected by this parameter and as such downslope sediment transport still occurs. It is therefore considered essential to differentiate reef sediment from "ordinary" sediment (i.e. spherical grains of quartz) to account for the immobility of reef sediment for advective transport while still simulating the transport of reef sediment downslope.

Hypothesis 3: Physiochemical processes alone cannot create apparently complicated carbonate stratigraphic sections.

The notion that carbonates are capable of forming chaotic stratigraphies stems from the fact that interacting non-linear processes may be responsible for the production and deposition of sediment (Nicolis and Nicolis, 1991). The forward model presented here includes several such non-linear interacting processes: light penetration, wave energy, supersaturation and sediment transport. To test the hypothesis that supersaturation affects the complexity that may be observed in carbonate deposits two identical runs were carried out with only a small change in initial conditions: a one metre difference in the antecedent topography in one cell (from 1225 cells). The results show that chaotic stratigraphy is not produced and in fact the vertical stratigraphy at a single location may well be predictable. However, the model produces output that is laterally discontinuous so a prediction based on one location will not hold at another. Therefore, physiochemical process alone can create stratigraphy that may appear chaotic when examined in the field.

Hypothesis 4: External forcings dominate internal processes and control the amount of carbonate deposition.

The causative factors of shallowing upwards peritidal carbonate cycles can be tested by subjecting a model that is capable of generating autocycles to an external forcing control, such as eustatic sea-level changes. This thesis has shown that large-scale oscillations (commonly referred to as 3rd and 4th order oscillations) do alter the stratigraphy deposited. However, 5th order changes coupled with autocyclic changes produce stratigraphy similar to that produced using autocyclic mechanisms alone. Therefore, external processes may dominate internal processes if those external processes are of sufficient magnitude above those tried here.

8.3 Conclusions

The general conclusions of this work are:

- Supersaturation is a key process in carbonate production and has an effect on the sedimentary geometries deposited.
- The binding of reefal sediments needs to be considered in order to correctly model sediment transport.
- It may be possible to predict a vertical section of carbonates based on a smaller portion of the section. However, this model may not be valid for any adjacent sections. In other words, a vertical section generated by Carbonate GPM is entirely compatible with a non-random creation process, but the time-dependent, three-dimensional shifting of the locus of sediment production and deposition makes a non-random forcing difficult, if not impossible, to detect.
- The effect of small amplitude, high frequency, sea-level oscillations may be impossible to differentiate from autocyclic effects.

8.4 Further Work

The main implication of this study on future work is that supersaturation must be included in a forward model of carbonate production and deposition. Unless there is specific need for a model that can complete in short amount of time, supersaturation should be modelled using the flow of water around the platform. This flow could be

derived from a number of sources, not just waves as is the case here. Modelling supersaturation using a distance from open marine sources is not adequate as the flow around a reef system is heavily dependent on the topography and the interaction of this topography with water currents.

The computer model used in this thesis is a typical geological forward model. Originally designed as a siliciclastic model, carbonate sedimentation has been added, which has enabled the carbonate sediment library created for this thesis to utilise all of the physical processes that are inherent to both carbonate and siliciclastic sediments; namely the physical processes of erosion, transport and re-deposition. In doing so, the transport algorithm needed to be altered beyond its original capabilities to account for the physical differences between reef sediment and small spherical grain for which it was designed. No other changes were included in the original GPM model and all other algorithms were entirely contained within the carbonate library. This separation of functionality enables a modular design for GPM, such that replacement libraries can be slotted in and only the interface is required to be the same. The separation also means that the validation, calibration and verification done on GPM in other studies are valid for Carbonate GPM also (Tetzlaff, 2005).

Despite these extensive tests, it is still not absolutely clear when the results of Carbonate GPM are stable and when not. Each individual process works correctly in isolation or when coupled with one other (see Chapter 4). However, when the whole suite of processes is used (i.e. a “normal” run), the interaction between algorithm components can produce unstable results when using numerical parameters that were stable when testing modules in isolation. To counter that, a comparatively small timestep was used for this study and was found to produce stable results. One of the aims of this study was to assess possible chaotic behaviour in carbonate deposition. This is an inherently unstable process where large, rapid shifts in deposition rates can occur. The difficulty that now arises is how one differentiates between physical instability, due to the interaction between non-linear processes (i.e. chaotic behaviour), and numerical instability, brought on by the interaction of a number of algorithmic processes. In this study there is an acceptance that there is some numerical instability, but by using a small enough timestep these instabilities are

much smaller than the difference caused by a small change in a physical parameter. This therefore gives confidence in the overall properties of the model output, but not on the small details (e.g., statistics such as the total amount of sediment deposited between 150,000 and 152,500 years of output or the exact number of cycles produced). Comparing model output to data recorded from various localities, both ancient and modern, adds much more confidence in the model output produced. However, it still does not necessarily follow that the model is correct. It is with these caveats in mind that these modelling results should be interpreted. This reasoning is true for any geological computer model (Watney *et al.*, 1999). This leads to an interesting future study on how one could test for numerical stability in a computer model that contains many interacting processes and could produce chaotic stratigraphy. Testing output between models is one avenue to explore and has been carried out in the past (Dalmasso *et al.*, 2001) and was also done in a limited way for this thesis (see Chapter 4).

The work presented here could be extended in several ways. Firstly, there are many other causes of currents around a reef system other than waves. Tides, storms and wind all influence the currents that occur. Secondly, only two sediment types were simulated. This could be extended to include common carbonate facies, such as ooid shoals. Thirdly, the effect of biology could be added to the model via methods described in chapter 3: cellular automata and predator-prey algorithms. These algorithms could use the environmental parameters simulated (wave energy, water depth and supersaturation) to simulate the colonisation of areas by carbonate producing biological organisms. As such, different facies could be produced, dependent on the "species" dominating an area. Finally, the small set of external forcings described here could be extended to include asymmetrical oscillations and a wider range of amplitudes and periods.

References

Adams, E.W., Schroder, S., Grotzinger, J.P., and McCormick, D.S., 2004, Digital Reconstruction and Stratigraphic Evolution of a Microbial-Dominated, Isolated Carbonate Platform (Terminal Proterozoic, Nama Group, Namibia): Journal of Sedimentary Research, v. 74, p. 479-497.

Adams, R.D., and Grotzinger, J.P., 1996, Lateral Continuity of Facies and Parasequences in Middle Cambrian Platform Carbonates, Carrara Formation, Southeastern California, USA: Journal of Sedimentary Research, v. 66, p. 1079-1090.

Algeo, T.J., and Wilkinson, B.H., 1988, Periodicity of Mesoscale Phanerozoic Sedimentary Cycles and the Role of Milankovitch Orbital Modulation: Journal of Geology, v. 96, p. 313-322.

Allen, J.R.L., 1994, Fundamental Properties of Fluids and Their Relation to Sediment Transport, *in* Pye, K., ed., Sediment Transport and Depositional Processes: Oxford, Blackwell Sciences.

Allen, M.R., Stott, P.A., Mitchell, J.F.B., Schnur, R., and Delworth, T.L., 2000, Quantifying the Uncertainty in Forecasts of Anthropogenic Climate Change: Nature, v. 407, p. 617-620.

Altiner, D., Yilmaz, I.O., Ozgul, N., Akcar, N., Bayazitoglu, M., and Gaziulusoy, Z.E., 1999, High-Resolution Sequence Stratigraphic Correlation in the Upper Jurassic (Kimmeridgian)-Upper Cretaceous (Cenomanian) Peritidal Carbonate Deposits (Western Taurides, Turkey): Geological Journal, v. 34, p. 139-158.

Andrefouet, S., Claereboudt, M., Matsakis, P., Pages, J., and Dufour, P., 2001a, Typology of Atoll Rims in Tuamotu Archipelago (French Polynesia) at Landscape Scale Using Spot Hrv Images: International Journal of Remote Sensing, v. 22, p. 987-1004.

Andrefouet, S., Pages, J., and Tartinville, B., 2001b, Water Renewal Time for Classification of Atoll Lagoons in the Tuamotu Archipelago (French Polynesia): Coral Reefs, v. 20, p. 399-408.

Archer, D., 1999, Modeling Co_2 in the Ocean: A Review, *in* Bouwman, A.F., ed., Scaling of Trace Gas Fluxes between Terrestrial and Aquatic Ecosystems and the Atmosphere, Volume 24: Developments in Atmospheric Science: Amsterdam, Elsevier Sciences, p. 169-184.

Arditi, R., and Saiah, H., 1992, Emperical Evidence of the Role of Hetrogeneity in Ratio Dependant Consumptions: Ecology, v. 73, p. 1544-1551.

Atkinson, M.J., Falter, J.L., and Hearn, C.J., 2001, Nutrient Dynamics in the Biosphere 2 Coral Reef Mesocosm: Water Velocity Controls Nh_4 and Po_4 Uptake: Coral Reefs, v. 20, p. 341-346.

Balog, A., Haas, J., Read, J.F., and Coruh, C., 1997, Shallow Marine Record of Orbitally Forced Cyclicity in a Late Triassic Carbonate Platform, Hungary: Journal of Sedimentary Research, v. 67, p. 661-675.

Balog, A., Read, J.F., and Haas, J., 1999, Climate-Controlled Early Dolomite, Late Triassic Cyclic Platform Carbonates, Hungary: Journal of Sedimentary Research, v. 69, p. 267-282.

Barnett, A.J., Burgess, P.M., and Wright, V.P., 2002, Icehouse World Sea-Level Behaviour and Resulting Stratal Patterns in Late Visean (Mississippian) Carbonate Platforms: Integration of Numerical Forward Modelling and Outcrop Studies: Basin Research, v. 14, p. 417-438.

Bellucci, A., Buffoni, G., Griffa, A., and Zambianchi, E., 2001, Estimation of Residence Times in Semi-Enclosed Basins with Steady Flow: Dynamics of Atmospheres and Oceans, v. 33, p. 201-218.

Bellwood, D.R., 1995a, Carbonate Transport and within Reef Patterns of Bioerosion and Sediment Release by Parrotfishes (Family Scaridae) on the Great-Barrier-Reef: Marine Ecology-Progress Series, v. 117, p. 127-136.

—, 1995b, Direct Estimate of Bioerosion by Two Parrotfish Species, *Chlorurus Gibbus* and *C. Sordidus*, on the Great-Barrier-Reef, Australia: Marine Biology, v. 121, p. 419-429.

—, 2003, Origins and Escalation of Herbivory in Fishes: A Functional Perspective: Paleobiology, v. 29, p. 71-83.

Berryman, A.A., 1992, Origins and Evolution of Predator Prey Theory: Ecology, v. 73, p. 1530-1535.

Bice, D., 1988, Synthetic Stratigraphy of Carbonate Platforms and Basin Systems: Geology, v. 16, p. 703-706.

Bitzer, K., and Salas, R., 2001, Simulating Carbonate and Mixed Carbonate-Clastic Sedimentation Using Predator-Prey Models, *in* Merriam, D., and Davis, J.C., eds., Luxer Academic/Plenum Publishers, p. 169-204.

—, 2002, SIMSAFADIM: Three Dimensional Simulation of Stratigraphic Architecture and Facies Distribution Modeling of Carbonate Sediments: Computers and Geoscience, v. 28, p. 1177-1192.

Borowitzka, M.A., 1981, Photosynthesis and Calcification in the Articulated Coralline Red Algae *Amphiroa Anceps* and *A. Foliacea*: Marine Biology, v. 62, p. 17-23.

Bosence, D., 2005, A Genetic Classification of Carbonate Platforms Based on Their Basinal and Tectonic Settings in the Cenozoic: Sedimentary Geology, v. 175, p. 49-72.

Bosence, D., and Waltham, D., 1990, Computer Modeling the Internal Architecture of Carbonate Platforms: Geology, v. 18, p. 26-30.

Bosence, D.W.J., Pomar, L., Waltham, D.A., and Lankester, T.H.G., 1994, Computer Modeling a Miocene Carbonate Platform, Mallorca, Spain: AAPG Bulletin, v. 78, p. 247-266.

Boss, S.K., and Rasmussen, K.A., 1995, Misuse of Fischer Plots as Sea-Level Curves: Geology, v. 23, p. 221-224.

Bosscher, H., and Schlager, W., 1992, Computer Simulation of Reef Growth: Sedimentology, v. 39, p. 503-512.

Bosscher, H., and Southam, J., 1992, CARBPLAT - a Computer Model to Simulate the Development of Carbonate Platforms: Geology, v. 20, p. 235-238.

Brander, R.W., Kench, P.S., and Hart, D., 2004, Spatial and Temporal Variations in Wave Characteristics across a Reef Platform, Warraber Island, Torres Strait, Australia: Marine Geology, v. 207, p. 169-184.

Bridges, P.H., Gutteridge, P., and Pickard, N.A.H., 1995, The Environmental Setting of Early Carboniferous Mud-Mounds, *in* Monty, C.L.V., Bosence, D.W.J., Bridges, P.H., and Pratt, B.R., eds., Volume 23, International Association of Sedimentologists, p. 171-190.

Broecker, W.S., and Takahashi, T., 1966, Calcium Carbonate Precipitation on the Bahama Banks: Journal of Geophysical Research, v. 71, p. 1575-1602.

Buddemeier, R.W., and Smith, S.V., 1999, Coral Adaptation and Acclimatization: A Most Ingenious Paradox: American Zoologist, v. 39, p. 1-9.

Burgess, P.M., 2001, Modeling Carbonate Sequence Development without Relative Sea-Level Oscillations: Geology, v. 29, p. 1127-1130.

—, 2006, The Signal and the Noise: Forward Modeling of Allocyclic and Autocyclic Processes Influencing Peritidal Carbonate Stacking Patterns: Journal of Sedimentary Research, v. 76, p. 962-977.

Burgess, P.M., and Emery, D.J., 2004, Sensitive Dependence, Divergence and Unpredictable Behaviour in a Stratigraphic Forward Model of a Carbonate System, *in* Curtis, A., and Wood, R., eds., Geological Prior Information, Volume Special Publication, Geological Society of London.

Burgess, P.M., and Wright, V.P., 2003, Numerical Forward Modelling of Carbonate Platform Dynamics: An Evolution of Complexity and Completeness in Carbonate Strata: Journal of Sedimentary Research, v. 73, p. 637-652.

Burgess, P.M., Wright, V.P., and Emery, D., 2001, Numerical Forward Modelling of Pertidal Carbonate Parasequence Development: Implications for Outcrop Interpretation: Basin Research, v. 13, p. 1-16.

Calantoni, J., Puleo, J.A., and Holland, K.T., 2006, Simulation of Sediment Motions Using a Discrete Particle Model in the Inner Surf and Swash-Zones: Continental Shelf Research, v. 26, p. 610-621.

Chalker, B.E., 1981, Simulating Light-Saturation Curves for Photosynthesis and Calcification by Reef-Building Corals: Marine Biology, v. 63, p. 135-141.

Chappell, J., 1980, Coral Morphology, Diversity and Reef Growth: Nature, v. 286, p. 249-252.

—, 2002, Sea Level Changes Forced Ice Breakouts in the Last Glacial Cycle: New Results from Coral Terraces: Quaternary Science Reviews, v. 21, p. 1229-1240.

Chazottes, V., Lecampionalsumard, T., and Peyrotclausade, M., 1995, Bioerosion Rates on Coral-Reefs - Interactions between Macroborers, Microborers and Grazers (Moorea, French-Polynesia): Palaeogeography Palaeoclimatology Palaeoecology, v. 113, p. 189-198.

Clarkson, E.N.K., 1998, Invertebrate Palaeontology and Evolution: Oxford, Blackwell Sciences.

Claudia, R.C., Claudia Di, N., Maurizio, G., Mario Mango, F., and Salvatore Di, G., 2001, A Network of Cellular Automata for a Landslide Simulation: Sorrento, Italy, ACM Press, 419-426 p.

Crossland, C.J., Hatcher, B.G., and Smith, S.V., 1991, Role of Coral Reefs in Global Ocean Production: Coral Reefs, v. 10, p. 55-64.

Cruz-Piñón, G., Carricart-Ganivet, J.P., and Espinoza-Avalos, J., 2003, Monthly Skeletal Extension Rates of the Hermatypic Corals *Montastraea Annularis* and *Montastraea Faveolata*: Biological and Environmental Controls: Marine Biology, v. 143, p. 491-500.

Curtis, A., 1999, Optimal Design of Focused Experiments and Surveys: Geophysical Journal International, v. 139, p. 205-215.

Dalmasso, H., Montaggioni, L.F., Bosence, D., and Floquet, M., 2001, Numerical Modelling of Carbonate Platforms and Reefs: Approaches and Opportunities: Energy Exploration and Exploitation, v. 19, p. 315-345.

Dargenio, B., Ferreri, V., Amodio, S., and Pelosi, N., 1997, Hierarchy of High-Frequency Orbital Cycles in Cretaceous Carbonate Platform Strata: Sedimentary Geology, v. 113, p. 169-193.

Darwin, C., 1842, On the Distribution of Coral Reefs with Reference to the Theory of Their Formation: London, Smith, Elder.

Davies, P.J., Bubela, B., and Ferguson, J., 1978, The Formation of Ooids: Sedimentology, v. 25, p. 703-729.

Deleersnijder, E., Tartinville, B., and Rancher, J., 1997, A Simple Model of the Tracer Flux from the Mururoa Lagoon to the Pacific: Applied Mathematics Letters, v. 10, p. 13-17.

Demicco, R.V., 1998, CYCOPATH 2D - a Two-Dimensional, Forward Model of Cyclic Sedimentation on Carbonate Platform: Computers and Geoscience, v. 24, p. 405-423.

Demicco, R.V., and Hardie, L.A., 2002, The "Carbonate Factory" Revisited: A Reexamination of Sediment Production Functions Used to Model Deposition on Carbonate Platforms: Journal of Sedimentary Research, v. 72, p. 849-857.

Diedrich, N.W., and Wilkinson, B.H., 1999, Depositional Cyclicity in the Lower Devonian Helderberg Group of New York State: Journal of Geology, v. 107, p. 643-658.

Donahue, J., 1969, Genesis of Oolite and Pisolite Grains: An Energy Index: Journal of Sedimentary Petrology, v. 39, p. 1399-1411.

Drew, E., 1983, Halimeda Biomass, Growth Rates and Sediment Generation on Reefs in the Central Great Barrier Reef Province: Coral Reefs, v. 2, p. 101-110.

Drummond, C.N., and Dugan, P.J., 1999, Self-Organising Models of Shallow-Water Carbonate Accumulation: Journal of Sedimentary Research, v. 69, p. 939-946.

Drummond, C.N., and Wilkinson, B.H., 1993a, Aperiodic Accumulation of Cyclic Peritidal Carbonate: Geology, v. 21, p. 1023-1026.

—, 1993b, Carbonate Cycle Stacking Patterns and Hierarchies of Orbitally Forced Eustatic Sealevel Change: Journal of Sedimentary Petrology, v. 63, p. 369-377.

—, 1993c, On the Use of Cycle Thickness Diagrams as Records of Long-Term Sealevel Change During Accumulation of Carbonate Sequences: Journal of Geology, v. 101, p. 687-702.

—, 1996, Stratal Thickness Frequencies and the Prevalence of Orderedness in Stratigraphic Sequences: Journal of Geology, v. 104, p. 1-18.

Duan, T., Cross, T.A., and Lessenger, M.A., 2000, 3-D Carbonate Stratigraphic Model Based on Energy and Sediment Flux.

Durbin, J., and Watson, G.S., 1950, Testing for Serial Correlation in Least Squares Regression. I: Biometrika, v. 37, p. 409-428.

—, 1951, Testing for Serial Correlation in Least Squares Regression. Ii: Biometrika, v. 38, p. 159-177.

Elgar, S., Guza, R.T., Raubenheimer, B., Herbers, T.H.C., and Gallagher, E., 1995, Observations of Wave Evolution During Duck94: EOS Transactions of American Geophysical Union, v. 76 p. 282.

Elrick, M., 1995, Cyclostratigraphy of Middle Devonian Carbonates of the Eastern Great-Basin: Journal of Sedimentary Research Section B-Stratigraphy and Global Studies, v. 65, p. 61-79.

Enos, P., 1991, Sedimentary Parameters for Computer Modeling: Bulletin of the Kansas Geological Survey, v. 233, p. 64-99.

Feely, R.A., Sabine, C.L., Lee, K., Berelson, W., Kleypas, J., Fabry, V.J., and Millero, F.J., 2004, Impact of Anthropogenic Co_2 on the $Caco_3$ System in the Oceans: Science, v. 305, p. 362-366.

Fischer, A.G., 1964, The Lofer Cyclothems of the Alpine Triassic: Kansas Geological Survey Bulletin, v. 169, p. 107-149.

Flemings, P.B., and Jordan, T.E., 1989, A Synthetic Stratigraphic Model of Foreland Basin Development: Journal of Geophysical Research, v. 94, p. 3851-3866.

Flood, P.G., 2001, The `Darwin Point' of Pacifc Ocean Atolls and Guyots: A Reappraisal: Palaeogeography, Palaeoclimatology, Palaeoecology, v. 175, p. 147-152.

Gattuso, J.-P., Allemand, D., and Frankignoulle, M., 1999, Photosynthesis and Calcification at Cellular, Organismal and Community Levels in Coral Reefs: A Review on Interactions and Control by Carbonate Chemistry: American Zoologist, v. 39, p. 160-183.

Gattuso, J.-P., and Buddemeier, R.W., 2000, Calcification and CO_2: Nature, v. 407, p. 311-312.

Gattuso, J.-P., Frankignoulle, M., Bourge, I., Romaine, S., and Buddemeier, R.W., 1998a, Effect of Calcium Carbonate Saturation of Seawater on Coral Calcification.: Global and Planetary Change, v. 18, p. 37-46.

Gattuso, J.P., Frankignoulle, M., Bourge, I., Romaine, S., and Buddemeier, R.W., 1998b, Effect of Calcium Carbonate Saturation of Seawater on Coral Calcification: Global and Planetary Change, v. 18, p. 37-46.

Ginsburg, R.N., 1971, Landward Movement of Carbonate Mud - New Model for Regressive Cycles in Carbonates: American Association of Petroleum Geologists Bulletin, v. 55, p. 340-&.

—, 2005, Disobedient Sediments Can Feedback on Their Transportation, Deposition and Geomorphology: Sedimentary Geology, v. 175, p. 9-18.

Glasgow, C., Parrott, A.K., and Handscomb, D.C., 1996, Particle Tracking Methods for Residence Time Calculations in Incompressible Flow, University of Oxford Numerical Analysis Group.

Goldhammer, R.K., 1988, Superimposed Platform Carbonate Cycles - Eustatic Response of an Aggradational Carbonate Buildup, Middle Triassic of the Dolomites: Aapg Bulletin-American Association of Petroleum Geologists, v. 72, p. 190-190.

Goldhammer, R.K., Dunn, P.A., and Hardie, L.A., 1987, High Frequency Glacio-Eustatic Sealevel Oscillations with Milankovitch Characteristics Recorded in the Middle Triassic Platform Carbonates in Northern Italy: American Journal of Science, v. 287, p. 853-892.

—, 1990, Depositional Cycles, Composite Sea-Level Changes, Cycle Stacking Patterns, and the Hierarchy of Stratigraphic Forcing: Examples from the Alpine Triassic Platform Carbonates: GSA Bulletin, v. 102, p. 535-562.

Goldhammer, R.K., and Elmore, R.D., 1984, Paleosols Capping Regressive Carbonate Cycles in the Pennsylvanian Black Prince Limestone, Arizona: Journal of Sedimentary Petrology, v. 54, p. 1124-1137.

Goldhammer, R.K., Lehmann, P.J., and Dunn, P.A., 1993, The Origin of High-Frequency Platform Carbonate Cycles and 3rd-Order Sequences (Lower Ordovician El-Paso Gp, West Texas) - Constraints from Outcrop Data and Stratigraphic Modeling: Journal of Sedimentary Petrology, v. 63, p. 318-359.

Granjeon, D., 2003, Outcrop and Seismic Constraints for 3d Numerical Stratigraphic Forward Modelling: Examples from Siliciclastic, Carbonate and Source Rock

Systems, Numerical and Physical Modelling of Sedimentary Systems: From Understanding to Prediction, Volume Abstract Only: Utrecht.

Granjeon, D., and Joseph, P., 1999, Concepts and Applications of a 3d Multiple Lithology, Diffusive Model in Stratigraphic Modelling, *in* Harbaugh, J.W., Watney, W.L., Rankey, E.C., Slingerland, R., Goldstein, R.H., and Franseen, E.K., eds., Numerical Experiments in Stratigrpahy: Recent Advances in Stratigraphic and Sedimentological Computer Simulations, Volume 1, SEPM, p. 197-211.

Graus, R.R., and Macintyre, I.G., 1989, The Zonation Patterns of Caribbean Coral Reefs as Controlled by Wave and Light Energy, Bathymetric Setting and Reef Morphology: Computer Simulation Experiments: Coral Reefs, v. 8, p. 9-18.

Graus, R.R., Macintyre, I.G., and Herchenroder, B.E., 1984, Computer Simultion of the Reef Zonation at Discovery Bay, Jamaica: Hurricane Disruption and Long-Term Physical Oceanographic Controls: Coral Reefs, v. 3, p. 59-68.

Griffiths, C., 2003: Cambridge.

Griffiths, C.M., Dyt, C., Paraschivioiu, E., and Liu, K., 2001, Sedsim in Hydrocarbon Exploration, *in* Merrian, D.F., and Davis, J.C., eds., Kluwer Academic/Plenum Publishers.

Grigg, R.W., 1998, Holocene Coral Reef Accretion in Hawaii: A Function of Wave Exposure and Sea Level History: Coral Reefs, v. 17, p. 263-272.

Grotsch, J., 1996, Cycle Stacking and Long-Term Sea-Level History in the Lower Cretaceous (Gavrovo Platform, Nw Greece): Journal of Sedimentary Research, v. 66, p. 723-736.

Grotzinger, J.P., 1986, Cyclicity and Paleoenvironmental Dynamics, Rocknest Platform, Northwest Canada: Geological Society of America Bulletin, v. 97, p. 1208-1231.

Hanks, T.C., Bucknam, R.C., Lajoie, K.R., and Wallace, R.E., 1984, Modification of Wave-Cut and Faulting-Controlled Landforms: Journal of Geophysical Research, v. 89, p. 5771-5790.

Harbaugh, J.W., and Bonham-Carter, G., 1970, Computer Simulation in Geology, John Wiley & Sons.

Hardisty, J., 1994, Beach and Nearshore Sediment Transport, *in* Pye, K., ed., Sediment Transport and Depositional Processes: Oxford, Blackwell Sciences.

Harrison, G.W., 1995, Comparing Predator-Prey Models to Luckinbills Experiment with Didinium and Paramecium: Ecology, v. 76, p. 357-374.

Hautmann, M., 2004, Effect of End-Triassic Co_2 Maximum on Carbonate Sedimentation and Marine Mass Extinction: Facies, v. 50, p. 257-261.

Hearn, C.J., Atkinson, M.J., and Falter, J.L., 2001, A Physical Derivation of Nutrient-Uptake Rates in Coral Reefs: Effects of Roughness and Waves: Coral Reefs, v. 20, p. 347-356.

Hillis-Colinvaux, L., 1986, *Halimeda* Growth and Diversity on the Deep Fore-Reef of Enewetak Atoll: Coral Reefs, v. 5, p. 19-21.

Hinnov, L.A., 2000, New Perspectives on Orbitally Forced Stratigraphy: Annual Review of Earth and Planetary Sciences, v. 28, p. 419-475.

Hinnov, L.A., and Goldhammer, R.K., 1991, Spectral-Analysis of the Middle Triassic Latemar Limestone: Journal of Sedimentary Petrology, v. 61, p. 1173-1193.

Hughes, T.P., 1999, Off-Reef Transport of Coral Fragments at Lizard Island, Australia: Marine Geology, v. 157, p. 1-6.

Hughes, T.P., Baird, A.H., Bellwood, D.R., Card, M., Connolly, S.R., Folke, C., Grosberg, R., Hoegh-Guldberg, O., Jackson, J.B.C., Kleypas, J., Lough, J.M.,

Marshall, P., Nystrom, M., Palumbi, S.R., Pandolfi, J.M., Rosen, B., and Roughgarden, J., 2003, Climate Change, Human Impacts, and the Resilience of Coral Reefs: Science, v. 301, p. 929-933.

Hüssner, H., Roessler, J., Betzlar, C., Petchick, R., and Peinl, M., 2001, Testing 3d Carbonate Simulation of Carbonate Platform Growth with Repro: The Micoene Llucmajor Carbonate Platform (Mallorca): Palaeogeopraphy, Palaeoclimatology, Palaeoecology, v. 175, p. 239-247.

Isern, A.R., McKenzie, J.A., and Feary, D.A., 1996, The Role of Sea-Surface Temperature as a Control on Carbonate Platform Development in the Western Coral Sea: Palaeogeography, Palaeoclimatology, Palaeoecology, v. 124, p. 247-272.

Kaufman, P., Grotzinger, J.P., and McCormik, D.S., 1991, Depth-Dependent Diffusion Algorithm for Simulation of Sedimentation in Shallow Marine Depositional Systems: Bulletin of the Kansas Geological Survey, v. 233, p. 489-508.

Kench, P.S., 1998, Physical Processes in an Indian Ocean Atoll: Coral Reefs, v. 17, p. 155-168.

Kenyon, P.M., and Turcotte, D.L., 1985, Morphology of a Prograding Delta by Bulk Sediment Transport: Geological Society of America Bulletin, v. 96, p. 1457-1465.

Kleypas, J.A., 1997, Modeled Estimates of Global Reef Habitat and Carbonate Production since the Last Glacial Maximum: Paleoceonography, v. 12, p. 533-545.

Kleypas, J.A., Buddemeier, R.W., Archer, D., Gattuso, J.-P., Langdon, C., and Opdyke, B.N., 1999a, Geochemical Consequences of Increased Atmospheric CO_2 on Coral Reefs.: Science, v. 284, p. 118-120.

Kleypas, J.A., Buddemeier, R.W., and Gattuso, J.P., 2001, The Future of Coral Reefs in an Age of Global Change: International Journal of Earth Sciences, v. 90, p. 426-437.

Kleypas, J.A., and Burrage, D.M., 1994, Satellite Observations of Circulation in the Southern Great Barrier Reef, Australia: International Journal of Remote Sensing, v. 15, p. 2051-2063.

Kleypas, J.A., McManus, J.W., and Meñez, L.A.B., 1999b, Environmental Limits to Coral Reef Development: Where Do We Draw the Line?: American Zoologist, v. 39, p. 146-159.

Koerschner, W.F., and Read, J.F., 1989, Field and Modeling Studies of Cambrian Carbonate Cycles, Virginia Appalachians: Journal of Sedimentary Petrology, v. 59, p. 654-687.

Kraines, S.B., Isobe, M., and Komiyama, H., 2001, Seasonal Variations in the Exchange of Water and Water-Borne Particles at Majuro Atoll, the Republic of the Marshall Islands: Coral Reefs, v. 20, p. 330-340.

Kraines, S.B., Suzuki, A., Yanagi, T., Isobe, M., Guo, X., and Komiyama, H., 1999, Rapid Water Exchange between the Lagoon and the Open Ocean at Majuro Atoll Due to Wind, Waves and Tides: Journal of Geophysical Research, v. 104, p. 15-635.

Leclercq, N., Gattuso, J.P., and Jaubert, J., 2000, Co_2 Partial Pressure Controls the Calcification Rate of a Coral Community: Global Change Biology, v. 6, p. 329-334.

Leeder, M.R., Gray, T.E., and Alexander, J., 2005, Sediment Suspension Dynamics and a New Criterion for the Maintenance of Turbulent Suspensions: Sedimentology, v. 52, p. 683-691.

Lehmann, C., Osleger, D.A., and Montanez, I.P., 1998, Controls on Cyclostratigraphy of Lower Cretaceous Carbonates and Evaporites, Cupido and Coahuila Platforms, Northeastern Mexico: Journal of Sedimentary Research, v. 68, p. 1109-1130.

Lehrmann, D.J., and Goldhammer, R.K., 1999, Secular Variation in Parasequence and Facies Stacking Patterns of Platform Carbonates: A Guide to Application of Stacking Pattern Analysis in Strata of Diverse Ages and Settings, *in* Harris, P.M., H., S.A., and Simo, J.A., eds., Advances in Carbonate Sequence Stratigraphy: Applications to Reservoirs, Outcrops and Models, Volume 63, SEPM Special Publication, p. 187-225.

Littler, M.M., Littler, D.S., and Lapointe, B.E., 1988, A Comparison of Nutrient- and Light-Limited Photosynthesis in Psammophytic Versus Epifithic Forms of Halimeda (Caulerpales, Halimedaceae) from the Bahamas: Coral Reefs, v. 6, p. 219-225.

Lugo-Fernández, A., Hernández-Ávila, M.L., and Roberts, H.H., 1994, Wave-Energy Distribution and Hurricane Effects on Margarite Reef, Southwestern Puerto Rico: Coral Reefs, v. 13, p. 21-32.

Lugo-Fernández, A., Roberts, H.H., and Suhayda, J.N., 1998a, Wave Transformation across a Caribbean Fringing-Barrier Coral Reef: Continental Shelf Research, v. 18, p. 1099-1124.

Lugo-Fernández, A., Roberts, H.H., and Wiseman, J.W.J., 1998b, Tide Effects on Wave Attenuation and Wave Set-up on a Caribbean Coral Reef: Esturine, Coastal and Shelf Science, v. 47, p. 385-393.

Martin, Y., 2000, Modelling Hillslope Evolution: Linear and Nonlinear Transport Relations: Geomorphology, v. 34, p. 1–21.

Mathieu, P.-P., Deleersnijder, E., Cushman-Roisin, B., Beckers, J.-M., and Bolding, K., 2002, The Role of Topography in Small Well-Mixed Bays, with Application to the Lagoon of Mururoa: Continental Shelf Research, v. 22, p. 1379-1395.

Mayer, H., 1993, Time-Series Analysis in Cyclic Stratigraphy - an Example from the Cretaceous of the Southern Alps, Italy: Mathematical Geology, v. 25, p. 975-1001.

McLaughlin, C.J., Smith, C.A., Buddemeier, R.W., Bartley, J.D., and Maxwell, B.A., 2003, Rivers, Runoff, and Reefs: Global and Planetary Change, v. 39, p. 191–199.

McLean, D.J., and Mountjoy, E.W., 1994, Allocyclic Control on Late Devonian Buildup Development, Southern Canadian Rocky-Mountains: Journal of Sedimentary Research Section B-Stratigraphy and Global Studies, v. 64, p. 326-340.

Miller, K.G., Sugarman, P.J., Browning, J.V., Kominz, M.A., Hernandez, J.C., Olsson, R.K., Wright, J.D., Feigenson, M.D., and Van Sickel, W., 2003, Late Cretaceous Chronology of Large, Rapid Sea-Level Changes: Glacioeustasy During the Greenhouse World: Geology, v. 31, p. 585-588.

Miller, K.G., Wright, J.D., and Browning, J.V., 2005, Visions of Ice Sheets in a Greenhouse World: Marine Geology, v. 217, p. 215-231.

Morse, J.W., Gledhill, D.K., and Millero, F.J., 2003, $Caco_3$ Precipitation Kinetics in Waters from the Great Bahama Bank: Implications for the Relationship

between Bank Hydrochemistry and Whitings: Geochimica Et Cosmochimica Acta, v. 67, p. 2819-2826.

Morse, J.W., Millero, F.J., Thurmond, V., Brown, E., and Ostlund, H.G., 1984, The Carbonate Chemistry of the Grand Bahama Bank Waters: After 18 Years Another Look: Journal of Geophysical Research, v. 89, p. 3604-3614.

Munk, W.H., and Sargent, M.C., 1948, Adjustment of Bikini Atoll to Ocean Waves: Transaction of the American Geophysical Union, v. 29, p. 855-860.

Newell, N.D., Purdy, E.G., and Imbrie, J., 1960, Bahamian Oölitic Sand: Journal of Geology, v. 68, p. 481-497.

Nicolis, G., and Nicolis, C., 1991, Nonlinear Dynamic Systems in the Geosciences: Bulletin of the Kansas Geological Survey, v. 233, p. 33-42.

Norland, U., 1999, Stratigraphic Modeling Using Common-Sense Rules, *in* Harburgh, J.W., Rankey, E.C., Slingerland, R., Goldstein, R.H., and Franseen, E.K., eds., Volume 62, SEPM, p. 245-251.

Opdyke, B.N., and Wilkinson, B.H., 1993, Carbonate Mineral Saturation State and Cratonic Limestone Accumulation: American Journal of Science, v. 293, p. 217-234.

Osleger, D., and Read, J.F., 1991, Relation of Eustasy to Stacking Patterns of Meter-Scale Carbonate Cycles, Late Cambrian, USA: Journal of Sedimentary Petrology, v. 61, p. 1225-1252.

Pentecost, A., 1978, Blue-Green-Algae and Freshwater Carbonate Deposits: Proceedings of the Royal Society of London Series B-Biological Sciences, v. 200, p. 43-61.

Pillans, B., Chappell, J., and Naish, T.R., 1998, A Review of the Milankovitch Climatic Beat: Template for Plio-Pleistocene Sea-Level Changes and Sequence Stratigraphy: Sedimentary Geology, v. 122, p. 5-21.

Pinet, P.P., 1992, Oceanography, West Publishing.

Pomar, L., 2001, Types of Carbonate Platforms: A Genetic Approach: Basin Research, v. 13, p. 313-334.

Pratt, B.R., and James, N.P., 1986, The St George Group (Lower Ordovician) of Western Newfoundland - Tidal Flat Island Model for Carbonate Sedimentation in Shallow Epeiric Seas: Sedimentology, v. 33, p. 313-343.

Press, W.H., Teukolsky, S.A., Vetterling, W.T., and Flannery, B.P., 1992, Numerical Recipes in C: The Art of Scientific Computing, Cambridge University Press.

Pye, K., 1994, Properties of Sedimentary Particles, *in* Pye, K., ed., Sediment Transport and Depositional Processes: Oxford, Blackwell Science, p. 398.

Rankey, E.C., 2002, Spatial Patterns of Sediment Accumulation on a Holocene Carbonate Tidal Flat, Northwest Andros Island, Bahamas: Journal of Sedimentary Research, v. 72, p. 591-601.

—, 2003, Carbonate Coasts as Complex Systems: A Case Study from Andros Island, Bahamas, Proceedings of the International Conference on Coastal Sediments.

—, 2004, On the Interpretation of Shallow Shelf Carbonate Facies and Habitats: How Much Does Water Depth Matter?: Journal of Sedimentary Research, v. 74, p. 2-6.

Raspini, A., 2001, Stacking Pattern of Cyclic Carbonate Platform Strata: Lower Cretaceous of Southern Apennines, Italy: Journal of the Geological Society, v. 158, p. 353-366.

Rasser, M.W., and Riegl, B., 2002, Holocene Coral Reef Rubble and Its Binding Agents: Coral Reefs, v. 21, p. 57-72.

Read, J.F., and Goldhammer, R.K., 1988, Use of Fischer Plots to Define Third-Order Sea Level Curves in Ordovician Peritidal Cyclic Carbonate, Appalachians: Geology, v. 16, p. 895-899.

Read, J.F., Grotzinger, J.P., Bova, J.A., and Koerschner, W.F., 1986, Models for Generation of Carbonate Cycles: Geology, v. 14, p. 107-110.

Read, J.F., Osleger, D., and Elrick, M., 1991, Two-Dimensional Modeling of Carbonate Ramp Sequences and Component Cycles: Bulletin of the Kansas Geological Survey, v. 233, p. 473-488.

Reynaud, S., Leclercq, N., Romaine-Lioud, S., Ferrier-Pages, C., Jaubert, J., and Gattuso, J.P., 2003, Interacting Effects of Co2 Partial Pressure and Temperature on Photosynthesis and Calcification in a Scleractinian Coral: Global Change Biology, v. 9, p. 1660-1668.

Roberts, H.H., 1974, Variability of Reefs with Regard to Changes in Wave Power around an Island, *in* Cameron, A.M., Campbell, B.M., Cribb, A.B., Endean, R., Jell, J.S., Jones, O.A., Mather, P., and Talbot, F.H., eds., Proceedings of the Second International Coral Reef Symposium, Volume 2: Brisbane, Australia, p. 497-512.

Roberts, H.H., Murray, S.P., and Suhayda, J.N., 1975, Physical Processes in a Fringing Reef System: Journal of Marine Research, v. 33, p. 233-260.

Roberts, J.M., Wheeler, A.J., and Freiwald, A., 2006, Reefs of the Deep: The Biology and Geology of Cold-Water Coral Ecosystems: Science, v. 312, p. 543-547.

Sadler, P.M., 1981, Sediment Accumulation Rates and the Completeness of Stratigraphic Sections: Journal of Geology, v. 89, p. 569-584.

Sadler, P.M., Osleger, D.A., and Montanez, I.P., 1993, On the Labeling, Length, and Objective Basis of Fischer Plots: Journal of Sedimentary Petrology, v. 63, p. 360-368.

Sandulli, R., and Raspini, A., 2004, Regional to Global Correlation of Lower Cretaceous (Hauterivian-Barremian) Shallow-Water Carbonates of the Southern Apennines (Italy) and Dinarides (Montenegro), Southern Tethyan Margin: Sedimentary Geology, v. 165, p. 117-153.

Saunders, P.M., Coward, A.C., and de Cuevas, B.A., 1999, Circulation of the Pacific Ocean Seen in a Global Ocean Model: Ocean Circulation and Climate Advanced Modelling Project (Occam): Journal of Geophysical Research-Oceans, v. 104, p. 18281-18299.

Schlager, W., 1992, Sedimentology and Sequence Stratigraphy of Reefs and Carbonate Platforms, AAPG.

—, 1999, Sequence Stratigraphy of Carbonate Rocks, Leading Edge.

Scoffin, T.P., 1993, The Geological Effects of Hurricanes on Coral Reefs and the Interpretation of Storm Deposits: Coral Reefs, v. 12, p. 203-221.

Shields A, 1936, Anwendung Der Ahnlichkeitmechanik Und Der Turbulenzforschung Auf Die Gescheibebewegung: Mitt. Preuss Ver.-Anst, v. 26.

Simone, L., 1980, Ooids: A Review: Earth-Science Reviews, v. 16, p. 319-355.

Stephens, N.P., and Sumner, D.Y., 2003, Famennian Microbial Reef Facies, Napier and Oscar Ranges, Canning Basin, Western Australia: Sedimentology, v. 50, p. 1283-1302.

Stoddart, D.R., 1969, Ecology and Morphology of Recent Coral Reefs: Biological Review, v. 44, p. 433-498.

Storlazzi, C.D., Logan, J.B., and Field, M.E., 2003, Quantitative Morphology of a Fringing Reef Tract Using High-Resolution Laser Bathymetry: Southern Molokai, Hawaii: GSA Bulletin, v. 115, p. 1344-1355.

Sumner, D.Y., and Grotzinger, J.P., 1993, Numerical Modeling of Ooid Size and the Problem of Neoproterozoic Giant Ooids: Journal of Sedimentary Petrology, v. 63, p. 974-982.

Suzuki, A., Nakamori, T., and Kayanne, H., 1995, The Mechanism of Production Enhancement in Coral Reef Carbonate Systems: Model and Empirical Results: Sedimentary Geology, v. 99, p. 259-280.

Szmant, A.M., 2002, Nutrient Enrichment on Coral Reefs: Is It a Major Cause of Coral Reef Decline?: Estuaries, v. 25, p. 743-766.

Tartinville, B., Deleersnijder, E., and Rancher, J., 1997, The Water Residence Time in the Mururoa Atoll Lagoon: Sensitivity Analysis of a Three-Dimensional Model: Coral Reefs, v. 16, p. 193-203.

Tartinville, B., and Rancher, J., 2000, Wave-Induced Flow over Mururoa Atoll Reef: Journal of Coastal Research, v. 16, p. 776-781.

Tetzlaff, D., 2005, Modelling Coastal Sedimentation through Geologic Time: Journal of Coastal Research, v. 21, p. 610-617.

Tetzlaff, D., and Harbaugh, J.W., 1989, Simulating Clastic Sedimentation, Van Nostrand Reinhold.

Tetzlaff, D., and Priddy, G., 2001, Sedimentary Process Modeling: From Academia to Industry, *in* Merrian, D.F., and Davis, J.C., eds., Kluwer Academic/Plenum Publishers.

Tetzlaff, D.M., 2004, Input Uncertianty and Conditioning in Siliciclastic Process Modelling, *in* Curtis, A., and Wood, R., eds., Geological Prior Information, Volume Special Publication, Geological Society of London.

Tinker, S.W., 1998, Shelf-to-Basin Facies Distributions and Sequence Stratigraphy of a Steep-Rimmed Carbonate Margin; Capitan Depositional System, Mckittrick Canyon, New Mexico and Texas: Journal of Sedimentary Research. 68, p. 1146-1174.

Tipper, J.C., 1997, Modeling Carbonate Platform Sedimentation - Lag Comes Naturally: Geology, v. 25, p. 495-498.

Tucker, M.E., and Wright, V.P., 1990, Carbonate Sedimentology, Blackwell Science.

Van Wagoner, J.C., Posamentier, H.W., Mitchum, R.M., Vail, P.R., Sarg, J.F., Loutit, J.S., and Hardenbol, J., 1998, An Overview of the Fundamentals of Sequence Stratigraphy and Key Definitions, *in* Wilgus, C.K., Hastings, B.S., Kendall, C.G.S.C., Posamentier, H.W., Ross, C.A., and Van Wagoner, J.C., eds., Sea-Level Changes: An Integrated Approach., Volume Special Publication 42: Tulsa, Society of Economic Paleontologists and Mineralogists, p. 38-45.

Walker, D.J., 1998, Modelling Residence Time in Stormwater Ponds: Ecological Engineering, v. 10, p. 247-262.

Walker, L.J., Wilkinson, B.H., and Ivany, L.C., 2002, Continental Drift and Phanerozoic Carbonate Accumulation in Shallow-Shelf and Deep-Marine Settings: Journal of Geology, v. 110, p. 75-87.

Ware, J.R., Fautin, D.G., and Buddemeier, R.W., 1996, Patterns of Coral Bleaching: Modeling the Adaptive Bleaching Hypothesis: Ecological Modelling, v. 84, p. 199-214.

Warrlich, G.M.D., Waltham, D.A., and Bosence, D.W.J., 2002, Quantifying the Sequence Stratigraphy and Drowning Mechanisms of Atolls Using a New Forward Modelling Program (Carbonate 3D): Basin Research, v. 14, p. 379-400.

Watney, W.L., Rankey, E.C., and Harbaugh, J.W., 1999, Perspectives on Stratigraphic Simulation Models: Current Approaches and Future

Opportunites, *in* Harbaugh, J.W., Watney, W.L., Rankey, E.C., Slingerland, R., Goldstein, R.H., and Franseen, E.K., eds., Numerical Experiments in Stratigraphy: Recent Advances in Stratigraphic and Sedimentological Computer Simulations, SEPM.

Whitaker, F., Smart, P., Hague, Y., Waltham, D., and Bosence, D., 1997, Coupled Two-Dimensional Diagenetic and Sedimentological Modeling of Carbonate Platform Evolution: Geology, v. 25, p. 175-178.

Wilkinson, B.H., Diedrich, N.W., and Drummond, C.N., 1996, Facies Successions in Peritidal Carbonate Sequences: Journal of Sedimentary Research, v. 66, p. 1065-1078.

Wilkinson, B.H., Diedrich, N.W., Drummond, C.N., and Rothman, E.D., 1998, Michigan Hockey, Meteoric Precipitation, and Rhythmicity of Accumulation on Peritidal Carbonate Platforms: Geological Society of America Bulletin, v. 110, p. 1075-1093.

Wilkinson, B.H., and Drummond, C.N., 2004, Facies Mosaics across the Persian Gulf and around Antigua - Stochastic and Deterministic Products of Shallow-Water Sediment Accumulation: Journal of Sedimentary Research, v. 74, p. 513-526.

Wilkinson, B.H., Drummond, C.N., Diedrich, N.W., and Rothman, E.D., 1999, Poisson Processes of Carbonate Accumulation on Paleozoic and Holocene Platforms: Journal of Sedimentary Research, v. 69, p. 338-350.

Wilkinson, B.H., Drummond, C.N., Rothman, E.D., and Diedrich, N.W., 1997, Stratal Order in Peritidal Carbonate Sequences: Journal of Sedimentary Research, v. 67, p. 1068-1082.

Williams, G.P., 1997, Chaos Theory Tamed: London, Taylor and Francis, 499 p.

Wolanski, E., and Spangnol, S., 2000, Sticky Waters in the Great Barrier Reef: Esturine, Coastal and Shelf Science, v. 50, p. 27-32.

Wood, R., 1998, The Ecological Evolution of Reefs: Annual Review of Ecology and Systematics, v. 29, p. 179-206.

—, 1999, Reef Evolution: Oxford, Oxford University Press.

Woodley, J.D., Chornesky, E.A., Clifford, P.A., Jackson, J.B.C., Kaufman, L.S., Knowlton, N., Lang, J.C., Pearson, M.P., Porter, J.W., Rooney, M.C., Rylaarsdam, K.W., Tunnicliffe, V.J., Wahle, C.M., Wulff, J.L., Curtis, A.S.G., Dallmeyer, M.D., Jupp, B.P., Koehl, M.A.R., Neigel, J., and Sides, E.M., 1981, Hurricane Allens Impact on Jamaican Coral Reefs: Science, v. 214, p. 749-755.

Wright, V., and Burgess, P., 2005, The Carbonate Factory Continuum, Facies Mosaics and Microfacies: An Appraisal of Some of the Key Concepts Underpinning Carbonate Sedimentology: Facies, v. 51, p. 17-23.

Xiao, Y., and Chen, L., 2002, A Ratio-Dependent Predator-Prey Model with Disease in the Prey: Applied Mathematics and Computation, v. 131, p. 397-414.

Yamano, H., Abe, O., Matsumoto, E., Kayanne, H., Yonekura, N., and Blanchon, P., 2003, Influence of Wave Energy on Holocene Coral Reef Development: An Example from Ishigaki Island, Ryukyu Islands, Japan: Sedimentary Geology, v. 159, p. 27-41.